Elin Storlien

Characterizing the demand response potential of thermal heat load in buildings

Master's thesis in Energy and Environmental Engineering

Supervisor: Laurent Georges

July 2020

Master's thesis

NTNU
Norwegian University of Science and Technology
Faculty of Engineering
Department of Energy and Process Engineering

NTNU
Norwegian University of
Science and Technology

Elin Storlien

Characterizing the demand response potential of thermal heat load in buildings

Master's thesis in Energy and Environmental Engineering
Supervisor: Laurent Georges
July 2020

Norwegian University of Science and Technology
Faculty of Engineering
Department of Energy and Process Engineering

NTNU
Norwegian University of
Science and Technology

Abstract

Utilizing the energy flexibility of buildings for demand response is stated as one of the solutions for maintaining the instantaneous balance in future energy systems, where intermittent renewable energy sources becomes more prominent. The aim of this thesis is to characterize the demand response potential of space heating load in Norwegian residential buildings, in order to facilitate the implementation of demand flexibility into energy planning models.

The embedded thermal mass in buildings can be utilized for thermal energy storage by periodically increasing and decreasing the space heating load relative to a reference heat load. This provides an opportunity to shift heat load to periods with lower demand, which could relieve grid stress, and reduce the energy costs for consumers. How much the heat load can deviate from a reference heat load, without affecting the thermal comfort, is investigated by using a combination of detailed dynamic simulations in IDA ICE and MATLAB. By introducing a step to the reference heat load profiles, the resulting step response of the indoor temperature could be analysed. Evaluations of the thermal comfort is done by introducing a restriction for the variation in indoor temperature during the thermal mass activation.

Simple models to represent buildings in energy system analysis are investigated. Based on physical knowledge about the thermal dynamics of buildings, a first-order and a second-order model is developed. Related step response equations are used to fit the models to the indoor temperature response obtained by IDA ICE. Model parameters such as the thermal capacitance, the overall heat transfer coefficient (U) and time constants are identified to characterize the demand flexibility.

Four variations of the building model used for the simulations are made, to study how indoor temperature fluctuations and model parameters are affected by insulation levels and energy performance. The model variations are defined based on Norwegian standards and regulations, including TEK87, TEK10, TEK17 and the passive house standard. Simulations were performed for each month of the heating season. It was found that the low insulated building had potential for both charging and discharging in nearly all months, with an allowed deviation in heat load of $\pm$4-6%. The parameter U was consistently high in all months, which is expected due to the amount of heat losses in low insulated buildings. The average value of the time constants was 40 hours. Due to the heating season being shorter in high insulated buildings, these models could only be discharged in the coldest months. The allowed deviation in heat load were found to be $\pm$5-8%. The parameter U decreased with higher insulation levels and better energy performance, while the time constants increased. The passive house model had an average time constant of 150 hours.

From the validation of model accuracy versus IDA ICE, it was found that due to the lack of fast dynamics, the first-order model could not obtain similar temperatures to those computed by IDA ICE. The second-order model could however obtain close to similar temperatures, with a deviation of 0.2-0.3°C for the high insulated models, and 0.5-0.6°C for the low insulated model. Over the course of three weeks, the deviation was still not changing. The second-order model is thus able to fairly predict the indoor temperature in buildings, both in the short-term and in the long-term. The modelling approach is thus proved to work, and the second-order model can potentially be used to represent buildings and their flexibility in energy planning models.

Sammendrag

Utnyttelse av energifleksibilitet i bygg er fremhevet som en av løsningene for å opprettholde balansen i fremtidens energisystem, hvor uregulerbare energikilder vil utgjøre en stadig større andel. Målet med denne masteroppgaven er å karakterisere energifleksibiliteten knyttet til varmelast i norske boligbygg, slik at denne fleksibiliteten kan implementeres i energiplanleggingsmodeller.

Den termiske massen som finnes naturlig i bygg kan utnyttes til termisk energilagring, ved å periodisk øke og redusere varmelast relativt til referanselasten. Dette muliggjør flytting av varmelast til perioder med lavere forbruk, slik at effekttoppene i kraftnettet og energiprisene reduseres. Hvor mye varmelast som kan flyttes uten at det påvirker termisk komfort, blir undersøkt ved å bruke en kombinasjon av dynamiske simuleringer i IDA ICE og MATLAB. Gjennom å introdusere et sprang på referanselasten, kan sprangresponsen til innetemperaturen undersøkes. Termisk komfort blir evaluert ved å innføre en restriksjon på variasjonen i innetemperatur under aktiveringen av den termiske massen.

Enkle modeller til å representere bygninger i energisystemanalyser blir undersøkt. En førsteordens og en andreordens modell er formulert på bakgrunn av de termiske egenskapene til bygg. Utledede ligninger for sprangrespons brukes til kurvetilpasning av modellene opp mot sprangresponsen for innetemperatur i IDE ICE. Modellparametere blir identifisert for å karakterisere bygningsfleksibiliteten, og inkluderer varmekapasitet, varmegjennomgangskoeffisient (U) og tidskonstanter.

For å analysere innvirkningen av isolasjonsnivå og energieffektivitet på svingninger i innetemperatur og modellparametere, defineres fire variasjoner av bygningsmodellen i IDA ICE. Disse er basert på norske forskrifter og standarder, inkludert TEK87, TEK10, TEK17 og standard for passivhus. Simuleringene av modellene gjennomføres for hver måned i fyringssesongen. Både økning og reduksjon av referanselast var mulig i den lavisolerte bygningsmodellen for nesten alle månedene, med et potensial for endring på 4-6%. Parameteren U var gjennomgående høy, som er forventet på bakgrunn av tapene som forekommer i lavisolerte bygg. Den gjennomsnittlige verdien på tidskonstantene var 40 timer. Høyisolerte bygg har gjerne kortere fyringssesong, noe som reflekteres i resultatene ved at reduksjon av referanselast bare var mulig for de kaldeste månedene. Den potensielle økningen og reduksjonen av referanselast var 5-8%. Parameteren U ble redusert i takt med økende grad av isolasjonsnivå og energieffektivitet, hvorav tidskonstantene økte. Den gjennomsnittlige verdien på tidskonstantene for Passivhusmodellen var 150 timer.

Nøyaktigheten til modellene ble vurdert opp mot IDA ICE gjennom en valideringsprosess. Førsteordens modellen klarte ikke å gjengi temperaturene fra IDA ICE, på grunn av manglende evne til å fange opp den raske dynamikken. Andreordens modellen klarte derimot å gjengi temperaturene med høy grad av nøyaktighet, med et avvik på 0.2-0.3°C for de høyisolerte modellene, og 0.5-0.6°C for den lavisolerte modellen. Disse avvikene endret seg heller ikke gjennom hele den simulerte perioden på tre uker. Andreordens modellen er dermed i stand til å ganske godt forutsi innetemperatur i bygninger, både på kort sikt og på lang sikt. Modelltilnærmingen er således bevist å fungere, og andreordens modellen kan potensielt brukes til å representere bygninger og tilhørende fleksibilitet i energiplanleggingsmodeller.

Preface

This master thesis concludes my Master of Science (MSc) degree in Energy and Environmental Engineering. It was written during the spring of 2020, at the department of Energy and Process Engineering at the Norwegian University of Science and Technology (NTNU). The problem description was developed in collaboration with SINTEF Energy, and the work is an extension of my specialization project written in the autumn of 2019.

I especially want to thank my supervisor Laurent Georges, for valuable guidance, devotion to helping me with solving problems, and providing me with the material needed to conduct the simulations. This has been very much appreciated. I would much like to thank my co-supervisor Magnus Askeland, for sharing his knowledge, and providing valuable help whenever needed. Additionally, I would like to thank Øystein Rønneseth and Igor Sartori, for providing the building models in IDA ICE, and all the related information.

Elin Storlien
Trondheim, July 2020

Table of Contents

List of Figures

List of Tables

Nomenclature

Abbreviations

AHU	Air handling unit
BEF	Building energy flexibility
BPS	Building Performance Simulation
DR	Demand response
HVAC	Heating, ventilation and air-conditioning
PMV	Predicted mean vote
PPD	Predictive percentage of dissatisfied
SFH	Single family house
SFP	Specific fan power
TES	Thermal Energy Storage
TMA	Thermal mass activation

Subscripts

conv	Convective heat
gen	Generated heat
inf	Infiltration loss
int	Internal heat gain
sh	Space heating
solar	Solar heat gain
st	Stored heat
trans	Transmission loss
vent	Ventilation loss

Symbols

λ	Thermal conductivity (W/mK)
τ	Building time constant (h)
T_i	Indoor temperature (°C or K)
T_o	Outdoor temperature (°C or K)
U_{val}	U-value (W/m^{2}K)
$\dot{Q}$	Heat transfer rate (W)
C	Thermal capacitance (J/K)
R	Thermal resistance (m^{2}K/W)
U	Overall heat transfer coefficient (W/K)
P	Space heating power (W)
Q	Heat transfer (J)
a	Thermal diffusivity (m^2/s)
c	Specific heat capacity (J/kgK)
h	Convective heat rate transfer coefficient (W/m^{2}K)
q	Heat flux (W/m^2)

Chapter 1

Introduction

1.1 Motivation

Greater commitment to renewable energy sources such as wind and solar power are means to create more sustainable energy systems, and reaching the climate goals [1]. With an increasing share of intermittent energy sources, flexible consumption is required to maintain the instantaneous balance in the energy system. Demand Response (DR) is introduced as a measure to ensure reliable and stable power supply during peak load hours, in which the consumption is adjusted according to the demand. Based on a price incentive, consumers are encouraged to reduce their energy consumption during peak load hours [2, 3]. Another way of obtaining this kind of demand flexibility is to utilize the building itself, or its technical systems, to shift in time the electric consumption. This is known as building energy flexibility (BEF).

Using building energy flexibility for demand response (DR) is stated to be one of the solutions to maintain balance in the future smart energy system [4, 5, 6]. IEA EBC Annex 67 - Energy Flexible Buildings, are currently developing standardized terminology and methodologies for characterizing the potential of BEF. They provide the following general definition of energy flexibility of buildings [4]:

> "*Energy flexibility of a building is the ability to manage its demand and generation according to local climate conditions, user needs and grid requirements.*"

Various methodologies for assessing the potential of BEF have been developed and studied in previous research. Lopes et al. [7], identified two general approaches used to deviate the electricity consumption from a reference case. The first approach is thermal energy storage (TES), where the thermal properties of the building (thermal mass) or the component itself can be utilized to postpone the electric consumption of heat pumps, electric radiators, water tanks etc. This approach was used by De Coninck and Helsen [8], which defined electricity costs as a constraint for flexibility. Furthermore, Le Dréau et al. [9], Reynders et al. [10] and Zhang et al. [11] used key performance indicators to define the demand response potential of thermal storage to evaluate BEF. Six et al. [12] used this approach to quantify the flexibility of heat pumps and a Combined Heat and Power system, both individually combined

with thermal energy storage. The second general approach is to implement controllers on electrical devices such as washing machines and dishwashers, to shift the consumption to periods with lower energy prices, or periods with high generation of renewable energy. This approach was used by D'hulst et al. [13].

Buildings were accountable for almost half of the Norwegian electricity consumption in 2016, according to the Norwegian Water Resources and Energy Directorate (NVE) [14]. Most of the electricity consumption in residential buildings are related to space heating systems, domestic hot water and electrical appliances. The energy demand varies depending on seasonal weather changes, system efficiency, building envelope, energy prices and occupant behaviour. On a daily basis, the demand usually peaks in early mornings and late afternoons. More energy efficient buildings and technological systems have reduced the energy use in recent years, and NVE predicts the energy use in buildings to be reduced by 1 TWh towards 2035. Although, this reduction is small compared to the total energy use, and so buildings would still have a considerable impact on the power grid in the future. Shifting the space heating load to more favorable periods of the day could relieve grid stress, and reduce the energy costs for consumers.

The embedded thermal mass in buildings can be utilized for thermal energy storage, which provides an opportunity for shifting or postponing the space heating load. How this flexibility of buildings could impact and potentially stabilize the power grid still needs to be investigated [4]. Additionally, it is important to account for the effect on the thermal comfort of occupants during the periods of load shifting. There is currently a desire for implementing the building energy flexibility into energy planning models, so that it can be included into the optimization of the energy system. In order to do so, this demand flexibility has to be characterised.

1.2 Objectives

This thesis aims to characterize the demand response potential of space heating load in buildings, in order to facilitate the implementation of demand flexibility into energy planning models. The following objectives are defined for this thesis:

1. Develop a framework in IDA ICE to be able to test the influence of space heating load profiles on the indoor temperature.
2. Investigate simplified models to represent buildings in energy system analysis, and identify the model parameters.
3. Analyse the influence of different insulation levels and energy performance on indoor temperature fluctuations and model parameters.
4. Validate the accuracy of the investigated models.

1.3 Scope and limitations

The scope of this thesis is to provide answers to the following essential questions; how much thermal energy can be shifted in time, and how can this flexibility be characterized?

The proposed method is to use detailed dynamic simulations in IDA ICE, on a building model representative for Norwegian residential buildings. Four different model variations of the building model are made in IDA ICE, to study how indoor temperature fluctuations and model parameters are affected by insulation levels and energy performance.

To identify the allowable deviation of space heating consumption from a reference heat load, the model variations are simulated for each month of the heating season. This is defined from January-March and October-December. Reference heat load profiles are modified in MATLAB by introducing a step, and the new heat load profiles are used as input to IDA ICE to run a second simulation. The resulting step responses of the indoor temperatures are analysed, to assure that thermal comfort is not comprised during the thermal mass activation. The thermal comfort of occupants is used as a constraint for the allowed deviation in heat load, by introducing a limit for the variation in indoor temperature. To limit the scope of work related to the simulations, only the main living zone of the building model is considered for changes in heat load.

Simplified mathematical models to represent buildings in energy system analysis will be investigated. This includes a first-order model and a second-order model, in which is developed based on the thermal dynamics of buildings. Step response equations are derived, and implemented into MATLAB to fit the models to the step response of the indoor temperature computed by IDA ICE. Related model parameters can then be identified to characterize the flexibility. Finally, the accuracy of these models are validated.

A lot of the work related to developing the framework in IDA ICE and the MATLAB scripts were done by the supervisor of this thesis, so that the focus could be kept on performing the simulations on the different model variations, and identify the model parameters.

1.4 Thesis structure

Chapter 2, *Background*, gives a brief introduction to the Norwegian energy system, and energy planning models. This provides background information that forms the basis for the defined objectives.

Chapter 3, *Theory*, provides theoretical background related to the thermal behaviour of buildings, thermal energy storage and the thermal environment. A literature review of thermal comfort evaluations during TMA is conducted, and an overview of the existing approaches used for modelling thermal mass is presented.

Chapter 4, *Methodology*, includes a description of the approaches related to formulating the mathematical models, use of IDA ICE for building performance simulation, defining the building model used in the simulations, the simulation approach, identification of model parameters and the simulation scenarios.

Chapter 5, *Simulation results*, presents the results obtained from the simulations, related to the allowable deviation from a reference heat load and the identified model parameters.

Chapter 6, *Analysis*, includes an analysis of the general trends and findings related to the results, and possible sources of error related to the simulations.

Chapter 7, *Validation*, presents the validation process, and an analysis of the findings related to model accuracy.

Chapter 8, *Conclusion*, presents the final evaluations based on the analysis. Further work is also proposed.

Remark: The contents in chapters 3 and 4 are either reused or based on previously written material from the specialisation project with the same title.

Chapter 2

Background

This chapter gives a brief introduction to how the traditional Norwegian energy system is currently transitioning into a smarter energy system, and how this is influencing the power grid. The purpose of using energy planning models is also introduced, and it is explained why there is a desire to implement building energy flexibility into such models.

2.1 The Norwegian Energy system

The main function of the energy system is to provide energy services for extracting primary energy, transport, conversion, storage, distribution and end use of energy [15]. These services are generally provided by different companies and operators with specific responsibilities.

Common energy sources in the Norwegian energy system includes hydro power, gas, oil, waste, biomass, and to some extent wind and solar power. Due to the natural access of hydro power, electricity has become the dominating energy carrier in Norway. Producers are responsible for generating the electricity, grid companies are responsible for operating and maintenance of the grid infrastructure, while the system operator is responsible for maintaining the energy balance and securing the supply. End users can choose between a variety of suppliers to buy the electricity from, and thus have the opportunity to choose the supplier with the lowest energy prices [16].

Electricity requires instant generation and consumption, and so the two must be balanced in some way. Traditionally, the supply side of the energy system has been responsible for ensuring that power generation is adjusted to the power consumption. In periods with lower energy demand, water can be stored in reservoirs, and later be used in periods with higher demand. This flexibility has been important for maintaining the instantaneous balance of the energy system, and the security of supply [17]. Additionally, the energy prices are kept fairly stable. With the increasing proportion of intermittent renewable energy sources, the instantaneous balance and energy prices are affected.

An important part of creating sustainable energy systems is to increase the share of renewable energy, and reduce the usage of fossil fuels. Wind power represents about 4% of the Norwegian power generation today, and with several new wind farms under development the installed effect will be doubled in the near future [18]. Additionally, solar power has become more profitable, and the amount of installed solar panels are increasing rapidly [19]. The generation of solar and wind power is strongly dependent on weather conditions, and may not be able to continuously deliver energy with an acceptable level of security. Additionally, solar radiation and wind cannot be stored naturally like water. In case of a shortage, the demand has to be covered by other energy sources to restore the balance of the energy system. This will increase the energy prices in cases where fossil fuels are used to cover the demand, due to higher generation costs. On a sunny or particularly windy day, the power generation may exceed the demand, in which the energy prices has to be dumped [20].

The development of smarter technology, and the increasing attention on reducing the environmental impact has changed the way energy systems are designed, constructed and operated. The Centre for Intelligent Electricity Distribution (CINELDI - SINTEF) is currently working on solutions for the future energy system, and aims to "*facilitate renewable energy generation, electrification of transport and more efficient use of energy*" [21]. Figure 2.1 shows this smart energy system of the future, which is an interconnected system with two-sided communication [22]. This is also referred to as a smart grid.

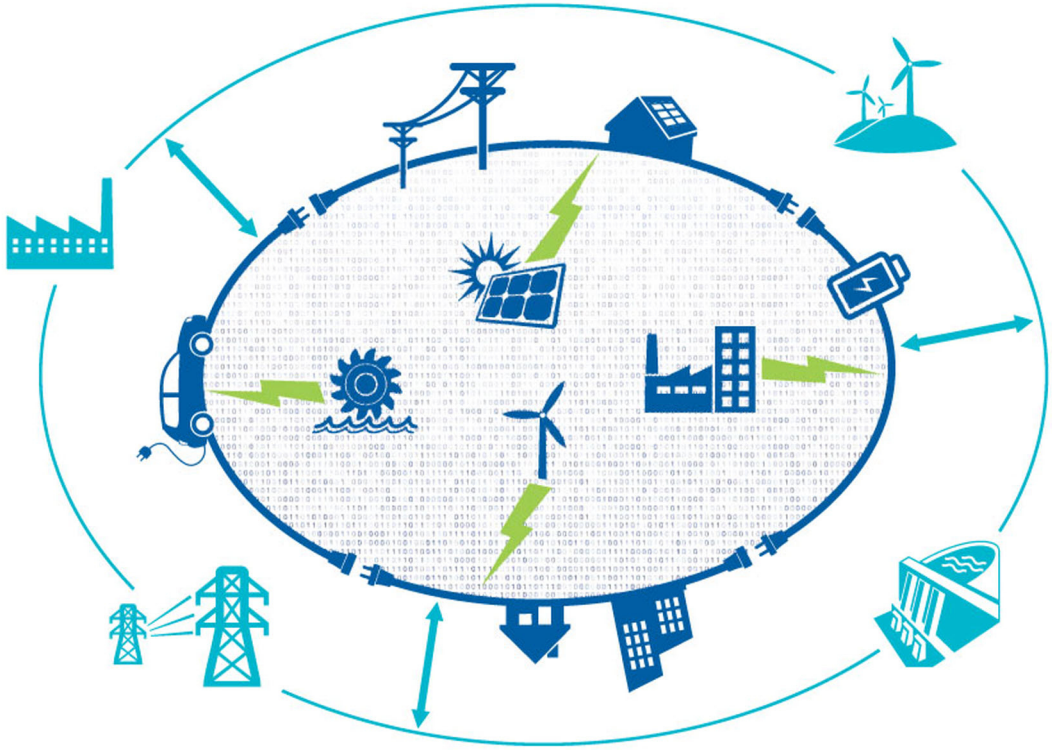

Figure 2.1: The smart energy system of the future [21].

Smart metering (AMS) is already implemented in all Norwegian households, which provides the opportunity to monitor energy consumption in real time. This is an important aspect of the future smart grid [22]. Furthermore, communication between suppliers and consumers makes the energy system more flexible. Consumers that produce their own energy locally, can transfer excess energy back to the grid (prosumers). Implementation of vehicle-to-grid strategies makes it possible for electric car owners to sell power to the grid whenever the car is parked.

As mentioned, demand response will be an important measure in future energy systems to maintain the instantaneous balance. The transition to a smarter energy system provides an opportunity to shift some of the responsibility to the demand side, where consumers adjust their power consumption according to the power generation. This could even out the energy prices during peak load hours, and even out the peak itself. Additionally, implementing batteries and other storage solutions in the system will contribute to maintaining the energy balance.

2.2 Energy planning models

Use of energy planning models is beneficial for making good investment decisions related to the development of the infrastructure, and for minimizing energy costs through identifying optimal solutions for energy generation and combination of energy carriers [23].

eTransport is an energy planning model developed by SINTEF Energy Research [23], which is used for local energy planning. It is designed to optimize load over a specified time period, based on minimizing the energy costs. Defined technology modules can be used as input to the model, which represents different energy sources, energy loads, forms of transport, technology for conversion/storage and more [24]. As of now, there is no module for building energy flexibility.

The load profiles used for representing the energy use of buildings in eTransport are based on historical data, and the only means is to cover this load. It is therefore desirable to formulate a module for building flexibility, which could realistically represent the flexible load of buildings [25]. In order to do so, the building energy flexibility needs to be characterized, and a simple model to represent buildings in energy system analysis is required. The first-order and second-order models developed in this thesis, are investigated for this reason. If the models are proven to accurately represent the thermal dynamics of the building, they can be used to formulate such a module.

By implementing a module for buildings, the flexible load can be included into the optimization of loads in energy systems. Even though eTransport is used as an example here, the results of this thesis can be used in any other energy planning model or energy system analysis.

Chapter 3

Theory

Knowledge about the thermal behaviour and thermal mass of buildings is essential to understand how buildings can be utilized for thermal energy storage, and it can also be used to formulate models to represent buildings in energy system analysis. The influence on thermal environment is an important factor to consider when evaluating the potential for energy flexibility in buildings, as it affects the thermal comfort. This chapter provides the theoretical background related to these concepts. Additionally, a literature review of how thermal comfort has been evaluated during thermal mass activation in previous studies, and commonly used modelling approaches for dynamic systems are presented.

3.1 Thermal behavior of buildings

The embedded thermal mass in buildings can be utilized for thermal energy storage, which is possible due to the transient thermal behaviour of buildings. The principles of heat transfer forms the basis of this behavior, and is also an important factor to consider when designing the building structure. Insulation levels are chosen according to climate conditions, and materials with high insulation properties are preferable to limit the heat loss. The material properties are also closely related to the ability to store heat, and the thermal inertia of buildings. For evaluation of thermal comfort, and to obtain a greater understanding of the building as a system, it is important to analyse the thermal energy balance. This chapter gives an introduction to some of the most important physical principles, laws and properties related to these concepts.

3.1.1 Principles of heat transfer

Heat transfer is the flow of thermal energy due to temperature differences in substances or between substances [26]. In building materials or building components, heat is mainly transferred by thermal conduction, convection and radiation. A simple representation of these principles are shown in figure 3.1.

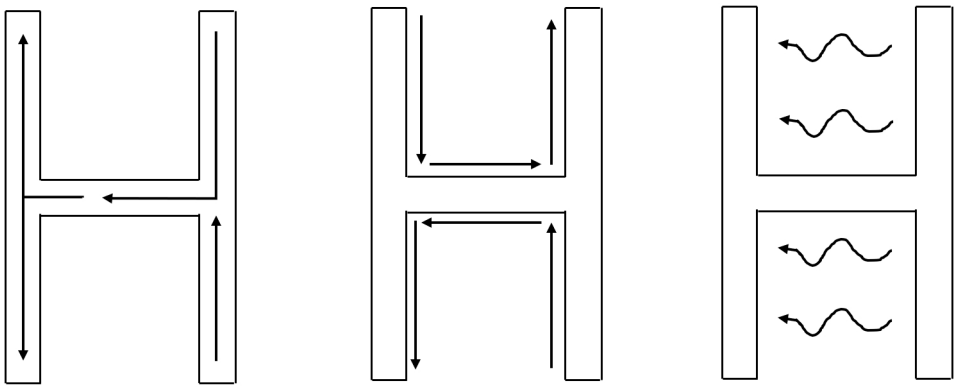

Figure 3.1: Principles of heat transfer. Adapted from [27].

Conduction

Energy transfer related to the interaction between particles of a substance is known as conduction. Collisions of molecules results in an energy exchange, where molecules with higher energy levels transfer some of their kinetic energy to molecules with lower energy levels. Whenever there is a temperature gradient present, heat transfer occurs by conduction [28]. This is described by Fourier's law, given in equation 3.1. The heat transfer rate per unit of area, also known as heat flux q (W/m^2), is proportional to the thermal conductivity λ (W/mK) and the temperature gradient dT/dx. The negative sign indicates that heat is transferred towards decreasing temperatures [26].

$$q = -\lambda \frac{dT}{dx} \tag{3.1}$$

Expressing conduction in terms of heat flow rate $\dot{Q}$ (W) through a surface A (m^2) yields equation 3.2.

$$\dot{Q} = qA = -A\lambda \frac{dT}{dx} \tag{3.2}$$

The thermal conductivity λ is a material property, which describes the ability to conduct heat. Materials with high conductivity conduct heat more easily, and the highest values are found in metals [28]. The conductivity of typical building materials are given in table 3.2 in Chapter 3.1.4.

Convection

Convection is a combination of energy transfer due to molecular interactions (heat conduction), and energy transfer due to the motion of a fluid. To illustrate, the surface of an exterior wall is constantly interacting with the surrounding outdoor air. In case of a temperature difference, heat transfer occurs in the boundary layer between the surface and air. Heat transfer by convection occurs when the air is in motion, and increases with higher air velocities. In close proximity to the wall, the velocity of air is zero due to the no-slip condition, and so the heat transfer occurs by conduction [28].

Heat transfer by convection is described by Newton's law of cooling, stating that the rate of heat loss from an object is proportional to the temperature difference between the object and its surroundings. In equation 3.3, the convective heat flux q_{conv} (W/m^2) is proportional to the difference between the surface temperature T_s (K) and the fluid temperature outside the boundary layer T_∞ (K) [26]. Equation 3.4 gives the convective heat flow rate Q_{conv} (W) through to a surface with area A (m^2).

$$q_{conv} = h_c(Ts - T_\infty) \tag{3.3}$$

$$\dot{Q}_{conv} = q_{conv}A = h_cA(Ts - T_\infty) \tag{3.4}$$

The convective heat rate transfer coefficient h_c (W/m^{2}K) is empirically determined depending on the properties of the fluid, geometry of the surface and the characteristic of the flow (laminar or turbulent). Furthermore, it depends on the driving force causing the motion of the fluid, which also characterizes the convection itself. Natural convection is associated with buoyancy driven flow, which occurs due to differences in temperature and density of the fluid. Forced convection is associated with flow driven by external forces such as wind or fans [26].

Radiation

All substances with a nonzero temperature emits electromagnetic radiation, which originates from movements of the molecules within the substance itself. The amount of radiation, its wavelength and the direction of the waves depends on the surface temperature. Higher temperatures yields shorter wavelengths. Solar radiation and the radiation from internal surfaces are examples of shortwave and longwave radiation respectively. Radiation can either be absorbed, transmitted through or reflected by materials [28].

3.1.2 Thermal resistance

Thermal resistance is analogous to electrical resistance, and is the ability to resist heat flow. To optimize the insulation properties of buildings, materials with high thermal resistance are thus preferable. Equation 3.5 is used to determine the thermal resistance R (m^2K/W), which depends on the thermal conductivity and thickness d (m^2) of a material.

$$R = \frac{d}{\lambda} \tag{3.5}$$

Figure 3.2 shows the temperature distribution in a typical wall structure under stationary conditions. The blue line represents the temperature, which increases through the different layers of materials moving from the outside to the inside of the wall. Each layer has a different conductivity λ and thickness d. Due to the temperature differences between the layers, heat is transferred by conduction.

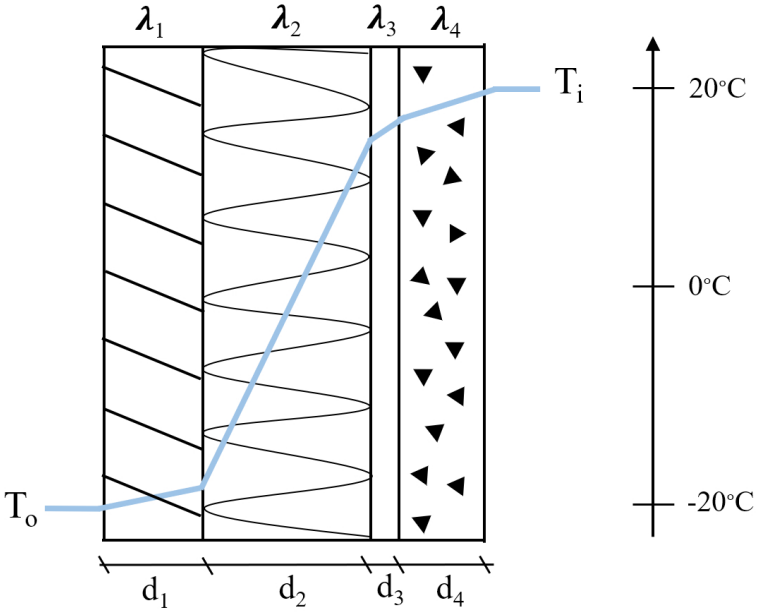

Figure 3.2: Temperature distribution in a typical wall structure under stationary conditions.

Using the electric circuits analogy, the thermal resistance of the layers equals electric resistances connected in series [28]. The total thermal resistance of the wall can thus be found using equation 3.6. Values of R_{so} and R_{si} are standardized in literature [29], made to represent the resistances of the outdoor and indoor surfaces respectively. Finally, the amount of heat flux transferred through the wall is given by equation 3.7, where T_i and T_o is the indoor and outdoor temperature respectively.

$$R_{tot} = R_{so} + \frac{d_1}{\lambda_1} + \frac{d_2}{\lambda_2} + \frac{d_3}{\lambda_3} + \frac{d_4}{\lambda_4} + R_{si} \tag{3.6}$$

$$q = \frac{T_i - T_o}{R_{tot}} \tag{3.7}$$

3.1.3 Thermal transmittance

Thermal transmittance, also known as the U-value, is used to describe the heat insulation properties of building components. Assuming one-dimensional flow and stationary conditions, the U-value can be defined as "*the heat transfer rate q through a building component when the air temperature difference across the component is 1 K*" [28]. This is shown in equation 3.8, where the thermal transmittance is denoted by U_{val} (W/m^{2}K).

$$U_{val} = \frac{q}{T_i - T_o} \tag{3.8}$$

By comparing this expression to equation 3.7, it follows that thermal transmittance can be defined as the inverse of the total thermal resistance. This is shown in equation 3.9.

$$U_{val} = \frac{1}{R_{tot}} \tag{3.9}$$

Based on the relation between U-values and the thermal resistance, it follows that low U-values are preferable. The U-value of building components determines how much heat is lost through the building envelope, and are thus closely related to the energy performance of buildings. Improving the U-values is an important measure to enhance the energy performance in new buildings and retrofit projects. This can be achieved by increasing the thickness of insulation in the envelope, and/or use materials with low conductivity. Additionally, well-insulated layered windows should be installed.

The Norwegian Building Acts and Regulation (TEK) provides general guidelines for energy efficiency measures, and minimum requirements for insulation properties in buildings. Both guidelines and requirements are continuously revised and updated, to comply with the most recent technology and research. Table 3.1 shows the requirements of U-values in building components from different issues of TEK, including TEK87, TEK10, TEK17 [30, 31, 32]. Additionally, the requirements for passive houses are given, which are found in the Norwegian standard NS 3700 [33].

Table 3.1: Requirements for U-values in different building regulations and standards.

Component	**U-values (W/m^{2}K)**		
	TEK87	**TEK10/TEK17**	**Passive House**
External wall	≤ 0.30	≤ 0.18	0.10 - 0.12
Roof	≤ 0.20	≤ 0.13	0.08 - 0.09
Floor	≤ 0.20	≤ 0.10	0.08
Windows	≤ 2.40	≤ 0.80	≤ 0.80

It is important to recognize that calculated U-values are related to some uncertainties, and may differ from the real U-value obtained in actual buildings. The assumptions concerning one-dimensional flow and stationary conditions are just simplifications of reality, and other external factors such as surface conditions and solar radiation may influence the real U-value. However, for calculations of energy demand, the estimated U-value will be sufficient [29].

3.1.4 Thermal capacitance

Thermal capacitance is a material property related to heat storage in building materials, and "*is an important characteristic for transient thermal behaviour*" [34]. In its simplest form thermal capacitance C (J/K) can be described by equation 3.10, where Q (J) is the amount of heat required to raise the temperature of an object by 1 K [35].

$$C = \frac{Q}{\Delta T} \tag{3.10}$$

Per unit mass, this is known as the specific heat capacity c (J/kgK), and is given by equation 3.11. It is defined as the amount of heat that 1 kg of a substance absorbs when the temperature is increased by 1 K (or the amount of heat released by a 1 K reduction) [28].

$$c = \frac{\Delta Q}{m \cdot \Delta T} \tag{3.11}$$

Materials with high specific heat capacity absorbs more energy for every unit change in temperature, and are thus preferable for heat storage. Defined values for the specific heat capacity of different building materials are given in Chapter 3.1.5. Note that these values are approximations based on average temperature conditions throughout the year [29]. The transient conditions in buildings are thus not reflected, but the defined values are useful to evaluate a materials ability to store heat.

When modelling the dynamics of thermal mass, it can be useful to combine the individual specific heat capacities of different building components into one lumped parameter C_{tot}. It has been argued that such lumped parameters are oversimplifying the heat storage ability of components, but using dynamic simulation tools to obtain numerical solutions of the model could provide sufficient estimates [34].

3.1.5 Thermal mass

Any mass within buildings that can be used for heat storage is defined as thermal mass [36], and concrete examples includes walls, floors and furniture. In order to achieve full utilization of thermal mass, it has to be placed correctly in the building structure, and be exposed to the indoor air [37, 38]. Whenever there is a temperature difference between thermal mass and indoor air, the thermal mass can absorb, store and release heat [39].

Materials defined by high specific heat capacity and high density ρ (kg/m^3) are preferable alternatives for thermal mass, as they enable storage of larger amounts of heat. Additionally, the thermal conductivity should be moderate. Materials with high conductivity will absorb and release heat to fast relatively to the daily cycle of the heating system [37]. Materials with low conductivity makes the process too slow. In both cases, this will cause unwanted temperature fluctuations in the indoor air.

The relation between specific heat capacity, density and thermal conductivity can be expressed by the thermal diffusivity, a (m^2/s), as shown in equation 3.12. This factor determines how fast a temperature change propagates in a material, and should preferably be high [39, 40].

$$a = \frac{\lambda}{c_p \cdot \rho} \tag{3.12}$$

Table 3.2 provides the thermal properties related to heat storage for some materials commonly used in buildings. Based on the presented values, concrete and brick satisfy the mentioned criteria and are thus suitable for heat storage. The specific heat capacity of wood and mineral wool are relatively high, but both the diffusivity and conduction is low. Heat will thus be absorbed/released too slow from these materials. On the contrary, steel has a very high thermal conduction, and so the heat will be absorbed/released too fast [38].

Table 3.2: Thermal properties related to heat storage in common building materials. Adapted from [40].

Material	**Density [kg/m^3]**	**Specific heat capacity [J/kgK]**	**Thermal conductivity [W/mK]**	**Thermal diffusivity [m^2/s]**
Steel	7800	500	55	$15 \cdot 10^{-6}$
Concrete	2300	950	1.7	$0.8 \cdot 10^{-6}$
Brick	1600	830	0.6	$0.5 \cdot 10^{-6}$
Wood	500	2800	0.14	$0.2 \cdot 10^{-6}$
Mineral wool	15-150	760	0.04	$0.3\text{-}3.3 \cdot 10^{-6}$

3.1.6 Building time constant

The thermal inertia of buildings is described by the time constant. In equation 3.13, the building time constant τ (h) is defined by the total thermal capacitance C (Wh/K) of the building, the convective heat loss coefficient and the area of which the heat is transferred through. The term hA can be replaced by U (W/K), defined as the overall heat transfer coefficient.

$$\tau = \frac{C}{hA} = \frac{C}{U} \tag{3.13}$$

The composition of the building structure, and the material properties described in Chapter 3.1.5 will influence the time constant. Buildings with brick or concrete structures are characterized as ”heavy-weight”, and are associated with the highest time constants (days/weeks). Buildings with a wooden structure are characterized as ”light-weight”, and are associated with lower time constants (hours/days). Which one is better depends on occupancy and the purpose of the building [41]. However, high thermal inertia is beneficial as it contributes to less temperature fluctuations within the building, and thus have a positive influence on the thermal comfort [39].

Figure 3.3 shows a scenario in which the time constant can be determined graphically. By introducing a sudden increase (step) in heat load at time zero, the indoor air temperature starts rising. Due to the resulting temperature difference between the air and exposed surfaces, heat is transferred to the surfaces by convection. The heat loss from the air to the thermal mass cause the increase in indoor temperature to slow down, and eventually reach equilibrium. The resulting tangent line of the step response and the equilibrium temperature determines the buildings time constant [42].

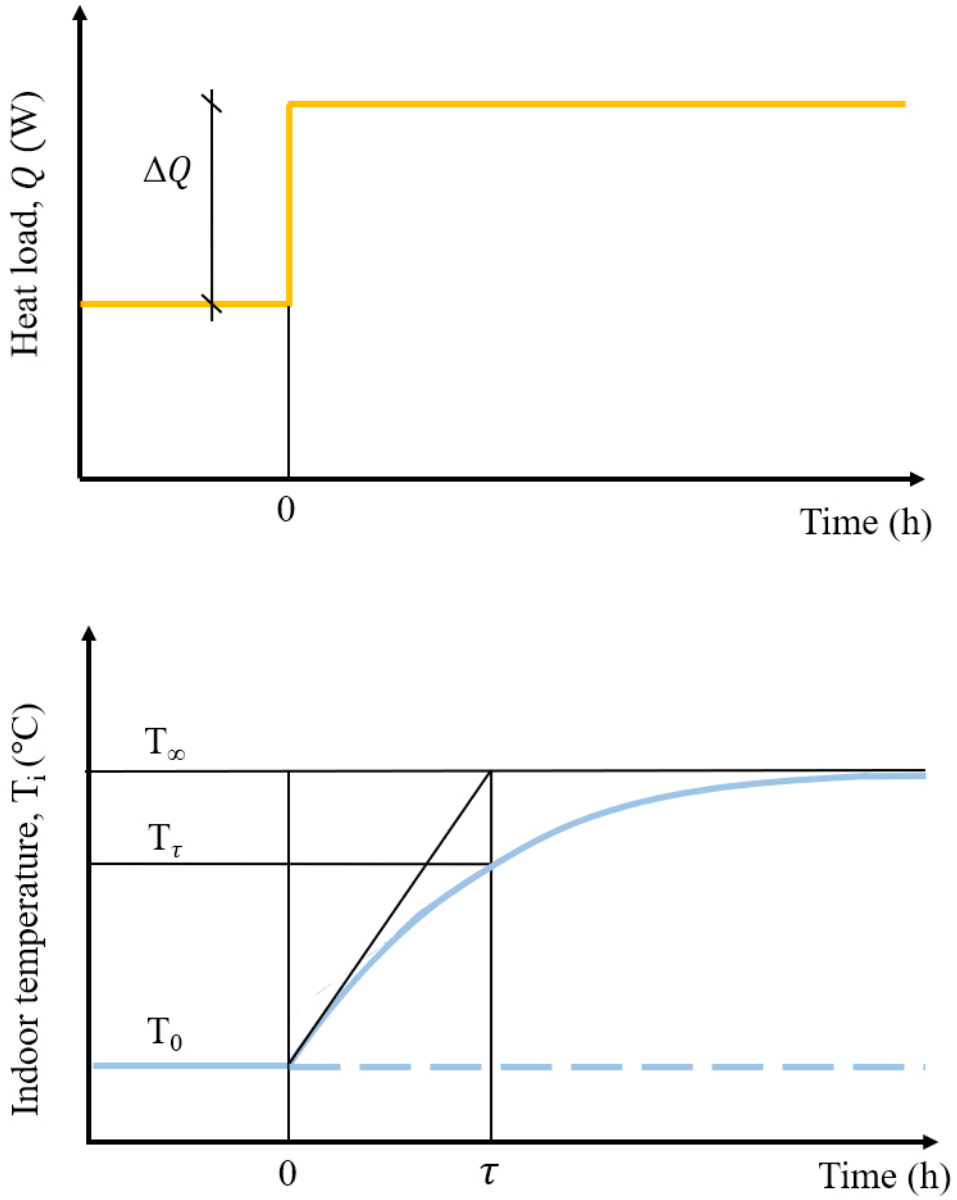

Figure 3.3: Change in indoor temperature due to sudden change in heat load. Adapted from [43].

3.1.7 Thermal energy balance in buildings

Analysing the thermal energy balance in buildings is important for the evaluation of thermal comfort, and for determining the total heat demand. Additionally, such analysis can be used to gain a better understanding of the building as a system.

The thermal balance is influenced by heat gains and heat losses related to the technical and physical processes within buildings. External factors such as weather conditions and occupant behaviour affects how the building is operated, and thus also the energy balance.

Heat gains

Space heating systems are the main supplier of heat in buildings. Electricity is the dominating energy carrier used for heating in Norwegian residential buildings, and the most used systems includes radiators, heat pumps and floor heating. The energy use related to electrical heating is approximately 54% of the total electricity consumption [14].

The point in which the average outdoor temperature drops below 11°C in the fall, marks the beginning of the Norwegian heating season. It then lasts until the temperature rises above 9°C in the spring. The duration of the heating season can however vary depending on the building insulation level [44]. Low insulated buildings are more exposed to outdoor temperature changes than high insulated buildings, and thus have a longer heating season.

Internal heat gains from people, lighting and technical equipment is another source of heating that should be included into the thermal energy balance of buildings. Normalised values are given in the energy calculation standard SN/TS 3031:2016 [45].

Finally, solar radiation could potentially be a substantial source of heating in buildings, especially if the building has large surfaces covered by windows. Usually some form of external shading are installed to avoid overheating during the summer.

Heat loss

Heat loss in buildings are mainly related to the heat transfer principles described in Chapter 3.1.1. Transmission loss is a form of conductive heat transfer, which occurs due to temperature differences over building components. It depends on the surface area and insulation properties of the individual components, and increases with higher ΔT. Thermal bridges are typical structures related to transmission loss. Infiltration loss is a form of natural convection, which occurs due to an air exchange through cracks and small openings in the building envelope. Ventilation loss is a form of forced convection, which depends on the amount of air exchange, the availability of installed heat recovery, and the temperature difference between the indoor and outdoor air [29].

Reducing heat loss will improve the energy performance of buildings, and thus reduce the energy demand. Assuring sufficient air tightness is crucial to limit infiltration loss, and transmission losses can be restricted by increasing the insulation level of the building envelope. Ventilation loss is desirable to some extent, and needed to sustain a sufficient indoor air quality. Installing energy efficient heat recovery will however reduce any unnecessary losses.

Thermal energy balance

In building physics, the energy conservation law is typically redefined for heat conservation within a control volume (CV) [29]. The inflow of heat Q_{in}, generated heat Q_{gen}, and the outflow of heat Q_{out} must equal the change in stored heat ΔQ_{st} within the CV over a certain period of time Δt. This is shown in equation 3.14, where the heat flows are measured in joules (J).

$$Q_{in} - Q_{out} + Q_{gen} = \Delta Q_{st} \tag{3.14}$$

Inserting the recently defined heat gains and heat loss found in buildings, yields the thermal energy balance in equation 3.15. The generated heat is represented by the space heating systems (Q_{sh}), and the internal heat gains (Q_{int}). Inflow of heat is defined as the solar radiation (Q_{solar}), and outflow as the transmission loss (Q_{trans}), infiltration loss (Q_{inf}) and ventilation loss (Q_{vent}). The stored heat ΔQ_{st} within in the CV represents the heat stored in the thermal mass.

$$Q_{solar} - Q_{trans} - Q_{inf} - Q_{vent} + Q_{sh} + Q_{int} = \Delta Q_{st} \tag{3.15}$$

Figure 3.4 illustrates a simple building model with a defined CV, where the defined heat flows related to the CV are included.

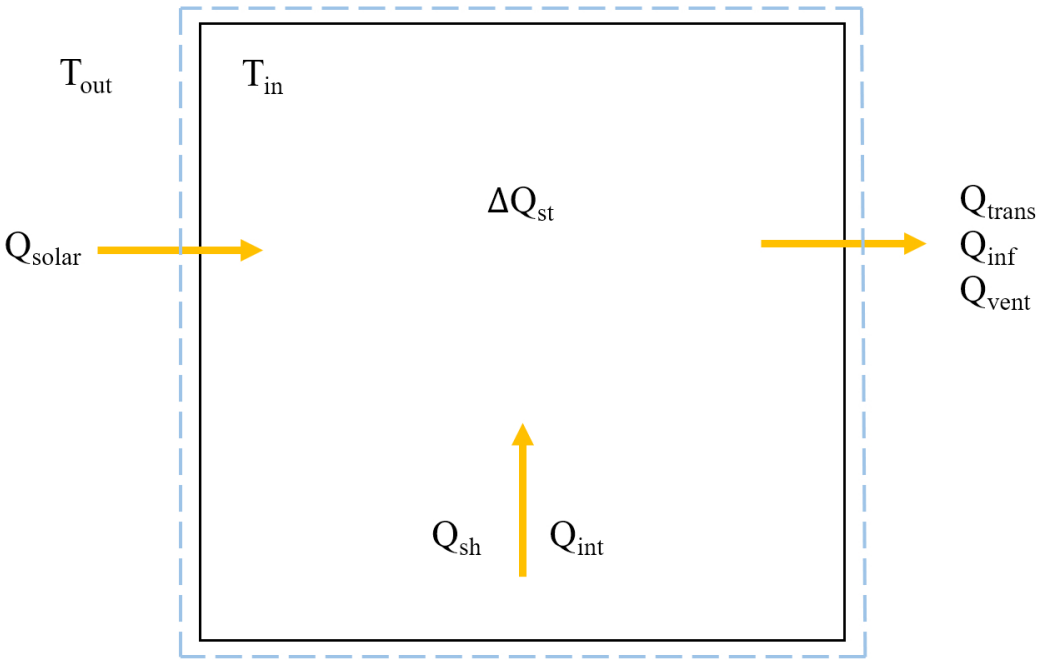

Figure 3.4: Heat flows in buildings with a defined control volume.

Expressing the thermal energy balance in terms of heat flow rates, measured in joules per second (J/S) or watt (W), yields equation 3.16.

$$\dot{Q}_{solar} - \dot{Q}_{trans} - \dot{Q}_{inf} - \dot{Q}_{vent} + \dot{Q}_{sh} + \dot{Q}_{int} = \frac{dQ_{st}}{dt} = \dot{Q}_{st} \tag{3.16}$$

Assuming that the indoor temperature T_i (K) is uniform within the control volume, the heat capacitance of the thermal mass and indoor air can be lumped into one parameter C (J/K). Hence, the stored heat can be described as in equation 3.17. The change in stored heat over a period of time $\dot{Q}_{st}$ (W) is shown in equation 3.18.

$$Q_{st} = CT_i \tag{3.17}$$

$$\dot{Q}_{st} = C\frac{dT_i}{dt} \tag{3.18}$$

Replacing $\dot{Q}_{st}$ in equation 3.16 with the relation from equation 3.18, the expression in equation 3.19 are obtained, which is a simple representation of the thermal energy balance in buildings.

$$\dot{Q}_{solar} - \dot{Q}_{trans} - \dot{Q}_{int} - \dot{Q}_{vent} + \dot{Q}_{sh} + \dot{Q}_{inf} = C\frac{dT_i}{dt} \tag{3.19}$$

3.2 Thermal energy storage

Thermal energy storage is accomplished by heating or cooling a storage media, and is useful when there is a need or beneficial to postpone energy use related to heating/cooling. Sensible and latent heat storage are two strategies of TES that can be applied in buildings. Sensible heat storage is defined as storing heat in liquids or solids, such as water tanks or building materials [46]. Latent heat storage is defined as storing heat in phase change materials (PCM), which can be implemented into wall surfaces and furniture [46, 47].

Utilizing thermal mass for TES is a form of sensible heat storage, and is the cheapest solution for storing energy as the thermal mass is already embedded into the building structure. It also provides the opportunity to shift heat load from peak hours to more favorable periods of the day. Figure 3.5 shows the different steps of TES, which is charging, storing and discharging.

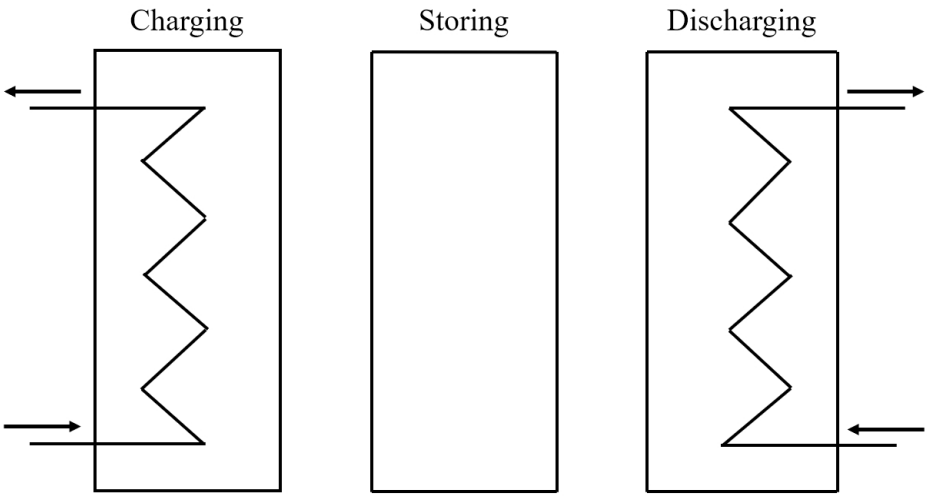

Figure 3.5: The steps of thermal energy storage. Adapted from [48].

In the charging phase, heat load is increased above the demand. This is equivalent to the scenario in figure 3.3 and the situation described in Chapter 3.1.6, where the surrounding surfaces absorbs heat due to a temperature difference. The heat is transferred further into the structure by conduction, and then stored in the thermal mass. In the discharging phase, heating load is decreased below the demand. The indoor temperature is thus reduced, and the stored heat will be released from the thermal mass to even out the temperature difference. This process of charging and discharging is also known as thermal mass activation (TMA), and an important prerequisite for using this approach is that occupants are willing to accept the changes in indoor temperature provoked by the TMA.

How long or how often the charging and discharging phases should be, depends on the material properties and the thermal inertia of the thermal mass [46, 39]. Peak load hours in buildings often occur in mornings and late afternoons, and this are the periods in which the discharging phase should be invoked. Charging of the thermal mass is usually referred to as pre-heating the building, and should be invoked a certain amount of time prior to the peak load hours depending on the mentioned properties of the thermal mass.

3.3 Thermal Environment

In addition to providing shelter from climate and weather conditions, it is required that modern buildings have technical systems that ensure a good indoor environment and thermal comfort for its occupants. Ventilation systems should provide a good indoor air quality by supplying fresh air and removing pollutants. Heating and cooling systems should sustain acceptable temperature levels. Considering the amount of time people spend inside buildings, the quality of the indoor environment is important to emphasise both during the planning process and operation of a building. Accordingly, several requirements regarding the indoor environment are stated in standards and building regulations.

Ensuring a good indoor environment is beneficial for several reasons. People in buildings with a bad indoor environment could often experience symptoms such as headaches, dizziness and skin irritations [40]. Failing to remove moisture from the air could lead to mold formation, which may cause both structural damages and health problems. Moreover, focus on having efficient technical systems to ensure a good indoor environment can reduce the energy use of buildings.

The thermal environment is one of the parameters affecting the indoor environment, in addition to the atmospheric, acoustic, actinic, aesthetic, psychosocial and mechanical environment [40]. Every parameter has an influence on the well-being of occupants, but the thermal environment is related to the thermal comfort.

3.3.1 Thermal comfort

Thermal comfort is defined as “the state of mind in which a person expresses satisfaction with the thermal environment” [40]. In simple terms this means that a person is thermally comfortable if not too warm or too cold. This balance is influenced by environmental and individual factors. Environmental factors include air temperature, mean radiant temperature, air velocity and relative humidity. Individual factors are generally related to the heat balance of the human body, and typically includes the activity level, clothing level, age, health and gender. Additionally, it is important to consider that local discomfort can occur even if the body as a whole is thermally neutral. Usually this could be caused by large variations in vertical temperature gradients, radiant asymmetry, cold floors or draft [40].

Each individual have their own experience and preference of the thermal environment, which from a general perspective makes it challenging to evaluate and predict thermal comfort. Standardized models for evaluating thermal comfort have thus been developed. The Fanger comfort model is a well recognized model based on the heat balance of the human body. From the indexes of predicted mean vote (PMV) and predictive percentage of dissatisfied (PPD), thermal comfort can be evaluated for an average group of people [49]. This model was developed based on steady state conditions, and considers people to be passive in relation to their environment. The willingness to adapt, typically by adding or removing pieces of clothing, is thus not acknowledged. Adaptive models were developed to account for these limitations of the Fanger model. Three main categories of adaption is described, in which the physiological adaption is related to the ability for acclimatization, psychological adaption is related to the expectations or former experiences of the thermal environment, and

behavioural adaption is the ability to take action to regulate thermal comfort. Generally, the thermal comfort of such models is evaluated based on the ”comfort temperature”, which is closely related to the outdoor temperature. A limitation of such models is that air velocity and air humidity are neglected [50].

3.3.2 Requirements for indoor temperature

The operative temperature is a combination of the air temperature and the mean radiant temperature, and is the temperature perceived by occupants. Thus, analysing the operative temperature gives a good indication of the thermal comfort in residential buildings. According to TEK17 [32], operative temperatures between 19-26°C are recommended for low activity levels. For the heating season specifically, operative temperatures between 20-24°C, or 22 $\pm$2°C, are recommended according to Sintef Byggforsk [49].

Large air temperature fluctuations over a short period of time are not preferable, as it may cause discomfort for the occupants. According to TEK17, the variation in air temperature over the course of one day should be limited to 4°C to avoid discomfort. More detailed requirements are given in ASHRAE 55-2004 [51], stating that the change in air temperature should be limited to 2.2°C and 3.3°C over one and four hours respectively.

3.4 Literature review

To gain some insight into the field of study relevant for this work, a literature review was conducted. The main purpose of the review was to study how thermal comfort previously has been evaluated during thermal mass activation.

Relevant studies were found by searching for key words such as thermal mass activation, demand response, building energy flexibility and thermal comfort. Additionally, literature reviews and reference lists in papers with related content was used as sources.

Studies regarding residential buildings in climates with a heating season were preferred, due to their similarities to this work. Five scientific journals were chosen for the literature review, which are shown in table 3.3.

Table 3.3: Scientific journals studied in the literature review.

Authors	Year	Title
J. Kensby, A. Trüschel J.O. Dalenbäck	2015	Potential of residential buildings as thermal energy storage in district heating systems – Results from a pilot test [52]
J. Le Dréau, P. Heiselberg	2016	Energy flexibility of residential buildings using short term heat storage in the thermal mass [9]
K. Zhang, M. Kummert	2018	Potential of building thermal mass for energy flexibility in residential buildings: a sensitivity analysis [11]
H. Wolisz, H. Harb, P. Matthes, R. Streblow, D. Müller	2013	Dynamic Simulation of thermal capacity and charging/discharging performance for sensible heat storage in building wall mass [53]
K. Foteninaki, R. Li, A. Heller, C. Rode	2018	Heating system energy flexibility of low-energy residential buildings [54]

It was found that thermal comfort evaluations were based on indoor temperatures, by introducing accepted limits or evaluating the time frame of which the temperatures changed. Additionally, the dynamic thermal behavior of buildings were studied by using building performance simulation tools. The study conducted by Kensby et al. [52] were the only study using measured data from a real building. Main aspects, scope and results of the studies are presented below.

1. Kensby et al.

Kensby et al. [52] studied the potential of using thermal mass as short-term TES to achieve more efficient heat generation in district heating systems. Five apartment blocks in Sweden were used in a pilot test, four in which was characterized as heavy-weight. The apartments were heated by water based radiators, and the supply water temperature was determined by the outdoor temperature.

The scope of the study was to identify the amount of storage that could be utilized without affecting the thermal comfort. The variation in indoor temperature was pointed out to be the limiting factor, and so it was measured and analyzed during the thermal mass activation. The charging and discharging periods were divided into nine hours, and then a period of three hours with normal operation made a total cycle of 21 hours. This would cause the individual periods to happen at different times each day, and made it possible to separate the variations due to the test from normal variations. Five different cycles were tested, in which the outdoor temperature signal was altered to initiate the charging and discharging periods. Data from a total of 19 weeks were used to obtain the results.

According to the test results, the heavy-weight buildings showed larger potential to be utilized for TES than the light-weight building. The average indoor temperature variation in the heavy-weight buildings was measured to ± 0.4°C or less during the testing period. Keeping this variation within ± 1°C was mentioned to be sufficient for sustaining thermal comfort, and so it was concluded that heavy-weight buildings were suitable for short-term TES.

2. Le Dréau & Heiselberg

Le Dréau and Heiselberg [9] conducted a study of two residential buildings in Denmark, to investigate the behaviour of thermal mass depending on insulation level, heating system and length of activation periods. Results from the study was used to propose control strategies to utilize the storage potential, taking energy use and thermal comfort into consideration.

Contrary to the study performed by Kensby et al., the activation periods in this study were separated. Instead of having subsequent periods of charging and discharging over several weeks, they were individually tested over periods of 2-24 hours. Initiating the charging and discharging periods were done by increasing and decreasing the set-point temperature respectively. Based on thermal comfort considerations, a temperature change of 2 K was chosen.

In the two buildings chosen for the study, both water based radiators and underfloor heating systems were evaluated. The first building, built in the 80s, was characterized by low insulation levels, and a time constant of 28 hours. It was found that activation periods between 2 and 6 hours would be preferable, as longer duration times could cause discomfort. The radiator caused more rapid changes in operative temperature than the underfloor heating, but the underfloor heating introduced a risk of overheating. In terms of activation method, it was found that discharging and charging would be most beneficial during the daytime and nighttime respectively.

The second building was characterized as a passive house, with high insulation levels, a time constant of 128 hours and a lower heating demand than the 80s house. The results showed

that the risk of overheating was high during charging periods, due to the well insulated walls and internal heat gains already contributing to increasing the temperature. Thus, the authors recommended to either avoid this strategy in such buildings, or use advanced controllers. Discharging with both radiators and underfloor heating showed promising results, and the thermal comfort was maintained. Additionally, the length of the activation periods could be longer without affecting comfort.

3. Zhang & Kummert

Based on a typical residential building in Canada, Zhang and Kummert [11] evaluated the energy flexibility by using thermal mass for TES. The building was characterized as light-weight, with a timber frame and brick exterior, and a time constant of 18 hours. Heat was distributed by a electric baseboard heating system.

Similar to the method used by Le Dréau and Heiselberg, the reference set-point temperature was changed by ± 2°C, and the activation periods were tested individually. Simulations for each day of the five months long heating season were conducted, and different lengths of the activation periods were tested. The authors found that 2-3 hours of activation was the best alternative to maintain thermal comfort.

In a sensitivity analysis of the energy flexibility, an increase of 2°C during the charging period was found to be preferable over an increase of 1°C. For the discharging period, a decrease of 2°C was only slightly better than a decrease of 1°C. The authors pointed this out as being interesting in cases where a decrease of 2°C would compromise the thermal comfort. However, due to the time constant, the temperature would decrease slowly and may not be of concern.

4. Henryk Wolisz et al.

Wolisz et al. [53] evaluated the thermal storage capacity of a German residential building, characterized by massive brick walls, concrete slab and insulation in the floors and roof only. Heat was supplied by a air-water heat pump, and distributed by a radiator system.

In order to separate the variations caused by the thermal storage from normal thermal variations, the authors neglected long wave solar radiation and elements inside buildings with their own thermal mass (furniture, flooring, fabrics). Based on an ambient temperature of 0°C, the set point temperature was defined to be 20°C.

Similar to studies 2 and 3 [9, 11], the activation periods were introduced by changing the set-point temperature of the heating system. However, the simulation approach was more similar to study 1 [52], in terms of having subsequent periods of overheating, cooling and normal operation. From a condition of steady state, two hours of overheating was followed by a week of normal operation, to discharge the thermal mass and again reach steady state conditions.

Considering that a set-point temperature of 20°C would give an operative temperature of about 19°C, the authors argued this to be an acceptable minimum temperature as it would provide a PPD of 65%. Moreover, it was proposed to introduce overheating in unoccupied

periods of the day, so that the low set-point of 20°C could function as a set-back temperature.

The overheating period caused an increase in temperature to 24.5°C, and thus an operative temperature of 22°C. With a PPD of 90%, this was considered to maintain thermal comfort. The upper limit of the air temperature was defined to be 25°C. Higher air temperatures could induce a greater difference between air and operative temperature, and eventually cause discomfort in terms of vertical temperature gradients. The radiant temperature from walls increased after the overheating period, which was beneficial for thermal comfort. During the discharging period this would cause the operative temperature to decrease more slowly. As the air temperature stabilized to set-point value, the operative temperature would cause a PPD of 80%.

5. Kyriaki Foteninaki et al.

Foteninaki et al. [54] evaluated the potential energy flexibility of using thermal mass for TES in Danish low-energy buildings, while still maintaining thermal comfort. One of the tested building types was a residential building, characterized as heavy-weight and well insulated. The heating was distributed by a water based radiator. Contrary to Wolisz et al., the internal thermal mass and solar radiation were included in this study.

The set-point temperature was defined to be 22°C. From simulating the reference case with a constant set-point temperature, the authors found that half of the supplied heat originated from a combination of solar radiation and internal gains. In order to sustain thermal comfort, the authors recommended to consider these factors before initiating activation periods in modern buildings.

Modification of set-point temperature was used to study the amount of energy that could be added or removed during activation periods. Based on thermal comfort standards, a change of ± 2°C in set-point temperature was introduced for the charging and discharging periods. Starting from the reference state of the building, the activation periods were individually tested.

The base case was defined to have charging and discharging periods of 8 hours, starting early in the morning. The ambient temperature was defined to represent a moderate winter day in Denmark. For the charging period, the maximum set-point temperature was obtained within 5 hours. In case of the discharging period, the set-point temperature did not reach the minimum value, due to the internal heat gains. The authors argued that this slow decrease in temperature was beneficial for thermal comfort. In situations where the heating load was removed completely, the building would maintain an acceptable temperature over 48 hours after the heating was shut off.

From the simulated results it was acknowledged that thermal comfort was one of the limiting factors of how much energy that could be added during activation periods. Similarly, the amount of energy reduction was dependent on the set-point temperature defined in the reference case.

3.5 Modelling approaches

Model formulation is an important part of the study and understanding of dynamic systems. It involves creating a mathematical model to represent the dynamic behaviour of a system, typically based on a set of differential equations [55]. By solving the equations, the characteristics of the system in terms of model parameters can be identified. The simplest models are based on first order differential equations, or dynamic linear equations. More complicated models are based on non linear differential equations [56].

It is evident from Chapter 3.1, that the thermal behaviour of buildings is influenced by several factors. Modelling of thermal mass could thus become quite complex. Different model formulations for representing thermal mass is found in literature, where the complexity of the models differ depending on the scope of the study. Some studies use simplified lumped parameters to describe the dynamic behaviour and thermal mass [57, 58], while others include detailed information of heat transfer and air flows [59]. It is also found that a distinction is made between including the thermal mass of furniture/internal components [59, 60, 61]. The numerical solutions are usually found by using dynamic simulation software, such as TRNSYS, EnergyPlus, Modelica and IDA ICE [9, 11, 53, 54].

Generally, the modelling approaches used to represent the building thermal mass can be divided into white box, grey box and black box models. Which of these approaches to use depends on the available information related to the physics describing the system. Figure 3.6 shows the general structure of such models. The mathematical relations between the input, parameters and output defines the model structure, and through dynamic simulation software the output is obtained [56].

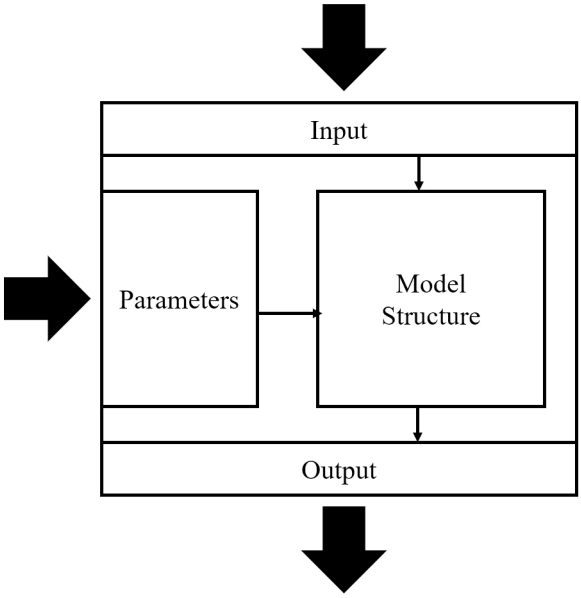

Figure 3.6: General structure of a model. Adapted from [62].

The modelling approach for white box, black box and grey box models are presented in the following. Main assumptions, applications, advantages and disadvantages of each approach are included, along with examples of related model types. Since the building thermal mass is best described through dynamic models, this will be the main focus.

3.5.1 White box models

White box models are based on the fundamental understanding of a particular system, and is characterized entirely by the equations related to physical laws. The most simple white box models are based on steady-state linear equations. Dynamic models are slightly more complicated as the parameters change with time, and the output are defined by various types of differential equations [56]. Perera et al. [59] used linear differential equations based on heat transfer to model the heat dynamics of a residential building, which was implemented into MATLAB to obtain the numerical solution. However, according to Li and You [5], the most common way of assessing building energy flexibility in terms of heating and thermal mass is by developing white box models in building simulation software.

In a literature review conducted by Foucquier et al. [63], the CFD approach (Computing Fluid dynamic), Zonal approach and the Multizone approach (Nodal approach) were presented as the main white box models used to describe the thermal behaviour in buildings. The basic idea of these models is to divide building zones into smaller parts, to obtain detailed information of the properties related to the defined space. The CFD approach is suitable for studying different flows within a zone, as each zone is divided into several control volumes with a uniform mesh. This method has the longest computational time of the three, but in return it provides far more detailed information. The zonal approach is derived from the CFD, but here one zone is divided into small cells. This provides local information of several parts of the zone, and give the opportunity of evaluating the temperature and pressure distribution. The computational time can however be long. Using the nodal approach reduces the computational time significantly, but has far less details than the other two methods. Here, each zone is divided into nodes. Based on the assumption that the zones are homogeneous, each node is described by unique state variables such as temperature and pressure. This method is thus suitable for estimating energy consumption.

One general advantage of using white box models is the understanding and valuable insight gained about the physics of the system. However, they are often related to long computational time for complex models, and sometimes the information needed to describe the physical processes of the model may not be available.

3.5.2 Black box models

Black box models can be used in cases where limited or no physical knowledge about the system is available. These models are entirely based on experimental data, often referred to as training data, and the system is defined by its inputs and outputs. What happens inside the model is unknown. For dynamic models, relevant parameters can be estimated using linear regression (less square method) or iterative methods [56].

In the context of building energy flexibility, Li and You [5] argued that black box models could be difficult to use due to limited available training data. They found that black box models were mainly used to predict energy performance, after sufficient data were obtained through building simulation software. Autoregressive model with exogenous inputs (ARX), and nonlinear autoregressive network with exogenous inputs (NARX) are examples of such black box models found in literature. In simple terms, these models predicts values based on previous outputs and inputs. Niu et al. [64] used ARX to predict the thermal load in

an industrial building, and the parameters were estimated using least square. Ferracuti et al. [65] compared the use of ARX and NARX to predict the short-term thermal behaviour of an office building connected to a district heating system. Real measured data from the building were used to identify the parameters, and both models demonstrated good predicting abilities.

The main advantage of black box models is the fast computation time. Contrary to white box models, no physical equations has to be solved, and thus heavy computation is avoided. The lack of insight into the physics is however a disadvantage with such models, and the results can not be interpreted in physical terms [63]. Sufficient training data is essential to get reliable results, and the precision of the model depends on the amount of data [66]. Even if large amounts of training data are available, the physical behavior of the system may not be reflected properly [58].

3.5.3 Grey box models

Grey box models are a combination of white box models and black box models, based on both physical laws and experimental data. Generally, physical laws is used to describe the model structure, and experimental data is used to identify the parameters [56]. Such models have less computational time than white box models, and some physical insight is available.

Low-order resistance–capacitance thermal networks (RC models) are suitable for describing building dynamics, due to the similarities between properties related to heat flow and those related to electric circuits. Although often used in relation to white box models [67], RC-models can advantageously be used in grey box modelling as it requires less physical information. Bidner and Thavlov [60] used RC modelling in a grey box approach to represent the heat flows in an office building.

RC-models represents the building thermal behaviour in terms of equivalent electric circuit variables, where R is the building resistance, C is the building capacitance, current represents heat flow, and nodal voltage represents a certain temperature [60, 68]. The equivalent circuit of a simple RC-model is shown in figure 3.7. This model can also be extended by adding more components, and thus increase the level of detail. The number of capacitance's determines the order of the model [66], and so the figure 3.7 illustrates a first-order model.

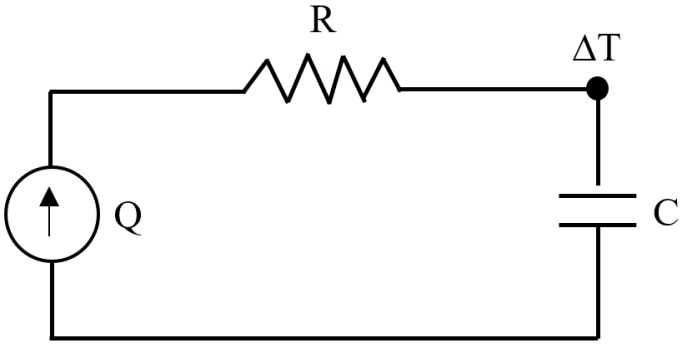

Figure 3.7: Electric circuit analogy to describe the thermal behaviour of buildings.

Chapter 4

Method

This chapter presents the different aspects of the method used to identify and characterize the demand flexibility related to thermal heat load in buildings. In order to describe the thermal dynamics of the building, two mathematical models are formulated. The related step response equations are derived, and an explanation of how to interpret the model parameters are given. Building performance simulation (BPS) is used to evaluate the energy flexibility potential in this thesis. A brief introduction to BPS and the chosen simulation software IDA ICE is given to explain why this is useful for studying the dynamic behaviour of buildings. The building model developed in IDA ICE to be used for the simulations are presented. Four variations of the building model are defined, and the related characteristics and input data is presented. Furthermore, the stages of the simulation approach is elaborated, and the procedure of identifying model parameters is described. To conclude this chapter, the simulation scenarios are introduced, along with related simplifications and a description of how thermal comfort is to be evaluated during thermal mass activation.

4.1 Model formulation

Using a grey box approach is considered to be the most suitable modelling approach in this thesis, as it enables both physical insight and interpretation of the system. The general structure of the models are formulated based on physical knowledge about the thermal behaviour in buildings, and the model parameters are identified by using a combination of IDA ICE and MATLAB. This will be further explained in Chapter 4.5.

Real buildings are non-linear systems, but for modelling purposes it is beneficial to assume that the thermal dynamics are linear [66]. In order to represent buildings in energy system analysis, simple modelling is also required. The simplest way of describing the thermal mass of buildings is to use a first-order model, which is based on the physical knowledge about the thermal energy balance. In this thesis, a model formulation for both a first-order and a second-order model is proposed. By identifying the related model parameters through derived step response equations, the demand flexibility can be characterised. The model formulations presented in the following subchapters was derived and provided by the supervisor of this thesis [69].

4.1.1 First-order model

The general structure of the first-order model is established based on the thermal energy balance defined in Chapter 3.1.7. Considering that the focus of this thesis is to study the deviation in indoor temperature, detailed descriptions of the thermal dynamics are neither interesting nor necessary. The model can thus be quite simplified.

The thermal energy balance in equation 3.19 requires a lot of information about the different heat flows in buildings. To simplify the expression, the total heat loss is described by Newton's law of cooling, introduced in Chapter 3.1.1. Here, the indoor temperature (T_i) represents the temperature of the object, and outdoor temperature (T_o) represent the temperature of the surroundings. Inserting this into the thermal balance yields equation 4.1. Note that the term hA is replaced with the overall heat transfer coefficient U (W/K).

$$C\frac{dT_i}{dt} = -U(T_i - T_o) + \dot{Q}_{sol} + \dot{Q}_{int} + \dot{Q}_{sh} \tag{4.1}$$

The next step is to incorporate the deviation in heating load and indoor temperature into the model, and so equations 4.2 and 4.3 are defined. The indoor temperature is a result of the reference temperature T_i^R and the change in temperature ΔT_i. The heat load is a result of the reference heat load $\dot{Q}_{heat}^R$ and the change in heat load $\Delta\dot{Q}_{heat}$. Inserting this into equation 4.1 gives the expression in equation 4.4.

$$T_i = T_i^R + \Delta T_i \tag{4.2}$$

$$\dot{Q}_{sh} = \dot{Q}_{sh}^R + \Delta\dot{Q}_{sh} \tag{4.3}$$

$$C\frac{dT_i^R}{dt} + C\frac{d\Delta T_i}{dt} = -U(T_i^R + \Delta T_i - T_o) + \dot{Q}_{sol} + \dot{Q}_{int} + \dot{Q}_{heat}^R + \Delta\dot{Q}_{sh} \tag{4.4}$$

The following assumptions and remarks are used to simplify the model further:

1. The step response of the indoor temperature are assumed to be independent of internal heat gains, solar radiation and outdoor temperature.
2. The reference indoor temperature (T_i^R) and reference heat load (Q_{sh}^R) are input values to the model.
3. The deviation in heat load is constant ($\Delta\dot{Q}_{sh} \rightarrow \Delta Q_{sh}$).

Finally, the model is reduced to the expression in equation 4.5. This is a linear, time continuous, first-order ordinary differential equation describing the thermal dynamics of buildings. The first part of the equation represents energy storage, which is equal to the storage losses ($U\Delta T_i$) and the heat in and out of the storage media (ΔQ_{sh}), which the thermal mass.

$$C\frac{d\Delta T_i}{dt} = -U\Delta T_i + \Delta Q_{sh} \tag{4.5}$$

Step response equation

Parameters are to be identified by introducing a step to the heat load ΔQ_{sh}, as shown in equation 4.6. Doing so introduces the possibility of creating a linear approximation for the indoor temperature change. Using Laplace transformation on equation 4.5 and rearranging it to represent the indoor temperature gives equations 4.7 and 4.8 respectively. Equation 4.9 is obtained by using Inverse Laplace transform. This is the step response equation for the first-order model, which can be used to identify the model parameters U, C and τ.

$$\Delta Q_{sh} = \Delta Q \delta(t) \tag{4.6}$$

$$(sC + U)\Delta T_i(s) = \frac{\Delta Q}{s} \tag{4.7}$$

$$\Delta T_i(s) = \frac{\Delta Q}{s(sC + U)} \tag{4.8}$$

$$\Delta T_i(t) = \frac{\Delta Q}{U}(1 - e^{(-U/C)t}) \tag{4.9}$$

When time equals zero (t=0), equation 4.9 gives a deviation in indoor temperature of zero. When the time approaches infinity (t=∞), the equation is reduced to $\Delta Q/U$. When a sudden change in heat load is introduced, the indoor temperature rises until the heat loss to the surfaces equals the change in heat load. This is shown in figure 4.1. The deviation in heating load, ΔQ and the deviation in indoor temperature, ΔT_i, are obtained from the dynamic simulations, and so the overall heat transfer coefficient can be determined. The resulting time constant of the building and equation 3.13 can be used to determine the thermal capacitance.

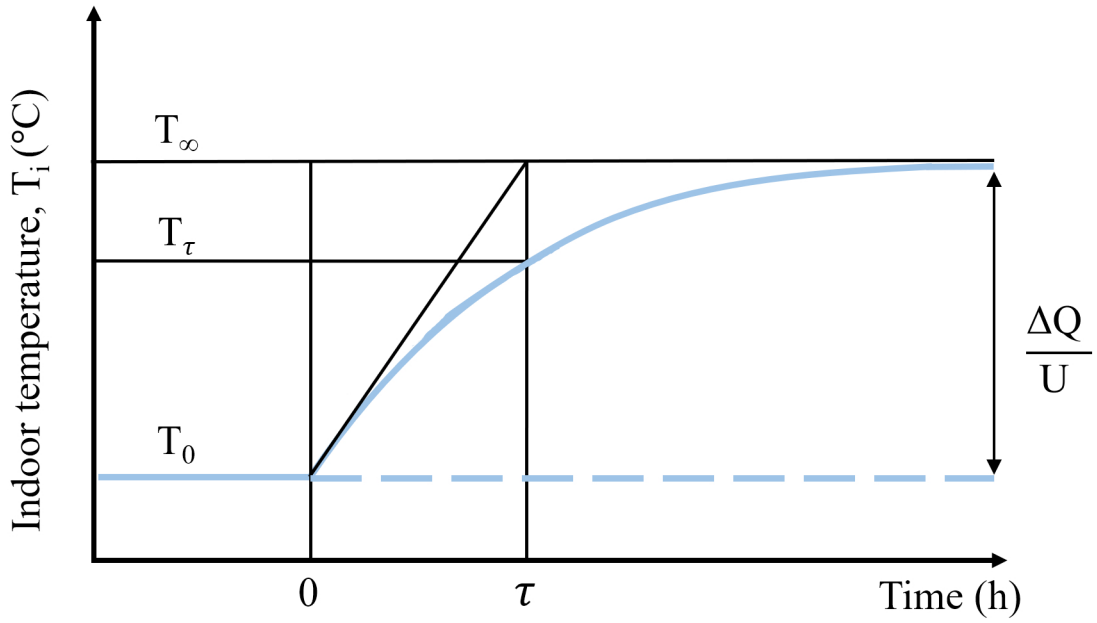

Figure 4.1: Identification of the parameters.

4.1.2 Second-order model

The mathematical formulation of the second-order model is complicated to derive, and will not be included in this thesis. It is based on the concept of representing thermal mass by a second-order RC model, with two resistances and two capacitances [69]. This is similar to the approach used by Yu et al. [66].

Parameters of the second-order model includes the overall heat transfer coefficient U, and the two time constants τ_1 and τ_2. Having two time constants makes it possible to account for both the fast and slow dynamics of the building. The first time constant describes the initial response to the step (fast dynamics), while the second time constant describes the response over a longer period of time (slow dynamics) [70].

Equation 4.10 presents the step response equation for the second-order model. Based on the relationship between coefficients α_1 and α_2 shown in equation 4.11, the step response can be altered to the expression given in equation 4.12. Here, α_1 is a weighting factor between the two time constants.

$$\Delta T_i(t) = \frac{\Delta Q}{U}(1 - \alpha_1 e^{-t/\tau_1} - \alpha_2 e^{-t/\tau_2}) \tag{4.10}$$

$$\alpha_1 + \alpha_2 = 1 \tag{4.11}$$

$$\Delta T_i(t) = \frac{\Delta Q}{U}(1 - \alpha_1 e^{-t/\tau_1} - ((1 - \alpha_1) e^{-t/\tau_2})) \tag{4.12}$$

4.2 Building performance simulation

Due to the complexity of buildings and their technical systems, using Building Performance Simulation is advantageous in order to make the best design decisions. The following definition of BPS is given in [71]:

"*Computational building performance modeling and simulation [...] is multi-disciplinary, problem-oriented and wide(r) in scope. It assumes dynamic (and continuous in time) boundary conditions, and is normally based on numerical methods that aim to provide an approximate solution of a realistic model of complexity in the real world.*"

The process of testing and evaluating the performance of building models is shown in figure 4.2. First step is to define a simplified model of the real case, and testing it based on certain performance criteria. Through analysing the simulation results, model parameters can be identified, and the overall performance can be evaluated against the set criteria. If these do not correlate in a sufficient way, changes are done to the model and the process is repeated. However, achieving a high performance in multiple categories is often challenging. As an example, high performance in energy efficiency may affect the thermal comfort, and a trade off may be considered [72].

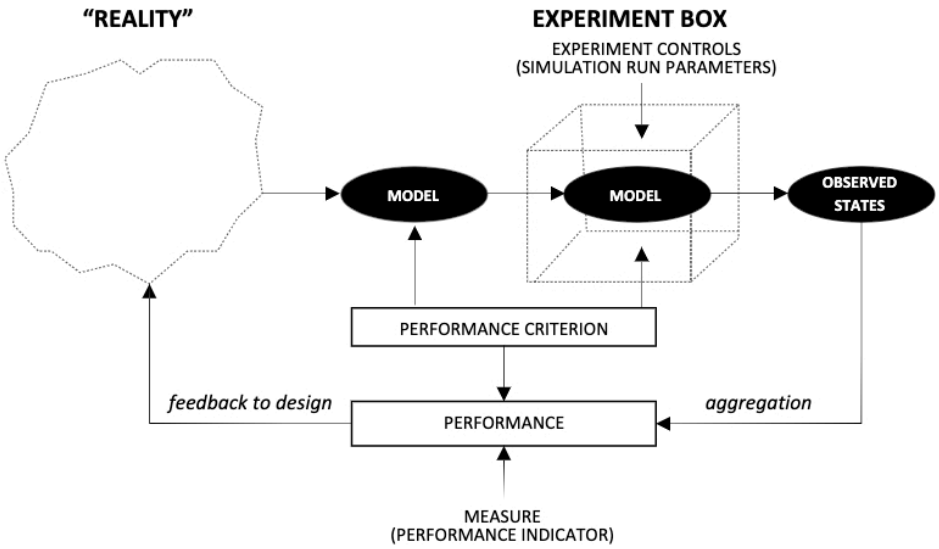

Figure 4.2: Process of testing the building performance. Figure obtained from [73].

It is important to recognize that the simulation results are only as good as the input data provided by the user. Accordingly, creating a model with well-defined parameters is crucial. BPS usually gives a good indication of the performance, but the results should be analysed carefully. Final design decisions should be rationally taken based on the results. Moreover, the best simulated case may not always be fully achievable in practice.

4.2.1 IDA Indoor Climate and Energy

IDA Indoor Climate and Energy (IDA ICE) is a dynamic multi-zone simulation software developed by EQUA Simulation AB, used for Building Performance Simulations (BPS) [74]. It enables users to model both simple and more complex buildings, and is flexible in terms of providing several options for user defined input. Construction materials, internal zoning, climate parameters, HVAC-systems, controllers, operation schedules and internal gains is just some of the available features that can be defined. The software also provides 3D view of the building model throughout the entire development process, which makes it easy to detect possible flaws in the design.

The simulation of the building model can be defined to focus only on certain aspects (heating, cooling, energy), or the building as a whole. A custom simulation with dynamic startup can be used to perform simulations for a specific period of time. This option requires the user to define a startup phase, which is an initialization phase simulated prior to the main simulation. The duration of the startup phase depends on how the building is characterized, where light-weight buildings require a shorter startup phase than heavy-weight buildings. Two weeks is however recommended to be sufficient in most cases [75].

Detailed results related to energy consumption and thermal indoor environment are provided for both the entire building and the individual zones. Both numerical values and graphs related to temperatures, air flows, heat flows and so on are provided for each zone. All this information gives an indication of the strengths and weaknesses of the modelling. If needed, measures can be taken to further improve the model and modelling inputs.

In the context of this thesis, IDA ICE is a suitable choice due to its ability to account for the detailed dynamics of a building, and the amount of information that is provided from the simulations. The custom simulation option enables each month of the heating season to be analysed individually. Moreover, the controllers in IDA ICE can be defined to take input from sources outside the software. This provides the opportunity to modify heat load in MATLAB.

4.3 Simulation model

In relation to the Zero Emission Neighborhoods project FME ZEN [76], Rønneseth and Sartori [77] developed several building models in IDA ICE to study the heating demand of Norwegian single-family houses (SFH). Each model represents an average building from a specific time period, where materials and U-values were chosen based on data from the IEE project TABULA [78]. Additionally, two variations of each model were made to represent different levels of energy performance; initial build and standard renovation. The building size, building body and internal structure were however kept the same for all models, as a general framework. Procedures for developing the models and their specifications are presented in the ZEN memo No 10; "Method for modelling Norwegian Single-family houses in IDA ICE" [77].

The building model used for the simulations in this thesis are based on the general framework made by Rønneseth and Sartori. Additionally, three of the model variations are used as a reference for the model variations defined in this thesis.

4.3.1 Model variations

Four different variations of the building model are made to study how the indoor temperature and model parameters are influenced by different insulation levels and energy performance. The first model variation is defined according to TEK87, and represents a low insulated building. The remaining three variations are defined according to more recent standards and regulations, including TEK10, TEK17 and the passive house standard. These model variations represents high insulated buildings.

Even though the requirements related to energy efficiency are practically the same in TEK10 and TEK17, a distinction is made to represent a middle ground in terms of energy performance. The insulation levels of the TEK10 model is defined similarly to the TEK17 model, but more losses through the building envelope is introduced due to a higher infiltration rate, lower efficiency for the ventilation system and lower insulated windows. This is further explained in Appendix A.

The SFH-05 model from the ZEN memo [77] represents residential buildings from 1991-2000, and the SFH-07 model represents residential buildings built after 2010. These are used as references for the model variations in this thesis:

- The TEK87 model is based on SH-05, variation 1
- The TEK10 model is to some extent based on SH-07, variation 1
- The TEK17 model is to some extent based on SH-07, variation 1
- The passive house model is based on SH-07, variation 2

4.3.2 Characteristics and input data

Considering that the main focus is to study the deviation in indoor temperature, the building model can be quite simple. However, it has to be realistic enough to provide meaningful results. Another important factor is to make sure that the system is kept constant during the simulations, to avoid any irregularities influencing the results. Certain building controllers are either defined to be constant, or removed from the system.

Some of the characteristics from the reference models are kept as is, and some alterations are introduced to adapt the models to the objective of this work. The general framework is kept the same for all variations, along with climate data and internal heat gains. Defined characteristics of the building model and the input data for the different model variations are presented in the following subchapters.

Climate and weather data

Energy use related to space heating is highly dependent on the outdoor temperature, which often differ every year. It is thus important that the weather data used in the simulations reflects the average trend, and are accurate in order to provide reliable results. The weather file used in IDA ICE is an IWEC-file for Fornebu in Oslo, retrieved from EnergyPlus [79]. This file includes temperature, wind speed, solar radiation and relative humidity for the chosen location. The year of 2015 is chosen as a basis for the simulations, and table 4.1 presents the related weather data in IDA ICE.

Table 4.1: Weather data for Oslo, Fornebu from the year of 2015. Obtained from EnergyPlus, and loaded into IDA ICE.

	Variables						
%	Dry-bulb temp °C	Rel humidity of air %	Direct normal rad W/m^2	Diffuse rad on hor surf W/m^2	Wind speed, x-comp m/s	Wind speed, y-comp m/s	Cloudiness
Jan	-7.2	85.3	59.0	9.0	0.1	-0.4	56.3
Feb	-4.9	81.0	103.7	24.feb	0.5	-0.3	57.6
Mar	-1.8	77.1	154.3	51.1	0.1	1.3	55.2
Apr	2.8	73.6	133.3	87.8	-0.5	-0.3	63.1
May	10.6	56.9	201.1	115.2	0.1	-0.8	59.1
Jun	13.2	65.0	183.2	133.6	0.2	0.6	64.5
Jul	15.6	67.6	185.5	125.4	0.2	-1.0	60.8
Aug	14.8	74.4	152.8	100.7	-0.6	-0.6	64.7
Sept	9.8	77.0	121.1	65.3	-0.2	0.5	62.7
Oct	4.9	85.8	101.2	32.8	-0.4	0.9	59.0
Nov	0.7	87.7	63.2	13.4	-0.3	1.4	63.1
Dec	-3.2	93.5	37.4	6.3	0.0	0.3	60.5
mean	4.6	77.1	124.8	63.9	-0.1	0.1	60.5
min	-7.2	56.9	37.4	6.3	-0.6	-1.0	55.2
max	15.6	93.5	201.1	133.6	0.5	1.4	64.7

Building envelope

The building has a simple geometry, with a rectangular shape and a flat roof. This design is beneficial for minimizing heat transfer, as it gives the lowest surface area. Avoiding complicated constructional details also reduce the number of thermal bridges and the risk of air leakages [80]. The building envelope is characterized by a wooden frame, with insulation levels according to the requirements given in Chapter 3.1.3. Floors are defined according to the reference model (concrete slab), and is the same for all model variations. Detailed information about material choices, structural composition, related U-values and other envelope characteristics are given in Appendix A. Figure 4.3 shows the complete model in IDA ICE. Note that shading objects are included to represent surrounding buildings.

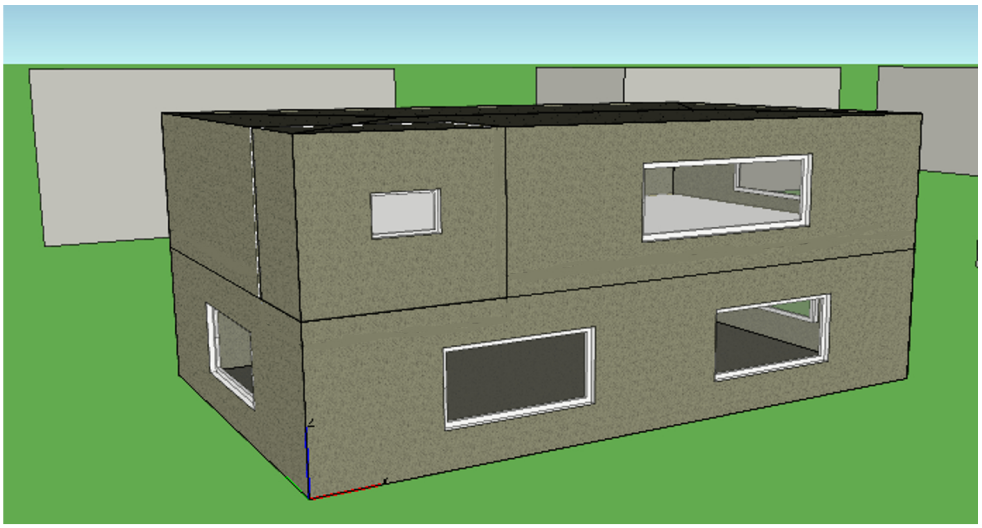

Figure 4.3: Screenshot of the building model in IDA ICE.

Windows are placed on all sides of the building to ensure daylight access. In order to make the model more realistic, the amount of windows and their size are altered from the reference model. The area ratio of windows relatively to the usable heated floor area (BRA) is calculated to be 20 %, which satisfies the requirement of TEK17 [32]. External blinds are installed, but defined to be ”always open” for each zone except for the bathroom, where it is defined as ”always closed” for privacy reasons. To compensate for the direct solar radiation, a recess depth of 0.1 m is introduced for all windows [81].

Zoning

The first floor is defined to be one large zone, functioning as a combined living room, kitchen and entrance. This zone will be referred to as the living room, and is shown in figure 4.4a. The second floor consist of two zones, including a bathroom and a bedroom. This is shown in figure 4.4b. The size of the bathroom is reduced from the reference model to be more realistic, and is defined according to the approved examples of bathrooms given in Sintef Byggforsk [82].

Defined area sizes of the three zones and general data related to the building size are summarized in table 4.2.

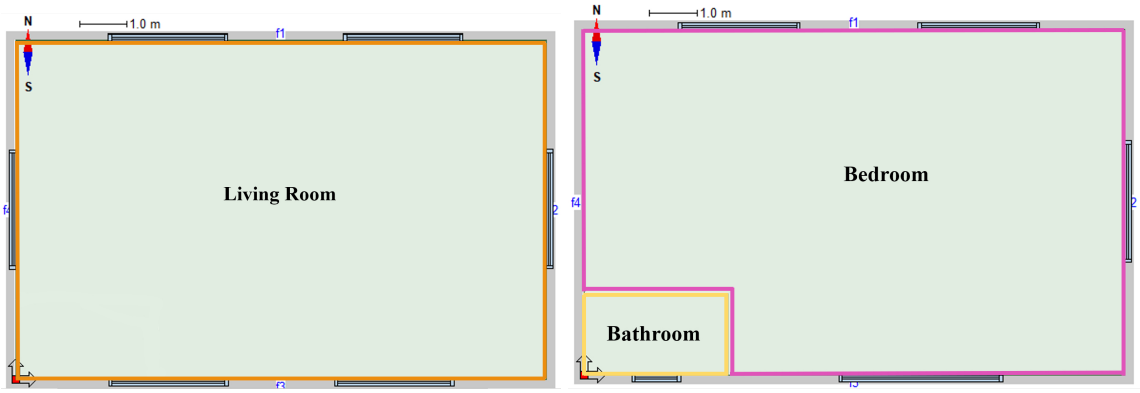

(a) 1st floor. **(b)** 2nd floor.

Figure 4.4: Floor plan of the building model in IDA ICE.

Table 4.2: General data related to the building model in IDA ICE.

Data	Value
Total area	162.3 m^2
Floor area	81.18 m^2
Area of Living room	81.18 m^2
Area of Bedroom	76.21 m^2
Area of bathroom	5.10 m^2
Number of floors	2
Footprint	11.3x7.2 m
Net ceiling height on each floor	2.4 m
Total height of the building	5.12 m

Heating System

All zones have electrical heating systems. Table 4.3 specify the type of heating system and set-point temperature defined for each zone, where the temperatures are retrieved from the ZEN memo [77]. PI controllers are used to regulate the power output of the heating systems, and customized to provide output data from the building model. This is further explained in Chapter 4.4.1.

Table 4.3: Heating system properties for each zone.

Zone	Set-point temperature (°C)	Supply system
Living room	22	Ideal heater
Bedroom	18	Ideal heater
Bathroom	24	Floor heating

Sizing of the heating system in each model variation is done by conducting heat load simulations in IDA ICE. The internal heat gains and solar radiation are excluded from this simulation, and a fixed ambient temperature at -20°C is chosen. The obtained values for nominal power P_n related to the zones in each model variation is shown in table 4.4.

Table 4.4: Values of nominal power P_n (W) related to the zones in each model variation.

	Nominal power (W)			
Zone	**TEK87**	**TEK10**	**TEK17**	**Passive**
Living room	4436	1903	1903	1567
Bedroom	3778	1615	1615	1159
Bathroom	1130	185.5	185.8	527.1

Ventilation and AHU

Balanced ventilation is used to ensure sufficient indoor air quality in the building, and air flow rates are defined according to TEK17 [32] for all model variations. Heat recovery is included for the high insulated models only. Table 4.5 presents the defined air flow rate, specific fan power (SFP) and heat exchanger efficiency for each model variation.

Table 4.5: Ventilation characteristics for each model variation.

Parameter	**Unit**	**Model values**			
		TEK87	**TEK10**	**TEK17**	**Passive**
Supply/return rate	m^3/m^2h	1.2	1.2	1.2	1.2
SFP factor	kW/m^2s	-	2.5	1.5	1.5
Heat exchanger efficiency	%	-	70	80	85

Modifications are made to the air handling unit (AHU) to make its behaviour close to linear. The set-point for supply air temperature is defined to be constant at 40°C, to keep the efficiency of the heat recovery constant. Additionally, heating and cooling coils are deactivated.

Internal Heat Gains

Internal heat gains are defined according to SN/TS 3031:2016 [45]. It is assumed that 100% of the energy from people and lighting are converted into heat, and 60% for equipment. Note that domestic hot water is not included in the building model.

Occupancy, activity level and clothing level are presented in table 4.6. Introducing limits for the clothing level allows IDA ICE to automatically adjust and adapt it to obtain thermal comfort.

Table 4.6: Occupancy, activity level and clothing level defined for each zone.

Zone	**Number of occupants**	**Activity level met**	**Clothing level clo**
Living room	1.16	1.0	0.85 $\pm$0.25
Bedroom	0.83	1.0	0.85 $\pm$0.25
Bathroom	0.35	1.0	0.85 $\pm$0.25

4.4 Simulation approach

The simulation approach used to determine the allowable deviation from a reference heat load, and to study the deviation in indoor temperature, is presented in this chapter. Dynamic simulations of the reference model and modification of its heat load was conducted in subsequent steps by using a combination of IDA ICE and MATLAB. The complete simulation approach is shown in figure 4.5, where each stage is presented as elements in a block diagram. Note that P (W) represents space heating power.

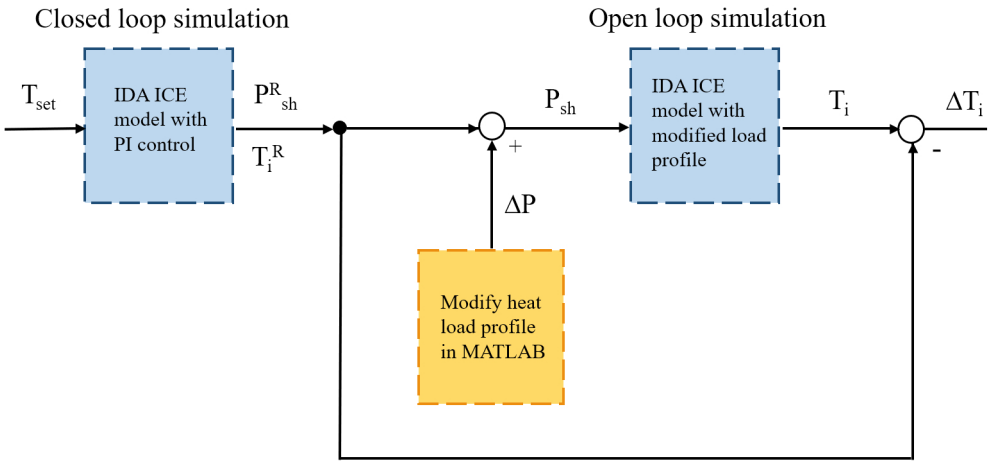

Figure 4.5: Block diagram of the simulation approach.

The different stages of the simulation approach can be summarized as follows:

1. Run a simulation of the building model in IDA ICE with the defined set-point temperatures (T_{set}). This is referred to as the closed loop simulation, where reference indoor temperatures (T_i^R) and reference heating power (P_{sh}^R) are obtained.
2. Modify the heat load profile in MATLAB, by introducing a step (ΔP).
3. Insert the modified heat load profile back into IDA ICE, and run a second simulation. This is referred to as the open loop simulation, where the indoor temperature (T_i) is obtained.
4. Compare the temperature (T_i) from the open loop, and the reference temperature (T_i^R) from the closed loop to obtain the deviation in indoor temperature (ΔT_i) in MATLAB.
5. Repeat the process from step 2, until a satisfactory result is obtained for the deviation in indoor temperature. The allowable deviation in heating load (ΔP) is then established.

The MATLAB script used in the simulation approach is given in Appendix B. An elaboration of the different stages is presented in the following subchapters.

4.4.1 Closed loop simulation

The first stage of the simulation approach is to establish the reference case in IDA ICE, based on the set-point temperatures and nominal power values defined in Chapter 4.3. To provide output from the model, a customized PI controller were defined as shown in figure 4.6.

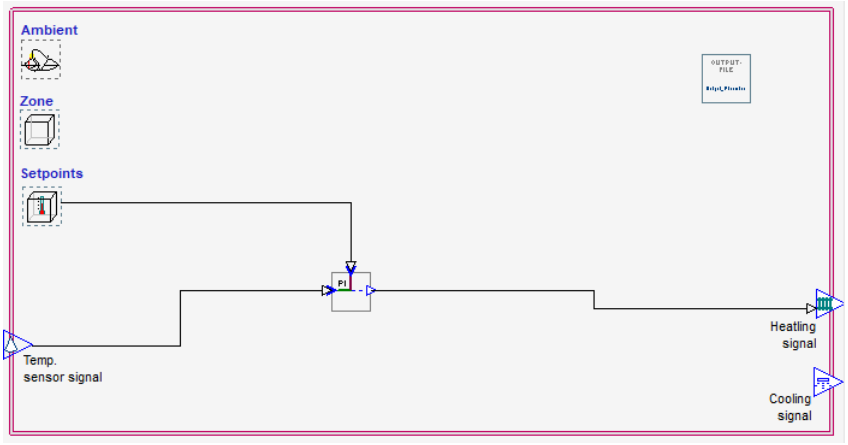

Figure 4.6: Screenshot of the PI controller in IDA ICE, closed loop simulation.

Inputs to the PI controller are defined as the real temperature value obtained by a zone sensor, and the temperature set-point defined for the zone. In case of a deviation between the set-point and the real temperature, the PI controller sends a signal to the heating system to correct it. This signal is a value between 0 and 1, which implies no power and maximum power respectively (maximum power equals the nominal power). Hence, the provided output is a list of signals for each time step defined in IDA ICE. To get a detailed list of outputs, the time step is defined to be 0.1 hour (every sixth minute).

The closed loop simulation is performed by using the custom simulation option, with a dynamic startup phase. The following guidelines are defined for the duration of the initialization and main simulation period:

- The initialization phase is set to 1 month in all model variations.
- For the low insulated model (TEK87), the main simulation period is set between 1 and 1.5 months.
- For the high insulated models, the main simulation period is set between 2 and 2.5 months.

Provided output from the simulation includes lists of indoor temperatures and space heating signals for each zone, according to the defined duration of simulation and time step. The elements in the list of temperatures are denoted as the reference indoor temperatures (T_i^R).

4.4.2 Modification of heat load profile

The second stage of the simulation approach is to modify the reference heat load profile obtained from the closed loop simulation. The list of power signals from a zone is imported into MATLAB, and changed into real values by multiplying each element with the nominal power P_n defined for this zone. The new list represents the reference heat load profile, and the elements of the list are denoted as the reference space heating power (P_{sh}^R).

Modification of the heat load profile is done by introducing a step, in which a constant value is added to or subtracted from each element P_{sh}^R. This value corresponds to the deviation in heat load ΔP. To indicate the point in the list where the step should be introduced from, a *start step* is defined in the MATLAB script. This is determined based on the potential for increasing/decreasing the reference heat load profile, and represents a particular date of the month. Values of P_{sh}^R prior to this start step remains unchanged.

The amplitude of the step can be determined graphically, by investigating the plotted graph of the reference heat load profile. The following restriction is introduced;

$$(P_{sh}^R \pm \Delta P) \in [0, P_n]$$

Figure 4.7 shows the reference heat load profile for January, obtained for the living room in the TEK87 model. The nominal power is defined in Chapter 4.3.2 to be 4436 W. Generally, by increasing the heating power ($P_{sh}^R + \Delta P$) the graph will shift upwards, and by decreasing the heating power (P_{sh}^R - ΔP) the graph will shift downwards. Based on the defined restriction, no points of the graph can exceed the value of 4436 when the graph is shifted upwards (indicated with a black line), or fall below 0 when the graph is shifted downwards.

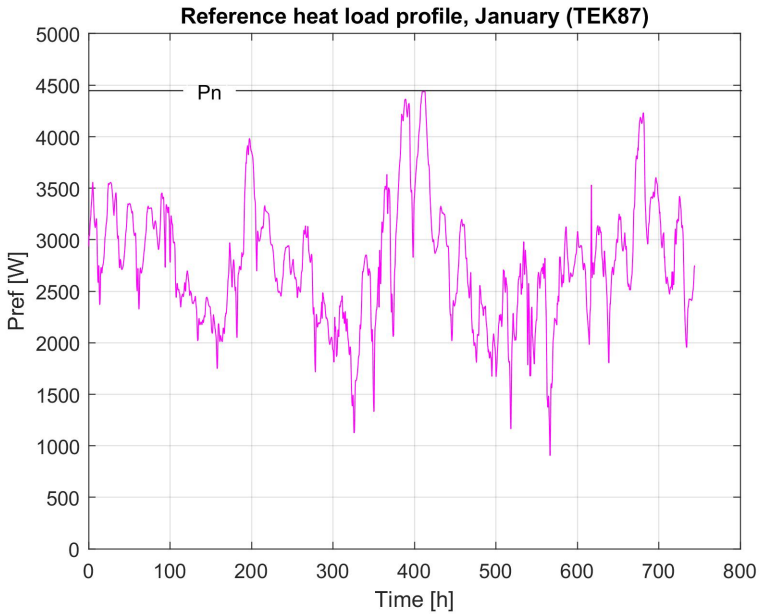

Figure 4.7: Hourly heating load profile for the month of January, obtained for the living room in the TEK87 model.

When the amplitude of the step is determined, the values of the heat load profile is changed back to signals between 0 and 1.

4.4.3 Open loop simulation

In the third stage of the approach, the modified heat load profile from MATLAB is used as input to the PI controllers in IDA ICE. This requires a new set of controllers that can take input from a source file, and so a new IDA ICE file is made with an identical building model. The new controllers are defined as in figure 4.8. Figure 4.8a shows the building central control, which is defined to take input from a source file, and deliver the new signals to each zone controller. Figure 4.8b shows the PI controller defined for each zone, where the heating signal gets input from the building central control.

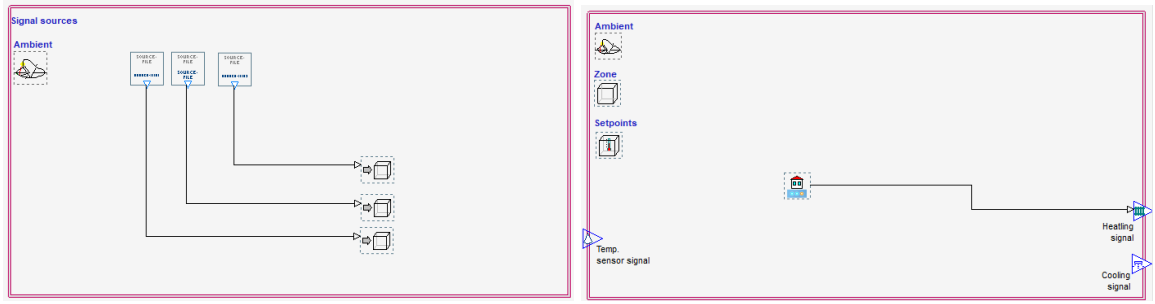

(a) Screenshot of the building central control. **(b)** Screenshot of PI controller.

Figure 4.8: Controllers defined for the open loop simulation in IDA ICE.

The open loop simulation is performed by using the custom simulation option, with a dynamic startup phase. The following guidelines are defined for the duration of the initialization and main simulation period:

- The initialization phase is set to 14 days in all model variations.
- For the step response to reach steady state, the main simulation is run up to four weeks after the defined start step.

Provided output from the simulation includes a new list of indoor temperatures T_i. The time step for the output is the same as for the closed loop simulation.

4.4.4 Comparison and evaluation of results

In the fourth stage of the approach, the indoor temperatures (T_i) obtained from the open loop simulation are imported into MATLAB. Plotting these temperatures provides the step response of the indoor temperature, which is expected to resemble the step response in figure 3.3.

The step response has to originate from the same point as the plotted graph for the reference temperatures (T_i^R) obtained in the closed loop simulation, in order for the case to be valid. If this proves to be difficult, a margin of error of ± 0.05°C is allowed. In case the deviation between the originating points are higher than the defined limit, one or both of the following two measures can be taken; (1) adjust the initialization phase of the open loop simulation, or (2) change the start step in MATLAB.

If the case is valid, the deviation in indoor temperature ΔT is obtained. Due to thermal comfort considerations, a limit is introduced to the value of ΔT, which is further explained in Chapter 4.6.2. In case of the deviation being too high, or has potential to be increased relatively to this limit, the value of ΔP is changed in MATLAB and the open loop simulation is repeated. The simulation process ends when a suitable deviation in temperature is obtained, and so the allowable deviation in heat load ΔP is established.

4.5 Identification of model parameters

The step response equations presented in Chapters 4.1.1 and 4.1.2 are implemented into the MATLAB script to fit the models to the step response of the indoor temperature computed by IDA ICE, and to estimate the model parameters after the open loop simulation.

Both models are fitted by using *nlinfit*, which is a nonlinear regression model function embedded in MATLAB [83]. Robust options is used for the nonlinear regression. In order to use *nlinfit* for the second-order model, an initial guess of the two time constants is required. As mentioned in Chapter 3.1.6, time constants vary depending on the insulation level, and the guess should be made accordingly. For the high insulated building models, at least one of the time constants should be in the range of several days [69].

After the model fitting is complete, the results must be checked visually to validate the fitting. This is done by comparing the plotted graphs for dT from the open loop simulation, dT from the first-order model and dT from the second-order model. If the three graphs originate from the same point, or within a margin of error of $\pm$ 0.05°C, the model fitting is considered to be valid. Figure 4.9 illustrates the visual check of the plotted graphs, where figures 4.9a and 4.9b shows an example of a valid and invalid case respectively.

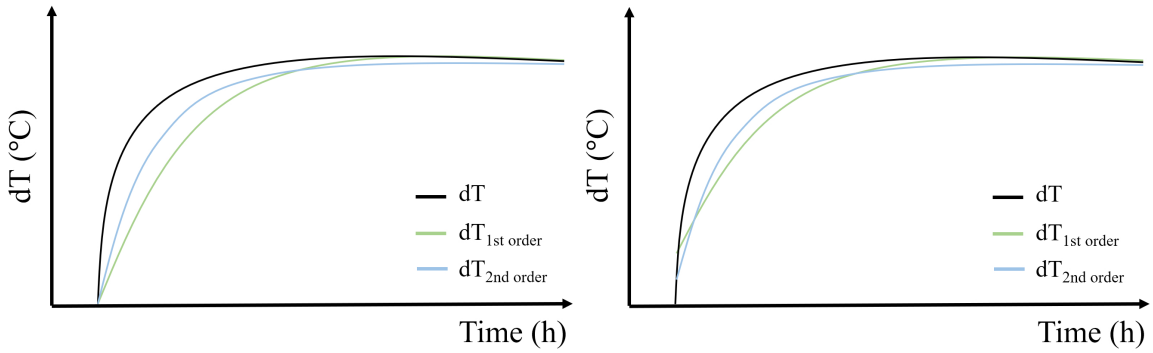

(a) Valid case. **(b)** Invalid case.

Figure 4.9: Visual check to validate the model fitting in MATLAB.

In case the model fitting is invalid, the measures from Chapter 4.4.4 can be used. In case the model fitting is valid, the model parameters are identified. The related code was developed by the supervisor of this thesis [69], and is found in line numbers 169-191 of the MATLAB script attached in Appendix B.

4.6 Simulation scenarios

The four model variations presented in Chapter 4.3 are simulated for each month of the heating season, and it is chosen to use weather data from the year of 2015 in IDA ICE. Based on the definition given in Chapter 3.1.7, the heating season is considered to be from January-March and from October-December. This gives a total of 24 simulation scenarios (cases).

In order to identify the potential of demand flexibility, the allowable deviation from a reference heat load is determined. This is done by using the approach presented in Chapter 4.4, and the restriction for the deviation in indoor temperature given in Chapter 4.6.2 has to be complied. Both increasing (charging) and decreasing (discharging) of heat load is evaluated in each simulation case. However, a step is only introduced in cases where one continuous week or more of the reference power profile has potential for charging/discharging within the defined limit (see Chapter 4.4.2). The step responses from the charging and discharging cases should preferably have a similar curve, but with opposite signs. Symmetry of the step responses is thus evaluated by inverting the plotted graphs of the discharging case.

Based on the results obtained in the open loop simulations, model parameters can be identified by using the approach presented in Chapter 4.5. This is considered to be the most important part of the simulations, as it enables a characterization of the building energy flexibility.

4.6.1 Simplifications

In order to limit the scope of work related to the simulations, only the heat load profile for the first floor is modified. The second floor consists of rooms that are generally less used than a living room. Also, the preferred temperature in bedrooms and bathroom are highly dependent on individual preferences, which makes it difficult to evaluate thermal comfort during thermal mass activation. Input to the zone controllers in the open loop simulation is thus provided by using the list of signals from the closed loop simulations directly.

It is still important to include the second floor in the simulations. The indoor temperature of the first floor depends on heat transfer through the floor divider, and thermal bridges in the building. To ensure that the right indoor temperature is reflected, this has to be accounted for.

4.6.2 Evaluation of thermal comfort

In the scope of this work, it is not meaningful to apply the thermal comfort models presented in Chapter 3.3 directly, due to the dynamic temperature changes during thermal mass activation. The proposed method of evaluating thermal comfort is however inspired by the adaptive models, where occupants are willing to adapt to changes in indoor temperature. Based on the information given in Chapters 3.3.2 and 3.4, the deviation in indoor temperature (ΔT_i) is restricted to ± 2°C during the thermal mass activation to ensure thermal comfort. Despite the limitations of this method, a good indication of the thermal comfort can be obtained as the indoor temperature often is the main contributor to discomfort.

Both air temperatures and operative temperatures are provided periodically for each zone in IDA ICE. Related numerical values and graphs can be used to compare against the requirements and recommendations given in Chapter 3.3.2, to evaluate the thermal comfort. It is chosen to use indoor air temperatures for the simulations, but operative temperatures are considered in the results.

4.6.3 Remarks about the results

The output from IDA ICE is given in terms of hours in the year, where 0 is the first hour, and 8760 is the last hour. The x-axix of the graphs presented in the results thus refers to the hourly number related to the month in which is simulated. Table 4.7 presents the hourly numbers for the first and last day of the relevant months.

Table 4.7: Hourly number defined for each simulated month.

Month	Fist hour of month	Last hour of month
January	0	743
February	744	1415
March	1416	2160
October	6552	7295
November	7296	8015
December	8016	8760

Chapter 5

Simulation results

This chapter presents the results obtained for the 24 simulation cases. Firstly, the deviation in heat load, symmetry of step responses, duration of simulation time and the identified model parameters for all model variations are presented for the individual simulated months. Secondly, the identified model parameters are compared for each model variation. This enables a comparison of the parameters during the entire heating season, and general trends or irregularities can more easily be identified within each model variation. At the end of this chapter, graphs obtained using the operative temperatures from IDA ICE is presented.

The identified model parameters are presented in tables. Due to limited space, the units of the parameters are not included, but they are defined as follows: U (W/K), C (Wh/K), τ (h).

5.1 January

Deviation in heat load

The allowable deviation from the reference heat load in January is presented for each model variation in table 5.1.

Table 5.1: Allowable deviation in heat load for each model variation in January.

Allowable deviation from reference heat load [%]				
	TEK87	**TEK10**	**TEK17**	**Passive**
Charge	4.5	7.6	6.6	6.4
Discharge	5.4	7.6*	6.6*	6.4**

*See figure 5.1 **See figure 5.2

Reference heat load profiles with discharging for the TEK10 and TEK17 models are shown in figures 5.1a and 5.1b respectively. Figure 5.2 shows the same for the passive house model. In all three cases, a compromise of violating the restriction from Chapter 4.4.2 allowed the possibility of discharge at the end on the month.

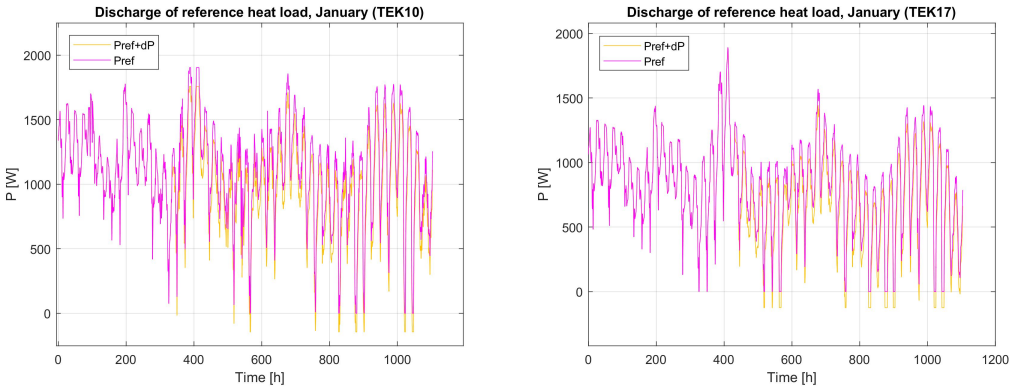

(a) TEK10 model. **(b)** TEK17 model.

Figure 5.1: Discharge of reference heat load for the TEK10 and TEK17 models in January.

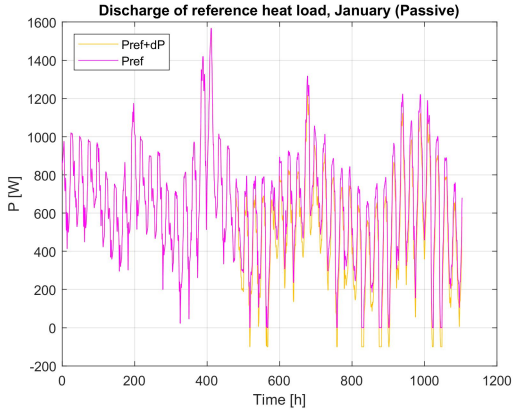

Figure 5.2: Discharge of reference heat load for the passive house model in January.

Symmetry

The step responses obtained by charging and discharging the reference heat load in the TEK87 model are shown in figures 5.3a and 5.3b respectively. For the charging case, the 24th of January was set as the start step, while the start step for the discharging case was set to the 23rd of January. A comparison between the temperatures from the closed loop (green) and open loop (blue) simulations are shown in figure 5.4, where figures 5.4a and 5.4b represents charging and discharging respectively. The open loop temperatures are the step response obtained by IDA ICE.

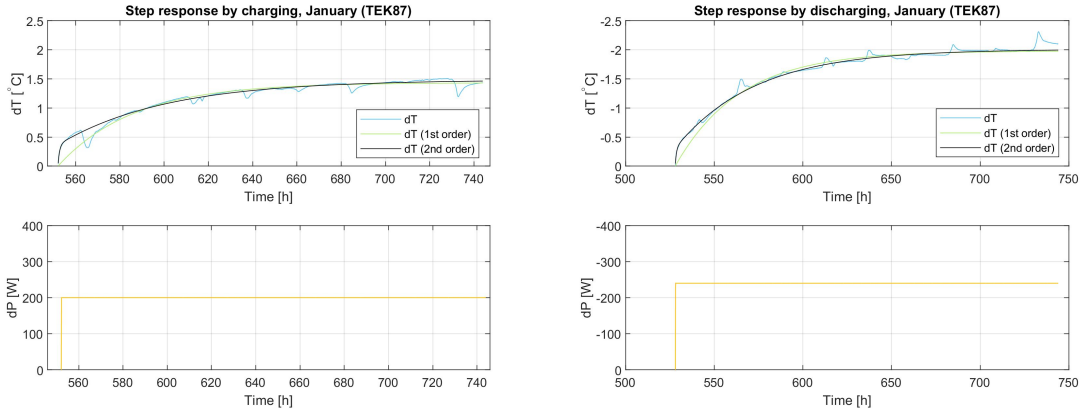

(a) Charging case. **(b)** Discharging case.

Figure 5.3: Comparison of step responses caused by charge/discharge (TEK87 model, January).

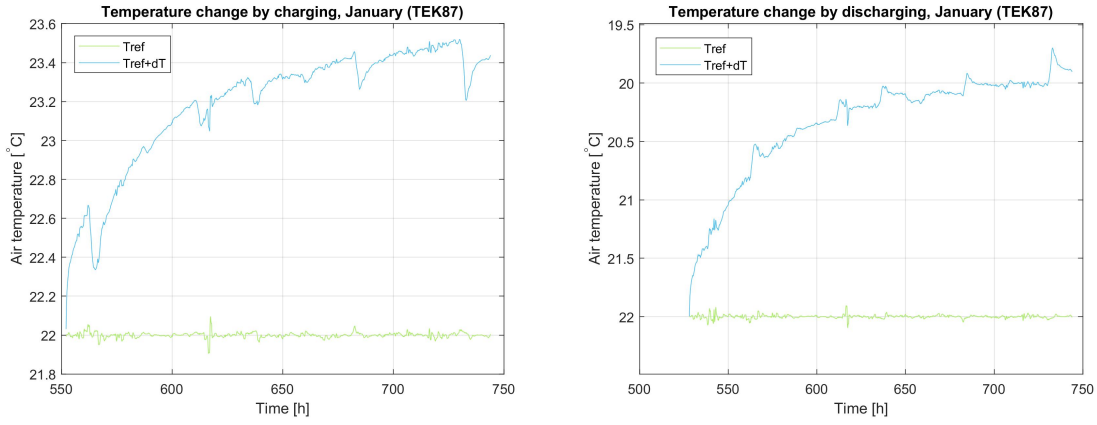

(a) Charging case. **(b)** Discharging case.

Figure 5.4: Comparison of $T_{ref} + dT$ caused by charge/discharge (TEK87 model, January).

Note that for the charging cases, the deviation in temperature is well below 2°C. This was a result of keeping the deviation in heat load within the defined restriction. However, the graphs are somewhat symmetrical.

The step responses from charging and discharging the reference heat load in the TEK10 model are shown in figure 5.5. For the charging case, the start step were set to the 19th of January, while the start step for the discharging case were set to the 15th of January. A comparison between the temperatures from the closed loop and open loop simulations are shown in figure 5.6. Even though the start step is different, the graphs are quite symmetrical.

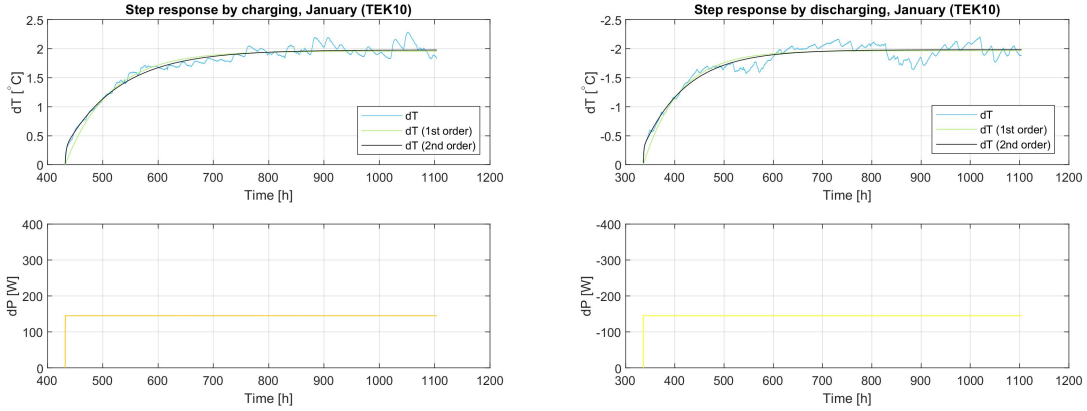

(a) Charging case. **(b)** Discharging case.

Figure 5.5: Comparison of step responses caused by charge/discharge (TEK10 model, January).

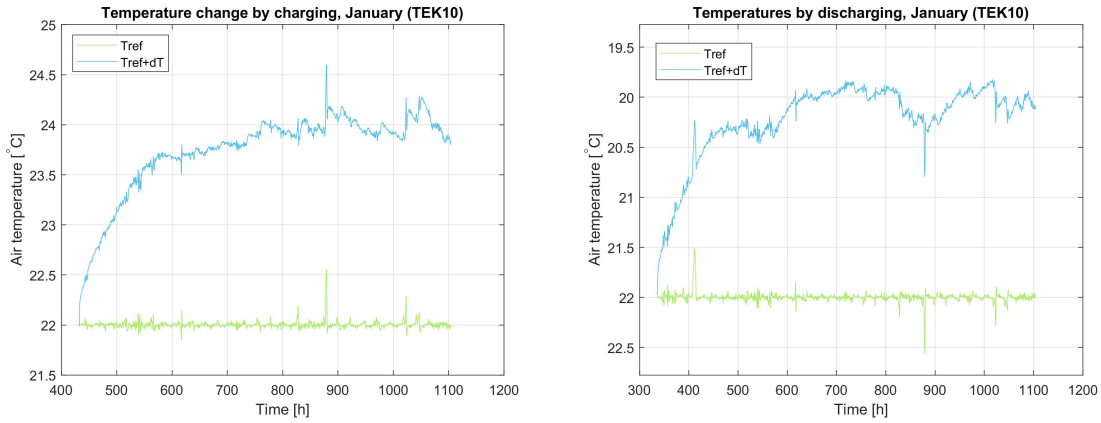

(a) Charging case. **(b)** Discharging case.

Figure 5.6: Comparison of $T_{ref} + dT$ caused by charge/discharge (TEK10 model, January).

For the TEK17 model, the reference heat load profile could be both charged and discharged from the 19th of January, which resulted in graphs with similar symmetry. The related step responses are shown in figure 5.7. A comparison between the temperatures from the closed loop and open loop simulations are shown in figure 5.8.

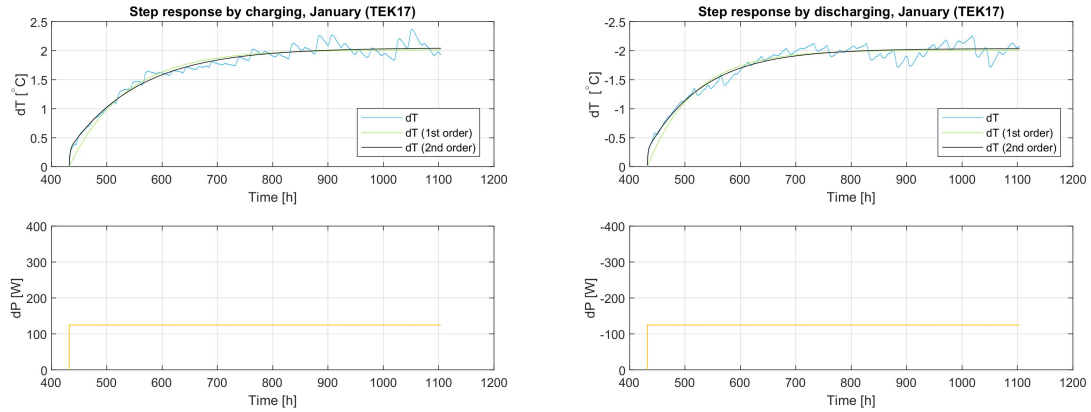

(a) Charging case. **(b)** Discharging case.

Figure 5.7: Comparison of step responses caused by charge/discharge (TEK17 model, January).

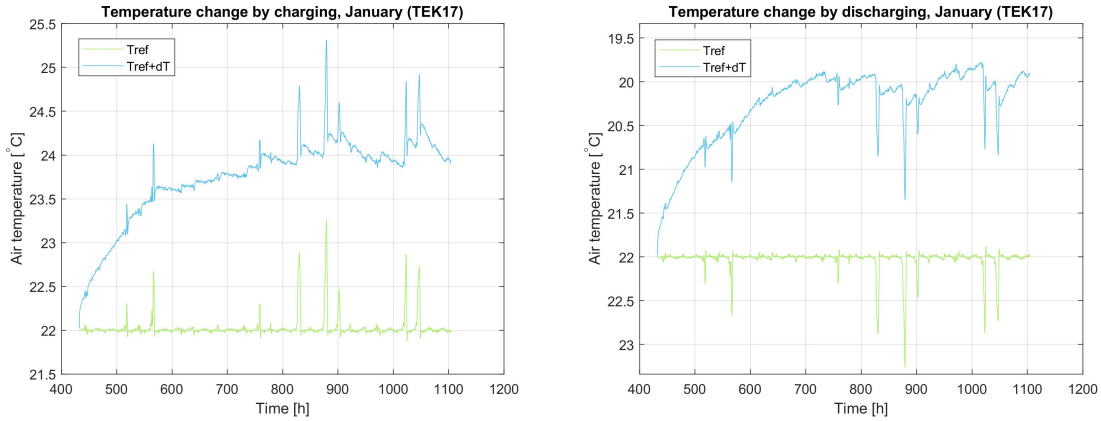

(a) Charging case. **(b)** Discharging case.

Figure 5.8: Comparison of $T_{ref} + dT$ caused by charge/discharge (TEK17 model, January).

The step responses from charging and discharging the reference load in the passive house model are shown in figure 5.9. For the charging case, the start step were set to the 23rd of January, while the start step for the discharging case were set to the 21st of January. A comparison between the temperatures from the closed loop and open loop simulations are shown in figure 5.10. Even though the start step is different, the graphs are quite symmetrical.

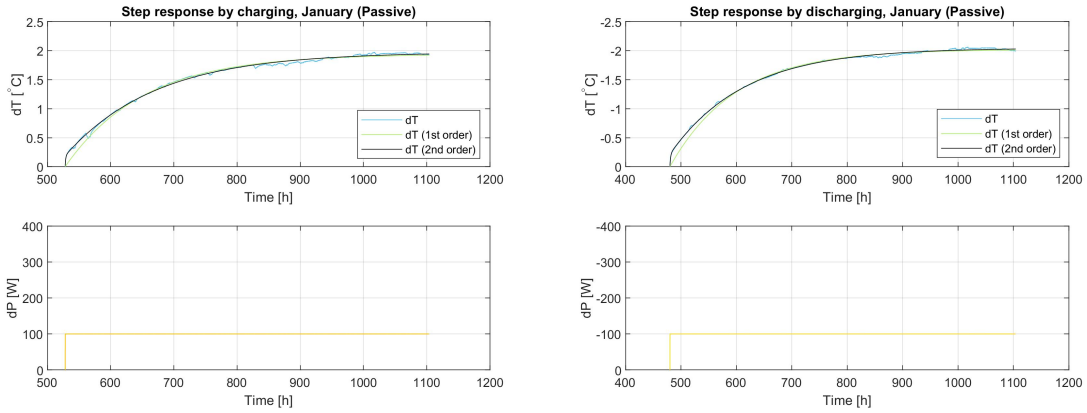

(a) Charging case. **(b)** Discharging case.

Figure 5.9: Comparison of step responses caused by charge/discharge (passive house model, January).

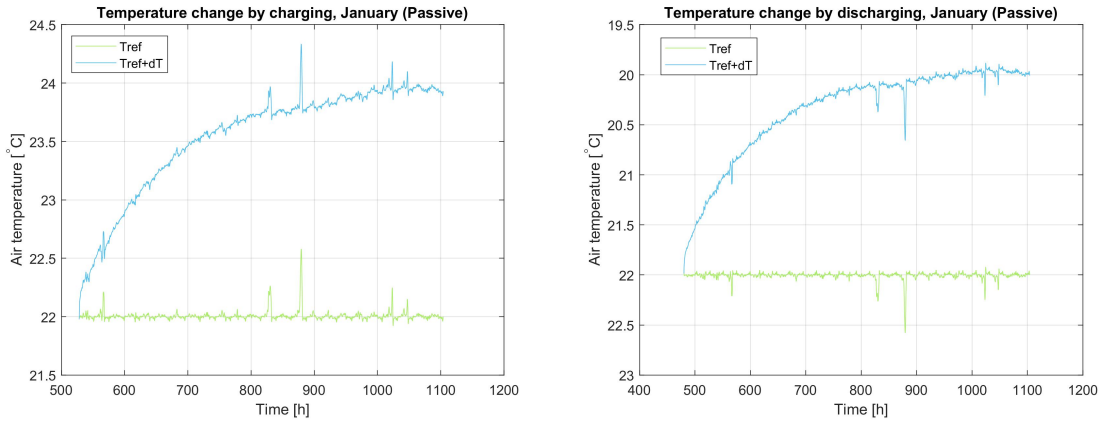

(a) Charging case. **(b)** Discharging case.

Figure 5.10: Comparison of $T_{ref} + dT$ caused by charge/discharge (passive house model, January.

Duration of simulation time

The duration of the initialization phase and the main simulation for all model variations in January are shown in table 5.2.

Table 5.2: Duration of the initialization phase and the main simulation for all model variations in January.

	Closed loop		**Open loop (charging)**		**Open loop (discharging)**	
	Initialization	Main	Initialization	Main	Initialization	Main
TEK87	1 month	1 month	14 days	11 days	3 days	11 days
TEK10	1 month	1.5 months	3 days	1.5 months	3 days	1.5 months
TEK17	1 month	1.5 months	5 days	1.5 months	2 days	1.5 months
Passive	1 month	1.5 months	11 days	1.2 months	5 days	1.4 months

Parameters

The parameters obtained for each model variation in January are presented in table 5.3.

Table 5.3: Identified parameters for each model variation in January.

	First-order model							
	TEK87		**TEK10**		**TEK17**		**Passive**	
	Charge	**Discharge**	**Charge**	**Discharge**	**Charge**	**Discharge**	**Charge**	**Discharge**
U	137.34	121.23	74.09	73.79	61.99	62.18	51.55	49.47
τ	35.97	36.55	80.06	72.64	101.43	84.25	123.68	118.54
C	4939.72	4431.16	5931.53	5360.39	6287.69	5238.64	6375.84	5863.81

	Second-order model							
	TEK87		**TEK10**		**TEK17**		**Passive**	
	Charge	**Discharge**	**Charge**	**Discharge**	**Charge**	**Discharge**	**Charge**	**Discharge**
U	134.01	119.41	73.28	73.18	60.97	61.40	50.63	48.86
τ_1	47.06	45.33	98.80	88.62	126.87	101.88	143.09	134.68
τ_2	0.89	0.69	1.74	0.97	1.61	1.16	0.95	1.29
α_1	0.81	0.85	0.85	0.85	0.85	0.86	0.90	0.89

5.2 February

Deviation in heat load

The allowable deviation from the reference heat load in February is presented for each model variation in table 5.4.

Table 5.4: Allowable deviation in heat load for each model in February.

Allowable deviation from reference heat load [%]				
	TEK87	**TEK10**	**TEK17**	**Passive**
Charge	5.6	7.9	5.7	5.7
Discharge	5.6	-	-	-

Due to high fluctuations in the reference heat load profiles, as shown in figure 5.11 for the TEK10 and TEK17 models, there was limited or no potential for discharging in the high insulated models. It was difficult to obtain any valid results, and was thus not considered any further. These fluctuations were also reflected in the temperatures obtained for the charging cases, as shown in figure 5.12.

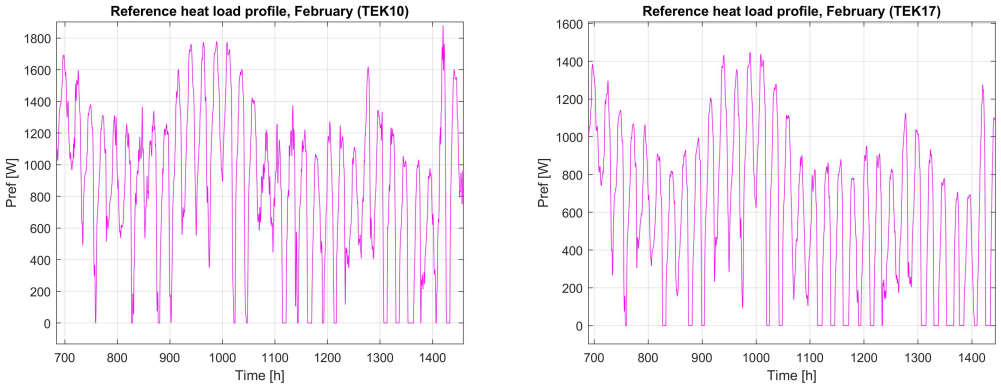

(a) TEK10. **(b)** TEK17.

Figure 5.11: Reference heat load profiles for the TEK10 and TEK17 models in February.

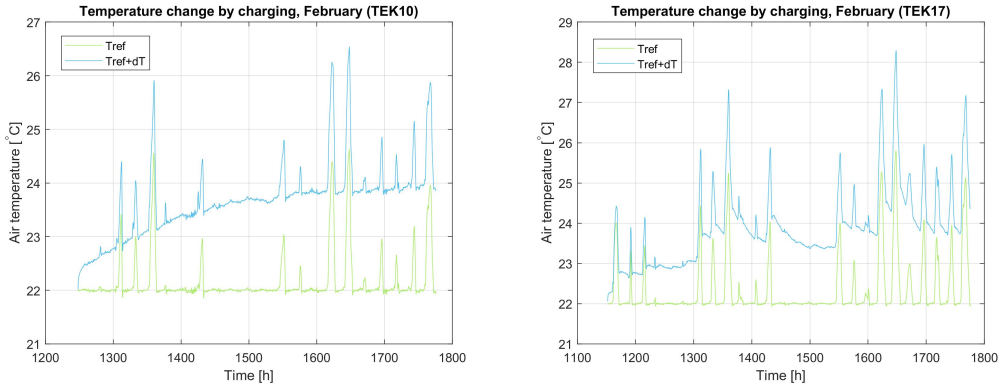

(a) TEK10. **(b)** TEK17.

Figure 5.12: $T_{ref} + dT$ caused by charging for TEK10 and TEK17 in February.

Symmetry

For the TEK87 model, the reference heat load profile could be both charged and discharged from the 15th of February, resulting in temperature graphs with similar symmetry. The step responses are shown in figure 5.13, where figures 5.13a and 5.13b presents charging and discharging respectively.

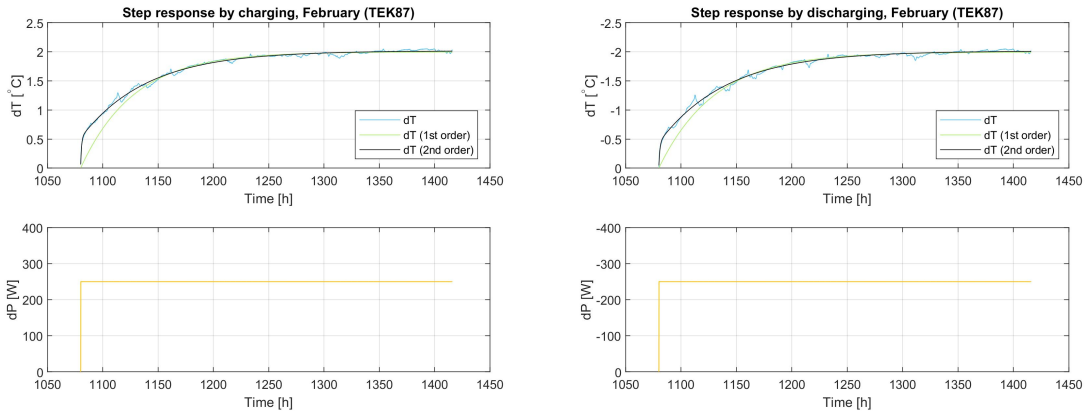

(a) Case of charging.

(b) Case of discharging.

Figure 5.13: Comparison of step response caused by charge/discharge (TEK87 model, February).

Figure 5.14 shows the comparison between the temperature graphs obtained from the closed loop and open loop, where figures 5.14a and 5.14b presents charging and discharging respectively.

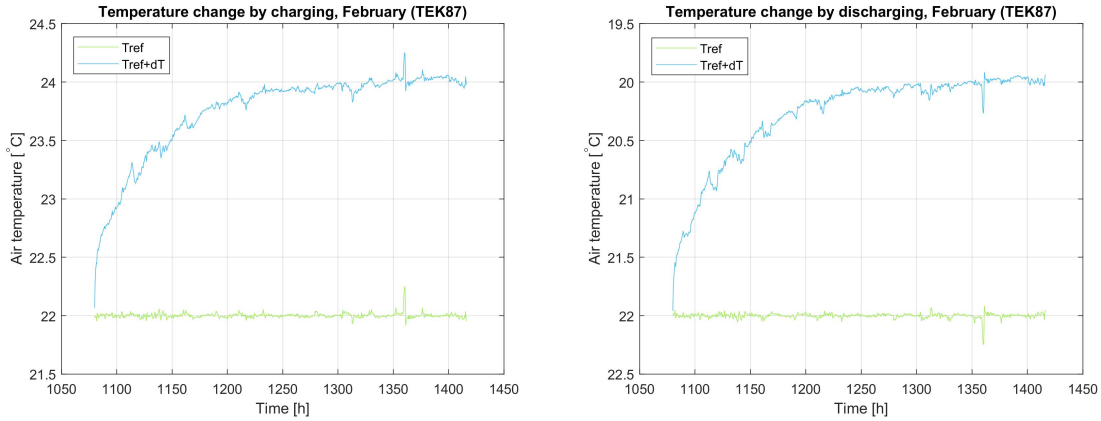

(a) Case of charging.

(b) Case of discharging.

Figure 5.14: Comparison of $T_{ref} + dT$ caused by charge/discharge (TEK87 model, February).

Duration of simulation time

The duration of the initialization phase and the main simulation for all model variations in February are shown in table 5.5.

Table 5.5: Duration of the initialization phase and the main simulation for all model variations in February.

	Closed loop		**Open loop (charging)**		**Open loop (discharging)**	
	Initialization	Main	Initialization	Main	Initialization	Main
TEK87	1 month	1.5 months	7 days	1 month	14 days	1 month
TEK10	1 month	2 months	14 days	1.5 months	-	-
TEK17	1 month	2 months	14 days	1.5 months	-	-
Passive	1 month	2 months	14 days	1.5 months	-	-

Parameters

The parameters obtained for each model variation in February are presented in table 5.6.

Table 5.6: Identified parameters for each model variation in February.

First-order model					
	TEK87		**TEK10**	**TEK17**	**Passive**
	Charge	**Discharge**	**Charge**	**Charge**	**Charge**
U	125.09	124.14	77.80	57.22	48.36
T	48.04	50.61	120.96	118.13	149.40
C	6008.84	6342.82	9411.16	6759.08	7225.67

Second-order model					
	TEK87		**TEK10**	**TEK17**	**Passive**
	Charge	**Discharge**	**Charge**	**Charge**	**Charge**
U	123.90	124.14	75.62	55.70	47.45
τ_1	59.95	61.65	152.89	150.13	186.21
τ_2	0.81	0.95	0.79	0.63	1.92
α_1	0.74	0.78	0.84	0.86	0.85

5.3 March

Deviation in heat load

The allowable deviation from the reference heat load in March for each model variation are presented in table 5.7.

Table 5.7: Allowable deviation in heat load for each model variation in March.

Allowable deviation from reference heat load [%]				
	TEK87	**TEK10**	**TEK17**	**Passive**
Charge	5.7	8.4	7.3	6.4

Due to high fluctuations in the reference heat load profiles, and generally low heating demand in the high insulated models, there was no potential for discharging in either of the model variations. This is shown for the TEK10 and passive house models in figures 5.15a and 5.15b respectively.

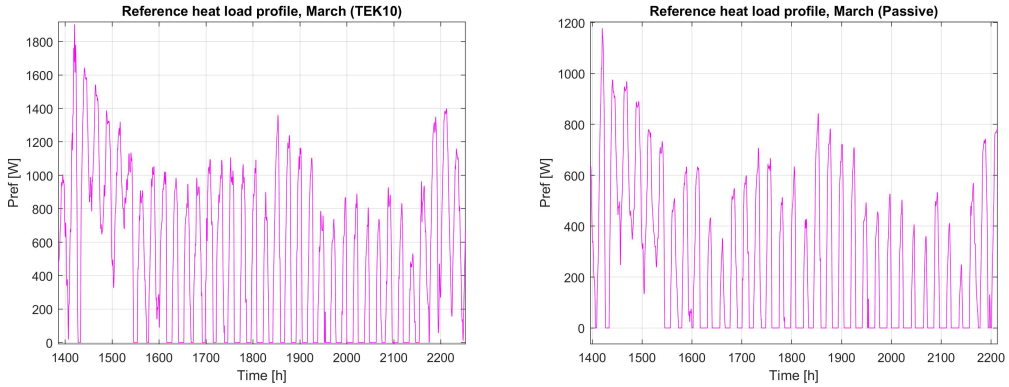

(a) TEK10. **(b)** Passive house.

Figure 5.15: Reference heat load profiles for the TEK10 and passive house models in March.

The fluctuations in heat load were also reflected in the temperatures obtained for the high insulated models this month. Figures 5.16 and 5.17 shows the step response and closed/open loop temperatures obtained for the TEK10 and passive house models respectively.

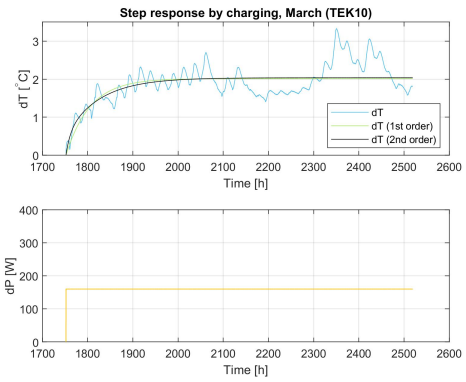

(a) Step response.

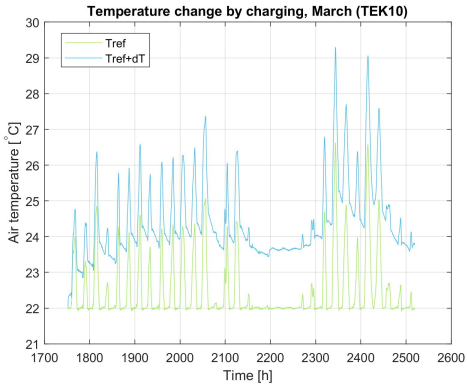

(b) Temperatures obtained from closed/open loop.

Figure 5.16: Results from charging the heat load in the TEK10 model (March).

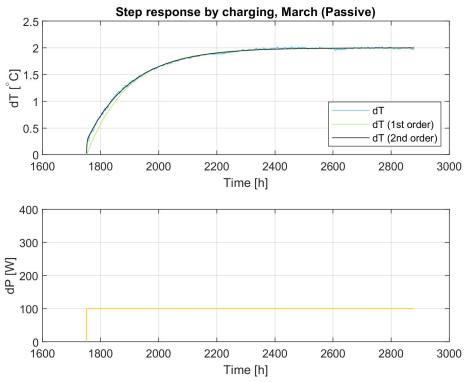

(a) Step response.

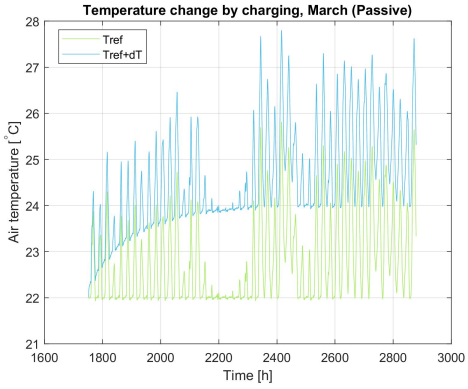

(b) Temperatures obtained from closed/open loop.

Figure 5.17: Results from charging the heat load in the passive house model (March).

The step response and closed/open loop temperatures obtained for the low insulated model are shown in figure 5.18. In this case, the temperature curves were smoother, which is a more preferable result than for the high insulated models.

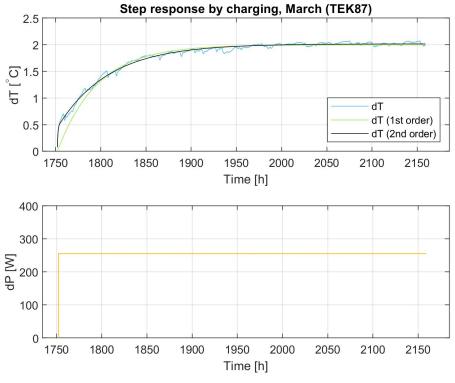

(a) Step response.

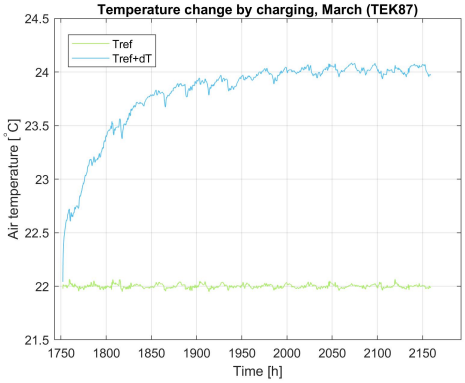

(b) Temperatures obtained from closed/open loop.

Figure 5.18: Results from charging the heat load in the TEK87 model (March).

Duration of simulation time

The duration of the initialization phase and the main simulation for all model variations in March are shown in table 5.8.

Table 5.8: Duration of the initialization phase and the main simulation for all model variations in March.

	Closed loop		**Open loop (charging)**	
	Initialization	Main	Initialization	Main
TEK87	1 month	1.5 months	14 days	1 month
TEK10	1 month	3 months	14 days	1.5 months
TEK17	1 month	3 months	14 days	1 month
Passive	1 month	3 months	14 days	2 months

Parameters

The parameters obtained for each model variation in March are presented in table 5.9.

Table 5.9: Identified parameters for each model variation in March.

	First-order model			
	TEK87	**TEK10**	**TEK17**	**Passive**
	Charge	**Charge**	**Charge**	**Charge**
U	127.69	79.37	77.63	50.09
τ	44.29	53.18	88.86	141.88
C	5654.84	4220.45	6897.99	7106.64

	Second-order model			
	TEK87	**TEK10**	**TEK17**	**Passive**
	Charge	**Charge**	**Charge**	**Charge**
U	126.47	78.53	77.77	49.96
τ_1	56.48	75.58	85.57	155.57
τ_2	0.52	9.37	0.92	1.31
α_1	0.78	0.73	1.0	0.87

5.4 October

Deviation in heat load

The allowable deviation from the reference heat load in October are presented for each model variation in table 5.10.

Table 5.10: Allowable deviation in heat load for each model variation in October.

Allowable deviation from reference heat load [%]				
	TEK87	**TEK10**	**TEK17**	**Passive**
Charge	5.7	8.1	7.3	6.4
Discharge	5.9	-	-	-

Due to high fluctuations in the reference heat load profiles, and generally low heating demand, there was no potential for discharging of the high insulated models this month. Reference heat load profiles for the TEK17 and passive house models are shown in figures 5.19a and 5.19b respectively.

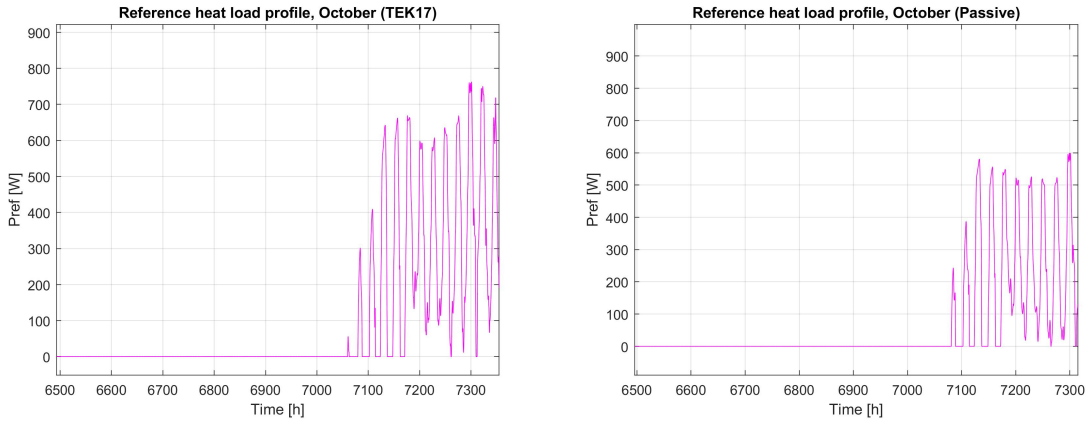

(a) TEK17. **(b)** Passive house.

Figure 5.19: Reference heat load profiles for the TEK17 and passive house models in October.

Symmetry

For the TEK87 model, the reference heat load profile could be both charged and discharged from the 22nd of October, resulting in temperature graphs with similar symmetry. The step responses is shown in figure 5.20, where figures 5.20a and 5.20b represents charging and discharging respectively.

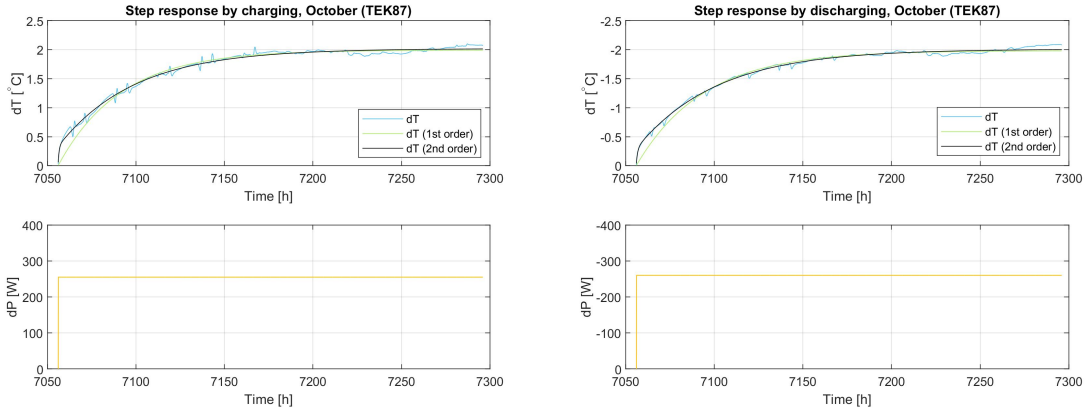

(a) Charging case. **(b)** Discharging case.

Figure 5.20: Step responses caused by charge/discharge (TEK87 model, October).

Figure 5.21 shows the change in temperature from the open loop compared to the closed loop, where figures 5.21a and 5.21b represents charging and discharging respectively.

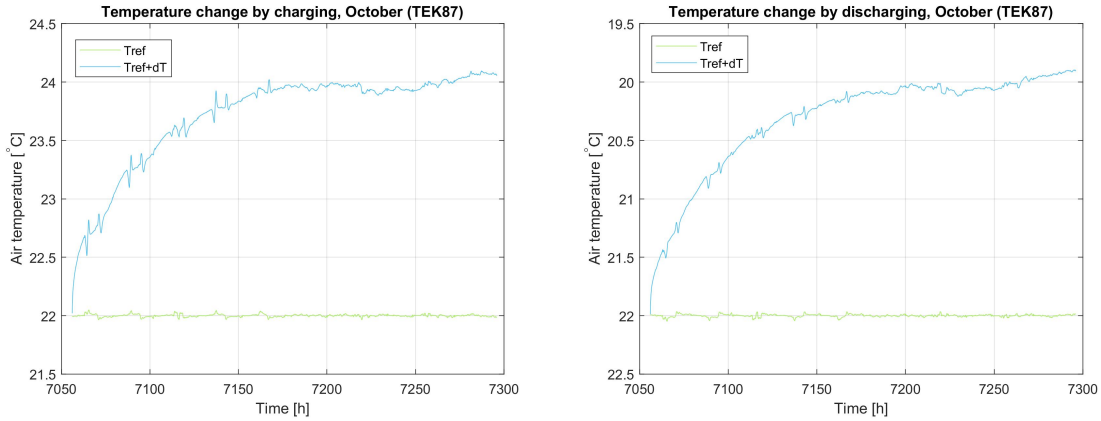

(a) Charging case. **(b)** Discharging case.

Figure 5.21: Comparison of $T_{ref} + dT$ caused by charge/discharge (TEK87 model, October).

Duration of simulation time

The duration of the initialization phase and the main simulation for all model variations in October are shown in table 5.11.

Table 5.11: Duration of the initialization phase and the main simulation for all model variations in October.

	Closed loop		**Open loop (charging)**		**Open loop (discharging)**	
	Initialization	Main	Initialization	Main	Initialization	Main
TEK87	1 month	1.5 months	14 days	11 days	7 days	20 days
TEK10	1 month	2.5 months	14 days	1.3 months	-	-
TEK17	1 month	2.5 months	14 days	1.3 months	-	-
Passive	1 month	3 months	14 days	2 months	-	-

Parameters

The parameters obtained for each model variation in October are presented in table 5.12.

Table 5.12: Identified parameters for each model variation in October.

First-order model					
	TEK87		**TEK10**	**TEK17**	**Passive**
	Charge	**Discharge**	**Charge**	**Charge**	**Charge**
U	127.98	131.13	79.76	70.89	49.59
τ	35.37	37.97	104.87	144.71	120.31
C	4525.84	4979.65	8364.28	10258.39	5966.42

Second-order model					
	TEK87		**TEK10**	**TEK17**	**Passive**
	Charge	**Discharge**	**Charge**	**Charge**	**Charge**
U	126.28	129.35	78.72	68.61	49.34
τ_1	43.27	45.47	120.34	176.68	137.86
τ_2	0.55	0.76	0.35	0.92	3.65
α_1	0.84	0.85	0.90	0.88	0.84

5.5 November

Deviation in heat load

The allowable deviation from the reference heat load in November are presented for each model variation in table 5.13.

Table 5.13: Allowable deviation in heat load for each model variation in November.

Allowable deviation from reference heat load [%]				
	TEK87	**TEK10**	**TEK17**	**Passive**
Charge	5.9	8.4	7.3	7.0
Discharge	5.9	7.4 *	6.2 *	-

* See figure 5.22.

Due to high fluctuations in the reference power profile, and a generally low heating demand, there was no potential for discharging of the the passive house model. Similar trends were detected for TEK10 and TEK17, but introducing a small compromise allowed the possibility of discharge. Reference heat load profiles with discharging are shown in figures 5.22a and 5.22b, for the TEK10 and TEK17 models respectively.

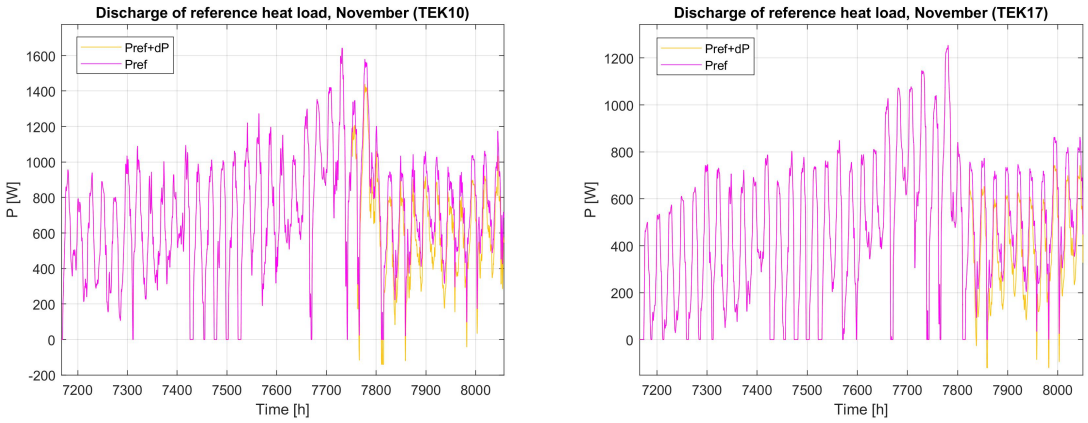

(a) TEK10. **(b)** TEK17.

Figure 5.22: Reference heat load profiles with discharge in November.

Symmetry

For the TEK87 model, the reference heat load profile could be both charged and discharged from the 19th of November, resulting in graphs with similar symmetry. Figures 5.23a and 5.23b shows the step responses obtained for the charging and discharging case respectively.

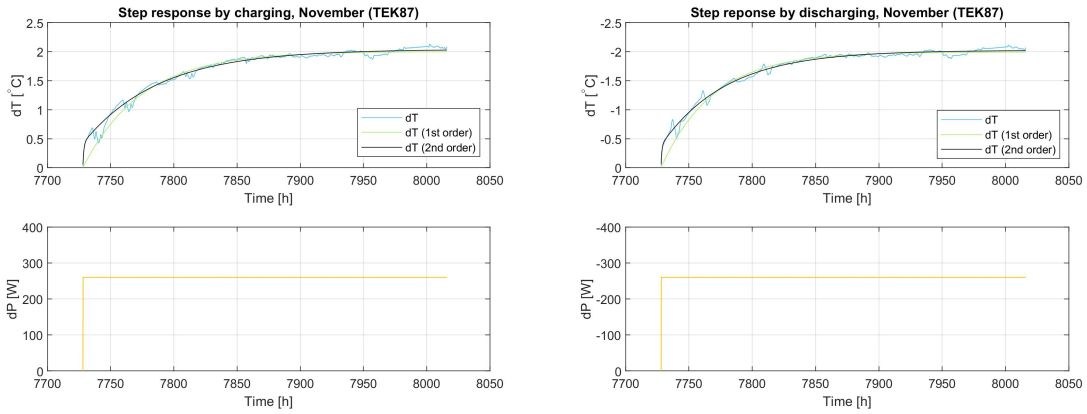

(a) Case of charging.

(b) Case of discharging.

Figure 5.23: Comparison of step responses caused by charge/discharge (TEK87 model, November).

The change in temperature from the open loop compared to the closed loop is shown in figures 5.24a and 5.24b, which represents charging and discharging respectively.

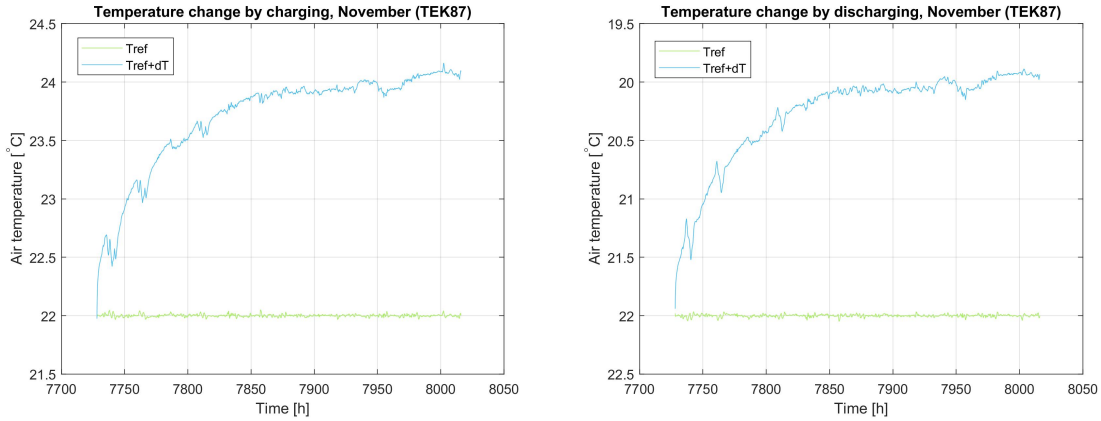

(a) Case of charging.

(b) Case of discharging.

Figure 5.24: Comparison of $T_{ref} + dT$ caused by charge/discharge TEK87 model, November).

For the TEK10 model, the reference heat load profile was charged from the 11th of November, and discharged from the 20th of November. Figures 5.25a and 5.25b shows the step responses obtained for the charging and discharging case respectively. In this case, the resulting graphs shows less symmetry.

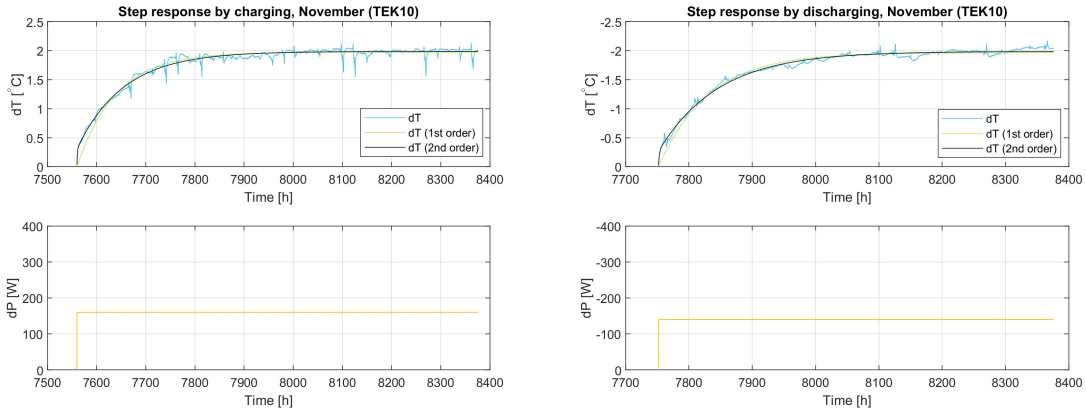

(a) Charging case. **(b)** Discharging case.

Figure 5.25: Step responses caused by charge/discharge (TEK10 model, November).

For the TEK17 model, the reference heat load profile was charged from the 11th of November, and discharged from the 23rd of November. Figures 5.26a and 5.26b shows the step responses obtained for the charging and discharging case respectively. In this case, the resulting graphs shows less symmetry.

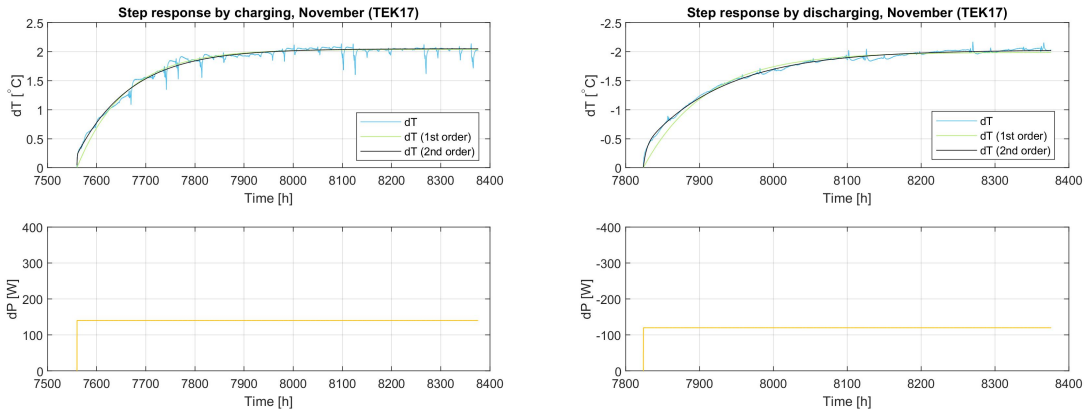

(a) Charging case. **(b)** Discharging case.

Figure 5.26: Step responses caused by charge/discharge (TEK17 model, November).

Duration of simulation time

The duration of the initialization phase and the main simulation for all model variations in November are shown in table 5.14.

Table 5.14: Duration of the initialization phase and the main simulation for all model variations in November.

	Closed loop		**Open loop (charging)**		**Open loop (discharging)**	
	Initialization	Main	Initialization	Main	Initialization	Main
TEK87	1 month	1.5 months	14 days	23 days	7 days	24 days
TEK10	1 month	2.5 months	14 days	1.5 months	14 days	1.5 months
TEK17	1 month	2.5 months	14 days	1.5 months	14 days	1.5 months
Passive	1 month	2.5 months	14 days	1.5 months	-	-

Parameters

The parameters obtained for each model variation in November are presented in table 5.15.

Table 5.15: Identified parameters for each model variation in November.

	First-order model						
	TEK87		**TEK10**		**TEK17**		**Passive**
	Charge	**Discharge**	**Charge**	**Discharge**	**Charge**	**Discharge**	**Charge**
U	129.80	130.40	81.07	71.23	68.62	60.31	54.12
τ	46.70	41.03	78.87	79.02	97.89	84.63	112.69
C	6061.15	5350.72	6394.59	5628.60	6717.23	5104.26	6098.47

	Second-order model						
	TEK87		**TEK10**		**TEK17**		**Passive**
	Charge	**Discharge**	**Charge**	**Discharge**	**Charge**	**Discharge**	**Charge**
U	127.36	128.49	80.52	70.46	68.26	59.10	53.42
τ_1	60.00	51.66	94.96	94.59	110.84	109.85	136.62
τ_2	0.77	0.65	0.88	1.30	0.50	4.20	2.54
α_1	0.79	0.81	0.84	0.87	0.89	0.82	0.86

5.6 December

Deviation in heat load

The allowable deviation from the reference heat load in December are presented for each model variation in table 5.16.

Table 5.16: Allowable deviation in heat load for each model variation in December.

Allowable deviation from reference heat load [%]				
	TEK87	**TEK10**	**TEK17**	**Passive**
Charge	5.7	8.4	6.5	6.4
Discharge	5.6	7.4	6.5	6.4

Symmetry

For the TEK10 model, the reference heat load profile could be both charged and discharged from the 12th of December, which resulted in graphs with similar symmetry. The step responses are shown in figure 5.27, while the changes in temperature are shown in figure 5.28.

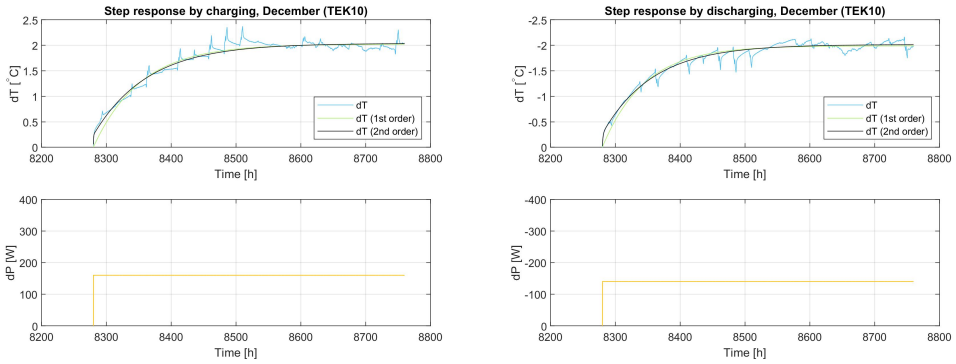

(a) Case of charging. **(b)** Case of discharging.

Figure 5.27: Comparison of step responses caused by charge/discharge (TEK10 model, December).

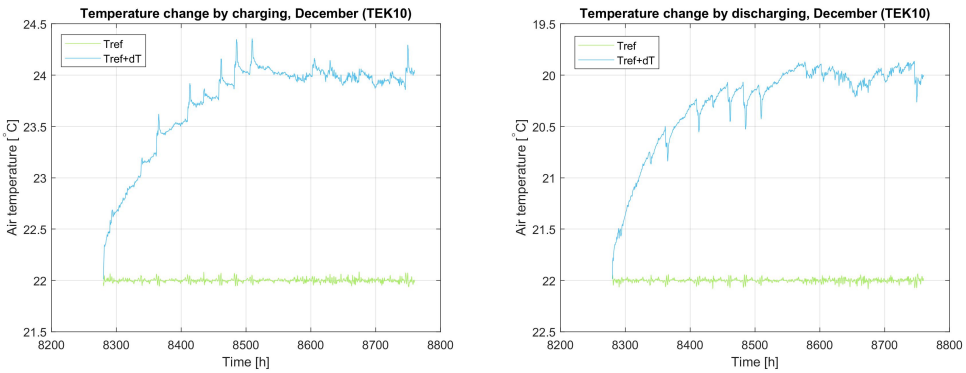

(a) Case of charging. **(b)** Case of discharging.

Figure 5.28: Comparison of $T_{ref} + dT$ caused by charge/discharge (TEK10 model,December).

Duration of simulation time

The duration of the initialization phase and the main simulation for all model variations in December are shown in table 5.17.

Table 5.17: Duration of the initialization phase and the main simulation for all model variations in December.

	Closed loop		**Open loop (charging)**		**Open loop (discharging)**	
	Initialization	Main	Initialization	Main	Initialization	Main
TEK87	1 month	1.5 months	14 days	1 month	5 days	16 days
TEK10	1 month	2 months	14 days	20 days	10 days	20 days
TEK17	1 month	2 months	14 days	1 month	14 days	1 month
Passive	1 month	2.5 months	14 days	2 months	14 days	2 months

Parameters

The parameters obtained for each model variation in December are presented in table 5.18.

Table 5.18: Identified parameters for each model variation in December.

	First-order model							
	TEK87		**TEK10**		**TEK17**		**Passive**	
	Charge	**Discharge**	**Charge**	**Discharge**	**Charge**	**Discharge**	**Charge**	**Discharge**
U	131.11	127.29	79.06	70.35	61.35	63.35	50.27	54.15
τ	37.68	36.06	72.84	64.67	95.46	87.61	104.90	144.44
C	4939.96	4590.67	5758.54	4549.57	5856.77	5550.48	5273.58	7821.35

	Second-order model							
	TEK87		**TEK10**		**TEK17**		**Passive**	
	Charge	**Discharge**	**Charge**	**Discharge**	**Charge**	**Discharge**	**Charge**	**Discharge**
U	129.94	125.54	78.49	69.44	60.69	62.79	49.82	53.19
τ_1	49.72	44.46	83.79	77.71	108.45	101.55	118.26	168.44
τ_2	0.67	0.73	0.38	1.05	0.67	1.66	0.59	3.39
α_1	0.76	0.80	0.88	0.87	0.90	0.86	0.89	0.90

5.7 Comparison of model parameters

In this chapter, the identified model parameters for the entire heating season are summarized to ease comparison in the individual model variations. Table 5.19 shows the model parameters for the TEK87 model, while tables 5.20, 5.21 and 5.22 shows the model parameters for the TEK10 model, TEK17 model and the passive house model respectively.

Table 5.19: Comparison of model parameters, TEK87 model

TEK87											
First-order model											
	Jan		**Feb**		**Mar**	**Oct**		**Nov**		**Dec**	
	C	D	C	D	C	C	D	C	D	C	D
U	139.46	121.23	125.09	125.33	127.69	127.98	131.13	129.80	130.40	131.11	127.29
τ	34.16	36.55	48.04	50.61	44.29	35.36	37.97	46.70	41.03	37.68	36.06
C	4763.47	4431.16	6008.84	6342.82	5654.84	4525.84	4979.65	6061.15	5350.72	4939.96	4590.67
Second-order model											
	Jan		**Feb**		**Mar**	**Okt**		**Nov**		**Dec**	
	C	D	C	D	C	C	D	C	D	C	D
U	134.73	119.41	123.90	124.14	126.47	126.28	129.34	127.36	128.49	129.94	125.54
τ_1	48.79	45.33	59.95	61.65	56.48	43.27	45.47	60.00	51.66	49.72	44.46
τ_2	0.71	0.69	0.81	0.95	0.52	0.55	0.76	0.77	0.65	0.67	0.73
α_1	0.75	0.85	0.74	0.78	0.78	0.84	0.85	0.79	0.81	0.76	0.80

Table 5.20: Comparison of model parameters, TEK10 model

TEK 10									
First-order model									
	Jan		**Feb**	**Mar**	**Oct**	**Nov**		**Dec**	
	C	D	C	C	C	C	D	C	D
U	74.09	73.79	77.80	79.37	78.35	81.07	71.23	79.06	70.35
τ	80.06	72.64	120.96	53.18	98.49	78.87	79.02	72.84	64.67
C	5931.53	5360.39	9411.16	4220.45	7716.44	6394.59	5628.60	5758.54	4549.57
Second-order model									
	Jan		**Feb**	**Mar**	**Oct**	**Nov**		**Dec**	
	C	D	C	C	C	C	D	C	D
U	73.28	73.18	75.62	78.54	77.45	80.52	70.46	78.49	69.44
τ_1	98.80	88.62	152.89	75.58	111.78	94.96	94.59	83.79	77.71
τ_2	1.74	0.97	0.79	9.37	0.40	0.88	1.30	0.38	1.05
α_1	0.85	0.85	0.84	0.73	0.90	0.84	0.87	0.88	0.87

Table 5.21: Comparison of model parameters, TEK17 model

TEK17									
First-order model									
	Jan		**Feb**	**Mar**	**Okt**	**Nov**		**Des**	
	C	**D**	**C**	**C**	**C**	**C**	**D**	**C**	**D**
U	61.99	62.18	54.37	77.63	70.89	68.62	60.31	61.35	63.35
τ	101.43	84.25	172.58	88.57	144.71	97.89	84.63	95.46	87.61
C	6287.69	5238.64	9383.45	6897.99	10258.39	6717.23	5104.26	5856.77	5550.48
Second-order model									
U	60.97	61.40	53.42	77.77	68.61	68.26	59.10	60.69	62.79
τ_1	126.87	101.88	202.82	85.57	176.68	110.84	109.85	108.45	101.55
τ_2	1.61	1.16	1.71	0.92	0.92	0.50	4.20	0.67	1.66
α_1	0.85	0.86	0.91	1.03	0.88	0.89	0.82	0.90	0.86

Table 5.22: Comparison of model parameters, Passive house model

Passive house								
First-order model								
	Jan		**Feb**	**Mar**	**Oct**	**Nov**	**Dec**	
	C	D	C	C	C	C	C	D
U	51.55	49.47	48.23	50.09	49.59	54.12	50.37	54.15
τ	123.68	118.54	147.22	141.88	120.31	112.69	106.06	144.44
C	6375.84	5863.81	7101.05	7106.64	5966.42	6098.47	5342.60	7821.35
Second-order model								
	Jan		**Feb**	**Mar**	**Okt**	**Nov**	**Dec**	
	C	D	C	C	C	C	C	D
U	50.63	48.86	47.32	49.96	49.34	53.42	49.94	53.19
τ_1	143.09	134.68	183.15	155.57	137.86	136.62	118.94	168.44
τ_2	0.95	1.29	1.59	1.31	3.65	2.54	0.63	3.39
α_1	0.90	0.89	0.85	0.87	0.84	0.86	0.90	0.90

5.8 Operative temperature

By changing from air temperatures to operative temperatures in the MATLAB script, the following results were obtained for the TEK17 model in January. Figure 5.29 shows the step response and comparison of closed/open loop temperatures for the charging case, while figure 5.30 shows the same graphs for the discharging case.

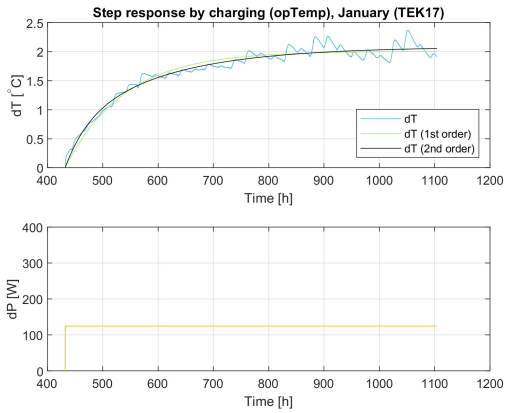

(a) Step response.

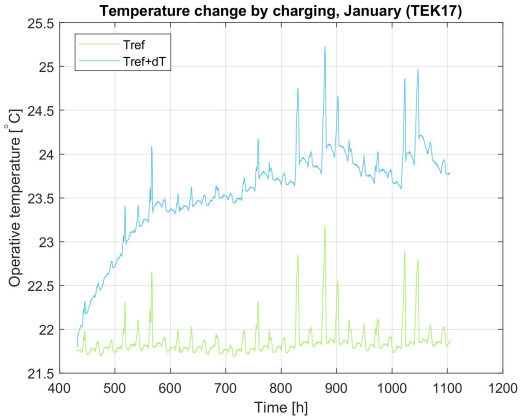

(b) Closed/open loop temperatures.

Figure 5.29: Graphs obtained for charging by using operative temperatures (TEK17 model, January).

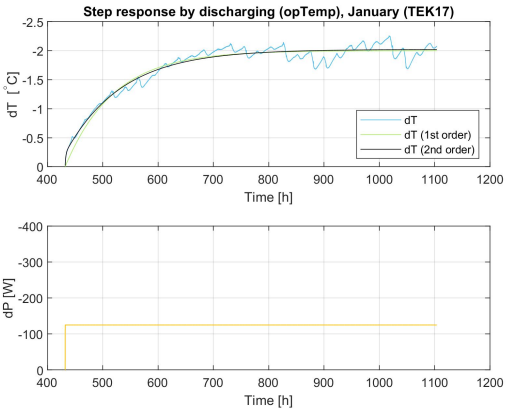

(a) Step response.

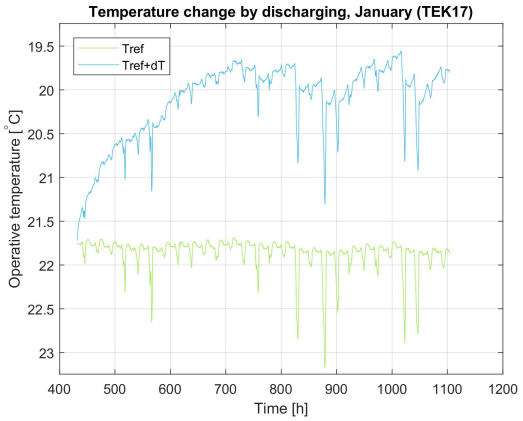

(b) Closed/open loop temperatures.

Figure 5.30: Graphs obtained for discharging by using operative temperatures (TEK17 model, January).

Chapter 6

Analysis

6.1 Potential for charging/discharging

The potential for charging and discharging was restricted by thermal comfort considerations, in terms of limiting the change in indoor temperature to ± 2°C during the thermal mass activation. Depending on the both the particular model variation, and the particular month in which was simulated, the potential for charging and discharging varied. The low insulated model had potential for both charging and discharging in all months, except for March where only charging was possible. Generally, the allowed deviation from the reference heat load was found to be 4-6%.

As previously mentioned, highly insulated buildings naturally have a shorter heating season, and this was also reflected in the results. Due to the generally low heating demand, discharging was only possible in the coldest months of the heating season for the high insulated models. The allowed deviation from the reference heat load were found to be 7-8% for the TEK10 model and 6-7% for the TEK17 and passive house models.

From the literature study in Chapter 3.4, it was argued by Le Dréau & Heiselberg that charging of a passive house may lead to overheating. A slightly lower potential for the TEK17 and passive house model was also found here. The heating systems in the TEK10 and TEK17 models were equally sized, and the insulation levels were quite similar. The reason for obtaining a slightly higher potential deviation in the TEK10 model may be explained by it having higher losses through the building envelope due to lower energy performance. More heat can thus be injected without causing a large temperature rise, because the heat will quickly be lost to the wall structures. This is also shown by the thermal inertia, which is lower in the TEK10 model than the other high insulated models. This means that the reaction to temperature change happens more quickly. The TEK87 model showed a slightly lower potential for charging, which was influenced by the generally high heating demand. In order to stay within the defined restriction, the increase in heat had to be limited.

Great fluctuations in the reference heat load profiles made it difficult to obtain valid results for discharging in the high insulated models. In an attempt to keep the heat load within the limit defined in Chapter 4.4.2, the main simulation period was reduced. As a result, the step response could not reach steady state. In the months of January and November, a compromise was therefore introduced. By violating the lower defined limit of heat load

near the end of the month, steady state could be obtained. Reasonable results were also obtained in these cases. An uncertainty is related to how IDA ICE handled this scenario. By violating the limit, negative control signals would go back into the ideal heater in the open loop simulation. It seems that IDA ICE may have corrected the negative signals to zero as the results were reasonable, but this was not confirmed. A test was made to violate the upper limit for a charging case in January. This showed similar results to the ones obtained by staying within the limit, which indicates that IDA ICE adjusted the heat signal.

Even though the TEK10 and TEK17 models in February showed some potential for discharging in figures 5.11a and 5.11b, a conscious decision was made not to violate the heat load limit in these cases. The reason being that more and higher fluctuations was observed earlier in the month, and the violation would be greater, and over a longer time period, than for the cases in January and November. Hence, discharging were disregarded in these models.

Except for the high insulated models in January and November, it was achieved to stay within the defined limit for heating load in every simulation scenario. Cases in which would cause a violation, were disregarded. This was true both for charging and discharging.

6.2 Evaluation of the step responses

Based on the graphs obtained for the step responses, the second-order model fits the step response from IDA ICE more accurately than the first-order model. This is can be observed in the graphs obtained for the TEK87 model in February (figure 5.13), and for the TEK87 model in November (figure 5.23). In both cases, the second-order model better fits the step response at the beginning of the period. As explained in Chapter 4.1.2, the second-order model is able to capture both the slow dynamics and the fast dynamics because it has two time constants. The first-order model lacks the fast dynamics as it only has one time constant, and cannot follow the step response from IDA ICE until some time has passed.

Whenever the start step for the charging and discharging cases were defined to be the same, or just two-three days apart, similar symmetry was observed in the graphs for the step responses. Note that the graphs for discharging were inverted, and are thus mirrored. In the graphs obtained for the high insulated models in January, a clear symmetry is observed between the charging and discharging cases.

In cases with a larger deviation between the start steps, the graphs seemed to be less symmetrical. An example of this was shown in figures 5.25 and 5.26, which presented the step responses for the TEK10 and TEK17 models in November. In this case, the main simulation time for discharging were shorter. By examining this particular time period in the graphs for charging, it is in fact quite similar to the discharging graph, which has just been stretched out due to the shorter time frame. Hence, symmetry are also to some extent obtained in these cases.

The assumption made in Chapter 4.1.1 related to the model formulation, can now be evaluated. The obtained symmetry of the charging/discharging graphs, along with the fact that the curve of the step responses resembles the desired form presented in Chapter 4.1.1, proves that the step response is independent of the outdoor temperature, solar radiation and internal heat gains.

6.3 General trends for the parameters

Overall heat transfer coefficient

From a building physics perspective, the highest values of the parameter U should be observed in the low insulated model, due to higher losses through the building envelope. With increasing insulation levels, this parameter should decrease. This was also found to be the general trend in the results from Chapter 5.7, where the highest U-values were obtained for the TEK87 model, and the lowest U-values were obtained for the passive house model. Even though the insulation levels in the TEK10 and TEK17 models are quite similar, the difference in energy performance resulted in slightly higher U-values in the TEK10 model, as expected.

The obtained U-values for the TEK87 model were quite consistent, at about 125-130 W/K for both the charging and discharging cases. Additionally, the obtained values for the first-order and second-order models were quite similar in all months. However, the month of January stands out as having a relatively high value for charging, and a slightly lower value for discharging compared to the general trend. The deviation is highest for the charging case of the first-order model. Figure 5.7a shows that the step response of the first-order model deviates from the step response obtained by IDA ICE to a greater extent, than in the other months (October, November). This ”poor” model fitting may be the reason for the deviating result. The second-order model fits the step response better, and the U-value in this case is more similar to the general trend. Another reason could be the restrictions related to the duration of simulation time in IDA ICE, which will be explained later in this chapter. Basically, January was the only month where the main simulation time had to be limited to one month for the TEK87 model. As seen in table 5.2, the initialization phase for the discharging case were limited to three days, which may explain the deviating result for the discharging case.

For the TEK10 model, the obtained U-values was found to be 70-80 W/K, and were quite similar for the first-order and second-order models within each month. November and December stands out as having a larger deviation between the charging and discharging cases. The potential of charging were higher than the potential for discharging in both months, which can be seen in figure 5.27 for December and in figure 5.25 for November. When charging, heat is lost from the indoor environment to the surrounding walls, and when discharging, heat stored in the walls is lost to the indoor environment. In both cases, this happens to even out the temperature between the wall surface and indoor air. Higher changes in heat load causes higher changes in temperature, and thus higher losses is caused to even out the temperature. This may explain why U is higher for the charging cases.

The obtained U-values for the TEK17 model ranged between 60-70 W/K in most of the simulated months, and for both the first-order model and second-order model. The values obtained for March was slightly higher, and the values obtained for February were slightly lower. Figure 5.12b shows great fluctuations in indoor temperature for February, and figure 5.16a shows similar trends for the temperatures in March (the TEK10 and TEK17 models had quite similar temperature graphs). These fluctuations may affected the results. For the passive house model, the obtained U-values was found to be 48-54 W/K, and were quite similar for the first-order and second-order models within each month.

Time constants

Based on the theory presented in Chapter 3.1.6, the time constants were expected to be lowest in the low insulated building, and increase with higher insulation levels. This was also found to be the general trend in the results. Based of the values obtained from the first-order model, the low insulated model had an average time constant of 40 hours. For the high insulated models, the average time constant was 80 hours for the TEK10 model, 100 hours for the TEK17 model, and 150 hours for the passive house model.

Generally, the second-order model provided higher time constants (τ_1) than the first-order model. In this case, the low insulated model had an average time constant of 50 hours. For the TEK10 and TEK17 models the average time constants were 100 hours and 125 hours respectively. The average time constant of the passive house model was however the same.

As previously mentioned, the second-order model is able to capture different reaction times of buildings, and will thus have different results for the time constants compared to the first-order model. The second time constant obtained with the second-order model generally ranged between 0.5-2 hours. Some exceptions were observed, such as for the TEK17 model in November (discharging), and the TEK10 model in March (charging). However, this is just reflections of how some phenomenons in buildings happens fast, while others develops are more slowly.

Thermal capacitance

The thermal capacitance determines the amount of heat that can be stored within the thermal mass. From the results, the values of thermal capacitance ranged from 4000 - 8000 Wh/K. These parameters were obtained by using equation 3.13 in the MATLAB routine for the first-order model, and are thus dependent on the parameters of U and τ obtained from the model fitting. This explains why there are some deviations from the general trend. For the TEK10 model in February, the high time constant results in the high thermal capacitance. Similar cases are found for the TEK17 model in January and October.

6.4 Evaluation of the guidelines

It was early recognized that the model parameters were sensitive to the duration of both the initialization phase and the main simulation period. The defined guidelines in Chapters 4.4.1 and 4.4.3 were thus valuable for being consistent in all the different simulation cases. The guidelines were defined based on the physical knowledge about buildings. High insulated buildings have a longer ”memory” of what has happened in the past due to their high time constants. It follows that the high insulated models would require a longer initialization period to establish a good reference case. On the other hand, low insulated buildings have a shorter ”memory” of what has happened in the past, due to their low time constants. The low insulated model should then have a shorter initialization period. By having a well defined initialization period, valid results could more easily be obtained.

The guidelines could however not be followed in all simulation cases. The main simulation

period of the closed loop simulation had to be extended to three months for all the high insulated models in March, and for the passive house model in October, in order to get valid results. The duration of the initialization phase for the open loop simulation had to be reduced to just a few days to obtain valid results in some months. This were especially true for the month on January.

The main simulation period defined in the closed loop simulation determines the period in which the initialization phase and main simulation can be defined in the open loop simulation. This is best explained by showing an example. Table 6.1 shows the defined initialization phase and main simulation period defined for the TEK87 model in March, for both the closed loop and open loop simulations.

Table 6.1: Example of defined simulation period for the TEK87 model in March.

	Closed loop	**Open loop**
Main	15.02.15 - 31.03.15	01.03.15 - 31.03.15
Initialization	14.01.15 - 14.02.15	15.02.15 - 28.02.15

From the given example, the first possible date to choose for the initialization phase in the open loop simulation is the 15th of February, as this is the first date defined for the main simulation in the closed loop. Similarly, the last possible date to choose for the main simulation period in the open loop is the 31st of March. This particular way of defining the duration of the simulations were used for the TEK87 model in all months, except for January. IDA ICE would not run the open loop simulation when starting from the 15th of December in the closed loop simulation. By initializing from December 2014, the hourly number for the first hour in January is 8761, and not 0. The main simulation in the closed loop was thus started from the 1st of January. This also had to be done in order to simulate the high insulated models, which is reflected by short initialization phases for the open loop simulation in table 5.2.

6.5 Robustness of the routine

A weighing between being consistent and obtain results that would fit the pattern was done throughout the simulations. In general, the parameters U, τ_1 and τ_2 increased by having a longer main simulation time in time the charging cases. By adjusting the main simulation time down, these parameters decreased. For the discharging cases, the opposite was true. Valid results could in fact be obtained in several ways for some cases. Which result to use was determined based on obtaining the smallest deviation between T_{ref} and $T_{ref} \pm dT$, following the guidelines, and if the results were reasonable in the context of the model variation and the particular month. However, this indicates how the results could be manipulated to fit a certain pattern.

The same MATLAB script was used to perform the different steps related to both the closed loop simulation and open loop simulation. This could affect the results if the work was not saved correctly between the steps. Additionally, the initial guess made related to the nlinfit function was not always intuitive. Several guesses for the time constant were sometimes required to complete the iteration process.

Due to the explained factors, the routine in both IDA ICE and MATLAB must be performed with great attention to details. The robustness of the routine may not be optimal. One measure to improve the robustness would be to separate the steps related to the closed loop simulation, and the steps related to the open loop simulation into two MATLAB scripts.

6.6 Temperature fluctuations

Based on the information given in Chapter 3.1.6, it was expected that the high insulated models would have less temperature fluctuations during the thermal mass activation. In January, the passive house model had less temperature fluctuations than the TEK17 model. This was however not always the case, and particularly large fluctuations in indoor temperature was observed for the high insulated models in February and March. This could be a result of how the building model in IDA ICE were initially designed. One source of error is the lack of external shading. As the building is faced south, solar radiation passing through the windows is a great source of heat during the day. According to table 4.1, both February and March are characterized by high amounts of solar radiation.

The shading controllers were removed to keep the system constant throughout the simulations. In further work, some type of constant shading should be installed to study if this could reduce the temperature fluctuations. An example would be to use half-closed internal blinds, to ensure some daylight access.

6.7 Thermal comfort

As explained in Chapter 3.3.1, several factors influence the thermal comfort of occupants. It is challenging to evaluate this correctly based on the simulation results, as there are no indications given for local discomfort. The approach of evaluating the thermal comfort was therefore to use the deviation in temperature as a constraint when determining the allowed deviation in heat load. A perquisite for allowing this deviation was however that occupants are willing to actively adapt to their thermal environment. Additionally, the time in which the temperature changes evolved could be analysed and compared to the requirements given in 3.3.2.

From analysing the temperature curves for the different months, it was found that the temperature changes generally evolved over several hours. Even for the TEK10 model in March, shown in figure 5.16a, the changes happened over the course of 6-7 hours. This is within the stated requirements. Generally, a decrease in temperature can be experienced as worse than an increase in temperature. Figure 5.8b showed the discharging case of the TEK17 model in January. The largest spike represents a decrease of 1°over the course of three hours, which is also within the stated requirements. This case where further chosen to study the change in operative temperatures versus air temperatures. From the graphs provided in Chapter 5.8, the deviation in temperature were still kept within the defined limit of ± 2°C. Additionally, the requirement of keeping the operative temperature within the range of 22 ± 2°C, were achieved when disregarding the occasional spikes. Similar trends were observed in other months and model variations.

Chapter 7

Model validation

For validation of the model accuracy, a new routine was made to be able to compare indoor temperatures obtained by the first-order and second-order models, with indoor temperatures computed by IDA ICE. This routine was developed by the supervisor [69], and includes two MATLAB scripts which are attached in Appendix C. In the following subchapters, a description of the routine and an analysis of the results are presented.

Modification of heat load

The first part of the script attached in Appendix C.1 was made to simulate how heat load could potentially be adjusted in relation to peak load hours. Instead of optimizing the heat load to minimize costs, as it could be in energy planning models, it was simply modified by a defined schedule.

Peak load hours were defined between 7-10 AM and 5-8 PM. Two hours prior to these peaks, the heating power was increased to pre-heat the building, which enabled a reduction in heat load during the peak hours without affecting the thermal comfort. The schedule of adjusting the heat load is summarized in the following list:

- From 5-7 AM: Pre-heat the building by increasing the heating power ($P_{sh}^{R} + dP$)
- From 7-10 AM: Reduce the heating power ($P_{sh}^{R} - dP$)
- From 3-5 PM: Pre-heat the building by increasing the heating power ($P_{sh}^{R} + dP$)
- From 5-8 PM: Reduce the heating power ($P_{sh}^{R} - dP$)

This sequence was repeated every day for three weeks, and the resulting heat load profile was used as input to the open loop simulation in IDA ICE. Figure 7.1 presents this approach as a block diagram, where the new indoor temperatures obtained with the modified heat load are the desired output.

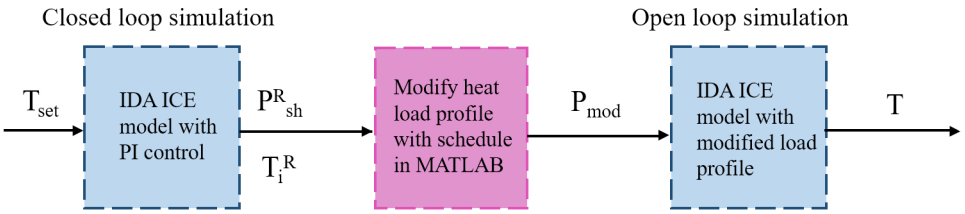

Figure 7.1: Block diagram of the approach in IDA ICE.

The same restriction introduced for the modification of heat load in Chapter 4.4.2 were used in this case, in which the new power could not exceed the defined nominal power of the particular model variation, or be reduced below zero.

State space models

In order to predict indoor temperatures with the first-order and second-order models, they were defined in terms of state space models in MATLAB [84]. This was done in the second part of the script attached in Appendix C.1. Note that the detailed approach used to define the second-order model is excluded from the script, as this is planned to be published in a scientific paper.

For the first-order model, the step response parameters (U_{tot}, C, τ_1) were converted into a first-order state space model. For the second-order model, the step response parameters (U_{tot}, τ_1, τ_2, α_1) were converted into a second-order state space model [69]. In both cases, the identified model parameters were used as input to compute the temperatures.

Analysis

Based on the results obtained in Chapter 5, the month of January was chosen for the validation. In this month, there was a potential for both charging/discharging in every model variation, and the step responses of charging and discharging were fairly symmetric. To compute temperatures with the first-order and second-order models, the identified parameters related to discharging were chosen as input.

The reference heat loads for each model variation were modified according to the defined schedule. Figure 7.2 shows the heat load schedule obtained for the TEK17 model. The new heat load profile used as input to the open loop simulation in IDA ICE is shown in figure 7.3. Note that heating power is within the defined restriction. The open loop simulation were run with the originally defined initialization phase and main simulation for the TEK17 model.

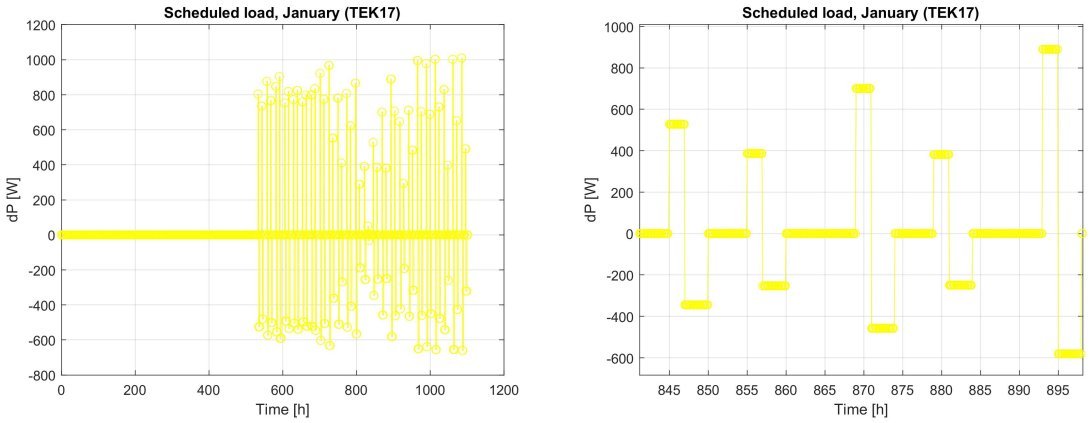

(a) Entire period. **(b)** Two days.

Figure 7.2: Heat load according to the defined schedule in MATLAB.

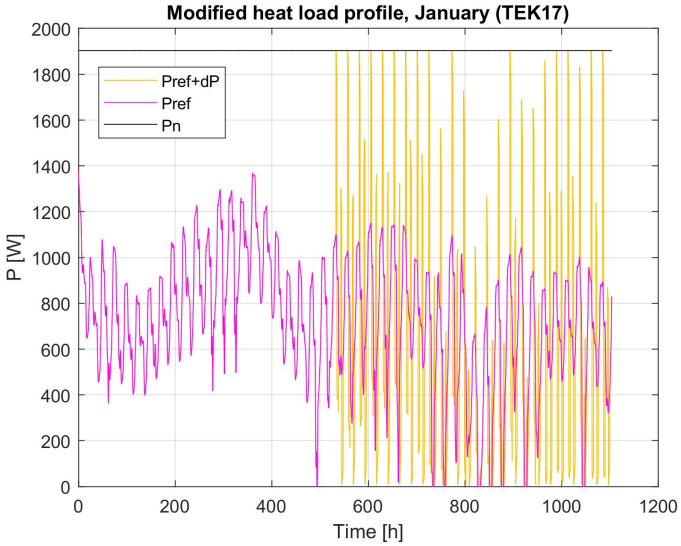

Figure 7.3: Modified heat load profile, used as input to the open loop simulation in IDA ICE.

After completing the open loop simulations, the resulting indoor temperatures from IDA ICE were imported back into MATLAB, and plotted against the temperatures computed by the models. This was done by using the script attached in Appendix C.2.

The model accuracy could be validated if the temperatures obtained by any of the models were equal to the temperatures computed by IDA ICE. Figures 7.4, 7.5 and 7.6 shows the temperatures obtained for the high insulated building models. Each figure consists of two graphs, where the first represents the temperatures obtained in the beginning of the simulated period, and the second represents the temperatures obtained at the end of the period.s

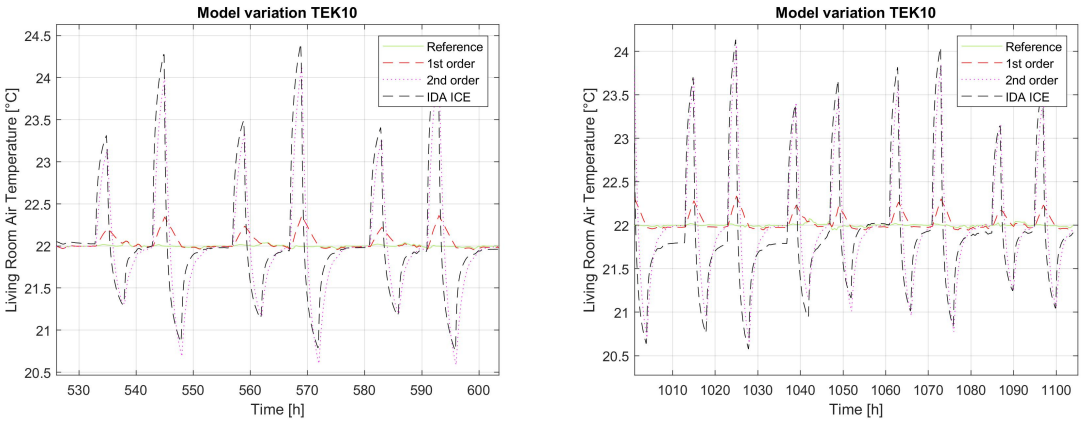

(a) Beginning of period. **(b)** End of period.

Figure 7.4: Comparison of temperatures obtained for the TEK10 model.

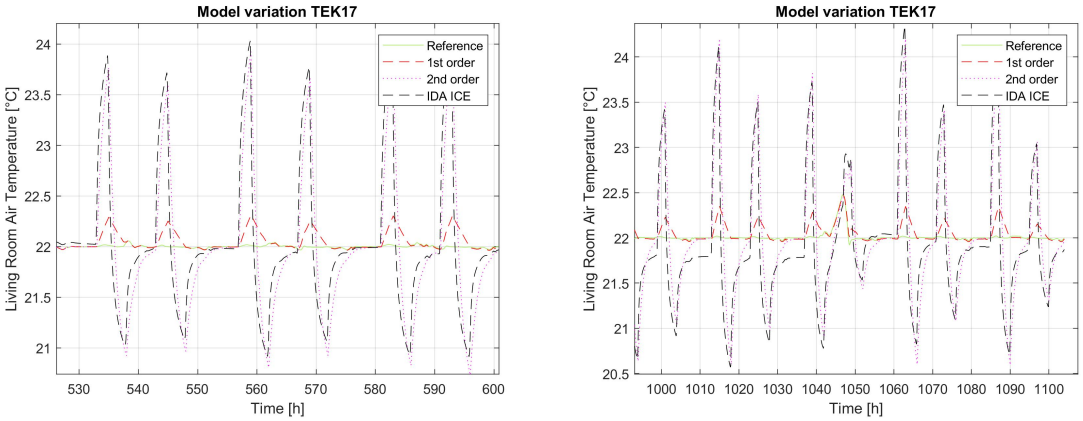

(a) Beginning of period. **(b)** End of period.

Figure 7.5: Comparison of temperatures obtained for the TEK17 model.

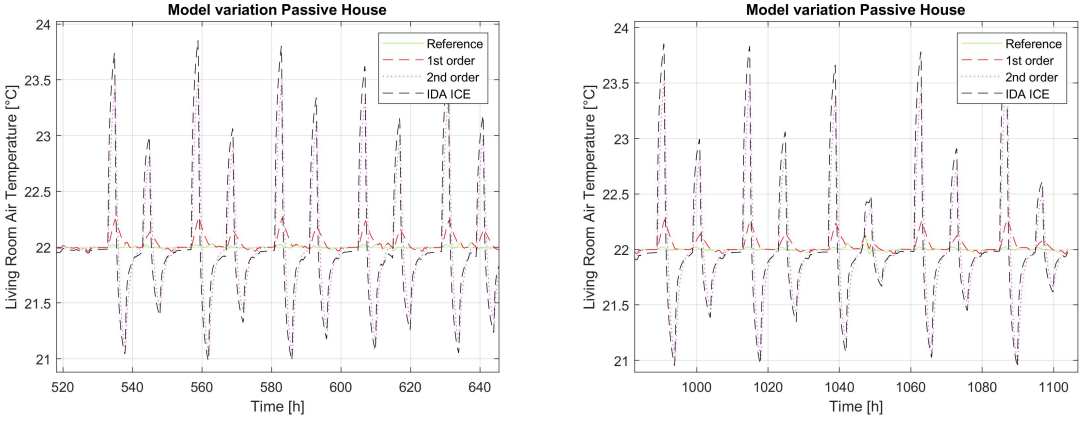

(a) Beginning of period. **(b)** End of period.

Figure 7.6: Comparison of temperatures obtained for the passive house model.

It is evident that the first-order model is not able to follow the temperatures obtained by IDA ICE in any of these model variations. On the other hand, the deviation between the obtained temperatures by IDA ICE and the second-order model is at most 0.2-0.3°C. This is shown in figures 7.7 and 7.8.

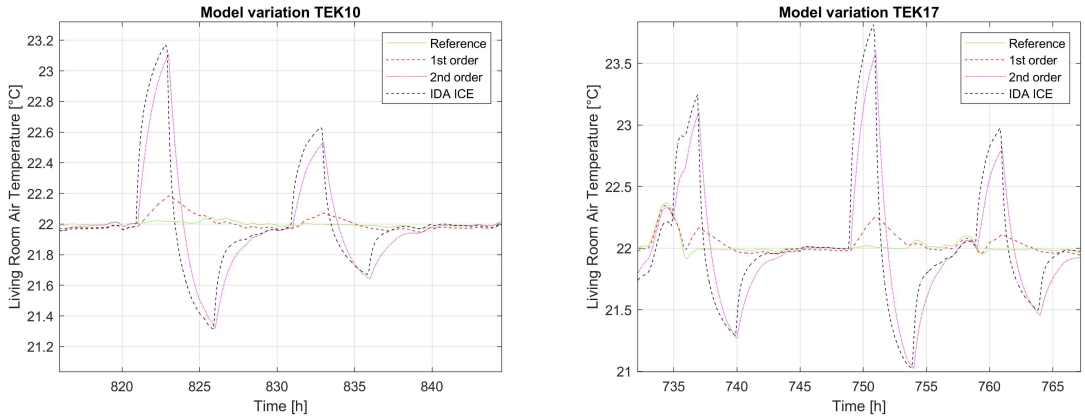

(a) TEK10 model. **(b)** TEK17 model.

Figure 7.7: Closer image of the temperatures obtained for the TEK10 and TEK17 models.

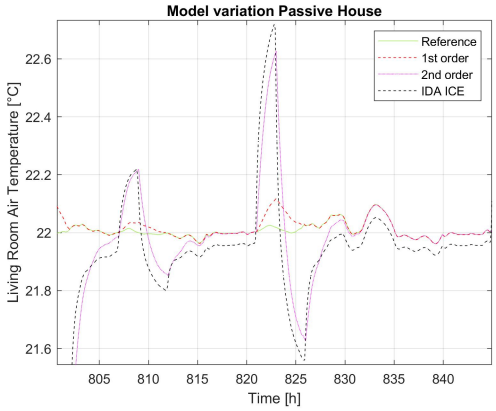

Figure 7.8: Closer image of the temperatures obtained for the passive house model.

Figure 7.9 shows the temperatures obtained for the low insulated building model. Similarly as for the high insulated models, the first-order model fails to follow the temperatures obtained by IDA ICE, while the second-order model shows more promising tendencies.

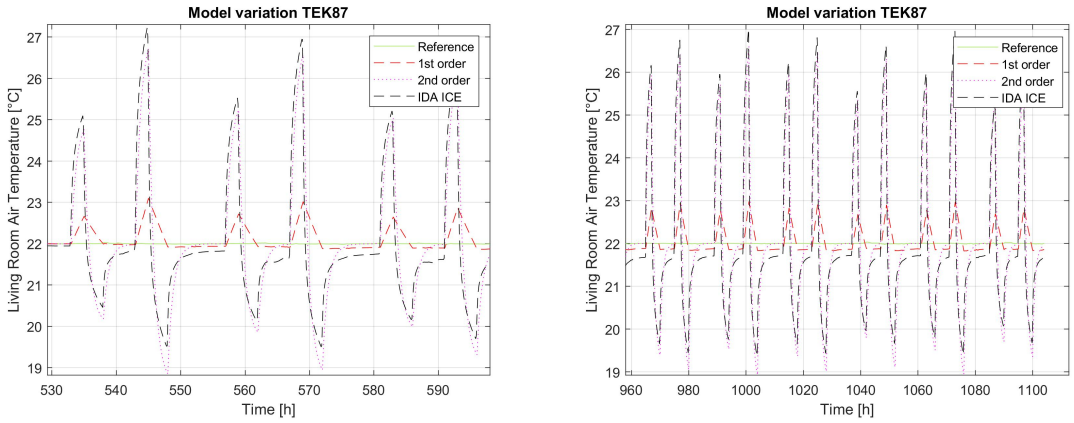

(a) Beginning of period. **(b)** End of period.

Figure 7.9: Comparison of temperatures obtained in the TEK87 model.

The deviation between the temperatures from IDA ICE and the second-order model is slightly higher compared to the high insulated buildings, at 0.5-0.6°C. This is shown in figure 7.10. However, this deviation is still small compared to the first-order model.

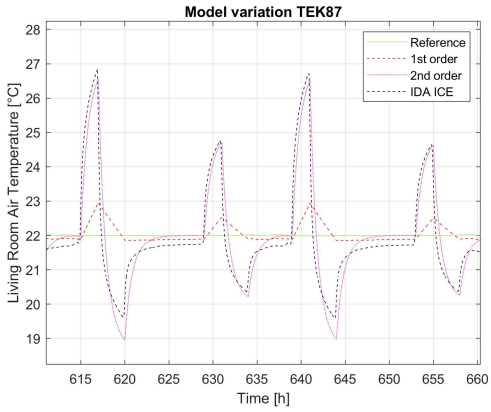

Figure 7.10: Closer image of the temperatures obtained for the TEK87 model.

Due to its general model structure, the first-order model cannot capture the fast dynamics, and is thus not accurate enough to predict the indoor temperature. The second-order model have two time constants, which makes is capable of capturing both the slow and fast dynamics. This is also shown by the fact that the small deviation from the IDA ICE temperature is kept constant from the very beginning of the period, and over the course of three weeks.

Based on the obtained results, it is shown that the second-order model is able to quite accurately follow the IDA ICE temperatures in all the variations of the building. The trade-off between accuracy and model complexity is as expected [69]. It is fair to conclude that this modelling approach has been proved to work, both in the short-term and long-term. The second-order model can therefore potentially be used for representing buildings in energy system analysis.

Chapter 8

Conclusion

The demand response potential of space heating load in Norwegian residential buildings was studied in the work of this thesis. By utilizing the thermal mass embedded in buildings for thermal energy storage, the electric consumption related to space heating load can be shifted to periods with lower energy demand. How much heating load that could be shifted in time, without compromising thermal comfort, was identified by using a combination of dynamic simulations in IDA ICE and MATLAB. Four variations of the building model used for the simulations were made, to study how indoor temperature fluctuations and model parameters were affected by insulation levels and energy performance. The model variations were defined based Norwegian standards and regulations, including TEK87, TEK10, TEK17 and the passive house standard.

Each model variation was simulated for each month of the heating season, defined to be from January-March and October-December. It was found that choosing a sufficient initialization phase for the simulations was decisive in order to obtain valid results. The high insulated models required a longer initialization phase than the low insulated model, which is natural due to the related time constants of the buildings.

The low insulated model had potential for both charging and discharging in nearly all months, and the allowed deviation from the reference heat load was 4-6%. Due to the generally low heating demand, discharging were only possible in the coldest months of the heating season for the high insulated models. The allowed deviation from the reference heat load were found to be 7-8% for the TEK10 model and 6-7% for the TEK17 and passive house models. By analysing the temperature curves for the different months, it was found that thermal comfort could be maintained during thermal mass activation.

Two simplified models to represent buildings in energy system analysis were investigated, including a first-order model and a second-order model. Related step response equations were derived, and implemented into MATLAB. Fitting the models to the step response in IDA ICE were done by non-linear regression. From the results it was found that the second-order model fitted the step response obtained by IDA ICE more accurately than the first-order model. The curves of the step responses had a desirable form, and good symmetry was found for the charging/discharging responses. This proved the assumption that the step response is independent of the outdoor temperature, solar radiation and internal heat gains.

The demand flexibility was characterized by identifying the model parameters. For the first-

order model, these included the overall heat transfer coefficient, thermal capacitance and one time constant (U, C, τ). For the second-order model, these included the overall heat transfer coefficient, two time constants, and a weighting factor between the time constants (U, τ_1, τ_2, α_1). The U-values were consistently high in all months for the TEK87 model. This was expected, due to the amount of losses in low insulated buildings. With increasing insulation levels and energy performance, the U-values decreased, which is also expected as the heat losses are restricted in high insulated buildings. Apart from some exceptions, the U-values were quite consistent for the first-order and second-order models, in both the charging and discharging cases. The time constants were found to increase with higher insulation levels, where the average value was 40 hours in the TEK87 model, and 150 hours for the passive house model. Generally, the second-order model provided higher time constants (τ_1) than the first-order model in all model variations, and for every month. The second-order model is able to capture different reaction times of buildings, and will thus have different results for the time constants compared to the first-order model.

From the validation of model accuracy versus IDA ICE, it was found that due to the lack of fast dynamics, the first-order model could not obtain similar temperatures to those computed by IDA ICE. The second-order model could however obtain close to similar temperatures, with a deviation of 0.2-0.3°C for the high insulated models, and 0.5-0.6°C for the low insulated model. Over the course of three weeks, the deviation was still not changing. The second-order model is thus able to fairly predict the indoor temperature in buildings, both in the short term and in the long term. The modelling approach is thus proved to work, and the second-order model can potentially be used to represent buildings and their flexibility in energy planning models.

Further work

There is still a need to characterize the demand response potential of heat load in other building types, but with some modifications the proposed simulation approach can also be used to study any other non-residential buildings. The simplified model formulation can also be applied for other building types.

To limit the scope of this work, the analysis of indoor temperature and change in heating load were restricted to one zone of the building model. For further work, it could be interesting to study how including more parts of the building would affect the heat load analysis and the model parameters. The simulation approach can easily be extended to include multiple zones. As the control system in the open loop simulation is already made to include input signals for all zones, the only change would be to extend the script in MATLAB to modify the inputs for every zone.

Further improvements on the building model in IDA ICE may help to obtain smoother curves for the indoor temperature, and avoid some of the temperature fluctuations observed in the results.

References

1. StatKraft. Strategi: Kraft til en grønn fremtid. 2020. Available from: https://www.statkraft.no/om-statkraft/strategi/. (Accessed on 27/05/2020)
2. Albadi MH and El-Saadany EF. A summary of demand response in electricity markets. Electric Power Systems Research 2008; 78:1989–1996
3. Kolokotsa D. The role of smart grids in the building sector. Energy and Buildings 2016; 116:703–708
4. Jensen SØ, Marszal-Pomianowska A, Lollini R, Pasut W, Knotzer A, Engelmann P, et al. IEA EBC Annex 67 Energy Flexible Buildings. Energy and Buildings 2017; 155:25–34
5. Li R and You S. Exploring potential of energy flexibility in buildings for energy system services. CSEE Journal of Power and Energy Systems 2018; 4:434–443
6. Junker RG, Azar AG, Lopes RA, Lindberg KB, Reynders G, Relan R, et al. Characterizing the energy flexibility of buildings and districts. Applied Energy 2018; 225:175–182
7. Lopes RA, Chambel A, Neves J, Aelenei D, and Martins J. A Literature Review of Methodologies Used to Assess the Energy Flexibility of Buildings. Energy Procedia 2016; 91:1053–1058. Available from: http://dx.doi.org/10.1016/j.egypro.2016.06.274
8. De Coninck R and Helsen L. Quantification of flexibility in buildings by cost curves - Methodology and application. Applied Energy 2016; 162:653–665. Available from: http://dx.doi.org/10.1016/j.apenergy.2015.10.114
9. Le Dréau J and Heiselberg P. Energy flexibility of residential buildings using short term heat storage in the thermal mass. Energy 2016; 111:991–1002
10. Reynders G, Diriken J, and Saelens D. A generic quantification method for the active demand response potential of structural storage in buildings. 14th International Conference of IBPSA - Building Simulation 2015, BS 2015, Conference Proceedings 2015 :1986–1993
11. Zhang K and Kummert M. Potential of building thermal mass for energy flexibility in residential buildings : a sensitivity analysis. Proceedings of eSim 2018, May 9-10, 2018 2018 :163–172
12. Six D, Desmedt J, Bael JVAN, and Vanhoudt D. Exploring the Flexibility Potential of Residential Heat Pumps. 21st International Conference on Electricity Distribution 2011 :6–9

13. D'hulst R, Labeeuw W, Beusen B, Claessens S, Deconinck G, and Vanthournout K. Demand response flexibility and flexibility potential of residential smart appliances: Experiences from large pilot test in Belgium. Applied Energy 2015; 155:79–90

14. Spilde D, Lien SK, Ericson TB, and Magnussen IH. Strømforbruk i Norge mot 2035. NVE report 2018; 43. Available from: www.nve.no

15. Novakovic V, Bolland O, Ulseth R, Hustad J, Gundersen T, Berg T, et al. TEP4225 Energi og Miljø. NTNU, 2014 :48–57

16. Wangensteen I. Power System Economics - the Nordic Electricity Market. 2nd ed. Chapter 5.5 Roles and responsibilities in a restructured system. Fagbokforlaget, 2012 :80–85

17. Energifakta-Norge. Security of Electricity Supply. 2019. Available from: https://energifaktanorge.no/en/norsk-energiforsyning/forsyningssikkerhet/. (Accessed on 27/11/2019)

18. Statkraft. Dette bør du vite om vindkraft i Norge. 2019. Available from: https://www.statkraft.no/Energikilder/Vindkraft/fordeler-med-vindkraft/. (Accessed on 27/11/2019)

19. NVE. Solkraft. 2019. Available from: https://www.nve.no/energiforsyning/kraftproduksjon/solkraft/?ref=mainmenu. (Accessed on 27/11/2019)

20. Statnett. Fleksibilitet i det nordiske kraftmarkedet, 2018-2040. 2018. Available from: https://www.statnett.no/globalassets/for-aktorer-i-kraftsystemet/planer-og-analyser/2018-Fleksibilitet-i-det-nordiske-kraftmarkedet-2018-2040. (Accessed on 29/05/2020)

21. CINELDI. FME II - CINELDI. The figure is used with permission from Gerd H. Kjølle. 2016. Available from: https://www.sintef.no/prosjekter/cineldi/. (Accessed on 25/04/2020)

22. Kjølle GH. Fremtidens elektriske energisystem (smart grids) og forsyningssikkerhet. 2019. Available from: https://www.sintef.no/globalassets/project/vulnerability-and-security/publications/papers/artikkel_gkj_fremtidens-elektriske-energisystem.pdf/. (Accessed on 25/04/2020)

23. SINTEF. eTransport. 2014. Available from: https://www.sintef.no/en/projects/etransport/. (Accessed on 25/04/2020)

24. Bakken BH, Skjelbred HI, and Wolfgang O. eTransport: Investment planning in energy supply systems with multiple energy carriers. Energy 2007; 32:1676–1689

25. Askeland M. Personal communication. PhD Fellow at SINTEF Energy Research, Department of Energy Systems. Co-supervisor for this thesis

26. Incorpera FP, Dewitt DP, Bergman TL, and Lavine AS. Incropera's Principles of Heat and Mass Transfer. 8, Global edition. Wiley, 2017 :2–11

27. Thue JV. Bygnigsfysikk Grunnlag. 1st ed. Figure 2.8.1, Prinsipper for varmeoverføring; p. 53. Fagbokforlaget, 2016 :53

28. Thue JV. Bygnigsfysikk Grunnlag. 1st ed. Kapittel 2, Fysikalsk grunnlag. Fagbokforlaget, 2016 :39–82

29. Thue JV. Bygnigsfysikk Grunnlag. 1st ed. Kapittel 4, Varmelære. Fagbokforlaget, 2016 :149–253

30. Direktoratet-for-Byggkvalitet. Byggeforskrift 1987. 1987. Available from: https://dibk.no/globalassets/byggeregler/tidligere_regelverk/historisk-arkiv-1949---1987/byggeforskrift-1987.pdf

31. Direktoratet-for-Byggkvalitet. Byggteknisk forskrift (TEK10). 2011. Available from: https://dibk.no/byggeregler/tek/

32. Direktoratet-for-Byggkvalitet. Byggteknisk forskrift (TEK17) med veiledning. 2017. Available from: https://dibk.no/byggereglene/byggteknisk-forskrift-tek17/

33. Standard-Norge. NS 3700 Kriterier for passivhus og lavenergibygninger - Boligbygninger. 2013. Available from: https://www.standard.no/nyheter/nyhetsarkiv/bygg-anlegg-og-eiendom/2013/ns-3700-kriterier-for-passivhus-og-lavenergihus---boligbygninger/

34. Antonopoulos KA and Koronaki E. APPARENT AND EFFECTIVE THERMAL CAPACITANCE OF. 1998; 23:183–192

35. Lillestøl E, Hunderi O, and Lien JR. Generell fysikk for universiteter og høgskoler - Bind 2 Varmelære og elektromagnetisme. 2nd ed. Universitetsforlaget, 2006 :21–171

36. Haase M and Andresen I. Thermal Mass Concepts - State of the art. Sintef Building and Infrastructure, Concrete Innovation Centre. 2007. Available from: https://www.sintef.no/globalassets/sintef-byggforsk/coin/sintef-reports/sbf-bk-a07030_thermal-mass-activation.pdf. (Accessed on 02/10/2019)

37. Saulles T de. Thermal Mass Explained. MPA - The concrete Centre. 2012. Available from: https://www.concretecentre.com/Performance-Sustainability-(1)/Thermal-Mass.aspx. (Accessed on 14/11/2019)

38. Sintef-Byggforsk. Termisk masse og klimatisering av bygninger. 2007. Available from: https://www.arkitektur.no/?nid=160747. (Accessed on 02/10/2019)

39. Verbeke S and Audenaert A. Thermal inertia in buildings: A review of impacts across climate and building use. Renewable and Sustainable Energy Reviews 2018; 82:2300–2318

40. NTNU and SINTEF. Energy Efficiency in Buildings – sustainable energy use. Trans. by LivLaga-SA. Vol. 3. English translation of the Norwegian textbook ”Enøk i bygninger - effektiv energibruk”. Gyldendal undervisning, 2007 :113–125

41. Bonilauri E. What’s the “time constant” of a building? 2015. Available from: https://emu.systems/2015/10/19/whats-the-time-constant-of-a-building/. (Accessed on 02/10/2019)

42. NTNU and SINTEF. Energy Efficiency in Buildings – sustainable energy use. Trans. by LivLaga-SA. Vol. 3. English translation of the Norwegian textbook ”Enøk i bygninger - effektiv energibruk”. Gyldendal undervisning, 2007 :393–396

43. NTNU and SINTEF. Energy Efficiency in Buildings – sustainable energy use. Trans. by LivLaga-SA. Vol. 3. Figure 7.4.3, Temperature development in a room where the thermal load increases suddenly after having been constant. Gyldendal undervisning, 2007 :396

44. Hagen H. Oppvarming av boliger. Energiforbruk og kostnader - Byggforskserien. Tech. rep. 552.103. SINTEF Byggforsk, 1990

45. Standard-Norge. SN/TS 3031:2016 for beregning av energibehov og energiforsyning. 2017. Available from: https://www.standard.no/nyheter/nyhetsarkiv/bygg-anlegg-og-eiendom/2016/snts-30312016-for-beregning-av-energibehov-og-energiforsyning/

46. Sarbu I and Sebarchievici C. A comprehensive review of thermal energy storage. Sustainability (Switzerland) 2018; 10

47. Johra H, Heiselberg P, and Dréau JL. Influence of envelope, structural thermal mass and indoor content on the building heating energy flexibility. Energy and Buildings 2019; 183:325–339

48. Cabeza LF. Thermal Energy Storage. *In: Comprehensive Renewable Energy*. Ed. by Sayigh A. Vol. 3. Figure 1, Steps involved in a complete TES system: charging, storing, and discharging; p. 213. Elsevier, 2012 :211–253

49. Mysen M. Termisk inneklima. Betingelser, tilrettelegging og målinger - Byggforskserien. Tech. rep. 421.501. SINTEF Byggforsk, 2017

50. Athienitis AK and O'Brien W. Modeling, Design, and Optimization of Net-Zero Energy Buildings. 5th ed. John Wiley & Sons Inc, 2015 :78–85

51. ASHRAE-Standard-55-2004. Thermal Environmental Conditions for Human Occupancy. American Society of Heating, Refrigerating and Air-Conditioning Engineers, Inc. 2004

52. Kensby J, Trüschel A, and Dalenbäck JO. Potential of residential buildings as thermal energy storage in district heating systems - Results from a pilot test. Applied Energy 2015; 137:773–781

53. Wolisz H, Harb H, Matthes P, Streblow R, and Müller D. Dynamic simulation of thermal capacity and charging/ discharging performance for sensible heat storage in building wall mass. *Proceedings of BS 2013: 13th Conference of the International Building Performance Simulation Association*. May 2017. 2013 :2716–2723

54. Foteinaki K, Li R, Heller A, and Rode C. Heating system energy flexibility of low-energy residential buildings. Energy and Buildings 2018; 180:95–108. Available from: https://doi.org/10.1016/j.enbuild.2018.09.030

55. Balchen JG, Andresen T, and Foss BA. Reguleringsteknikk. 6th ed. Institutt for tekniks kybernetikk, Norges teknisk-naturvitenskapelig universitet (NTNU), 2016 :33–40

56. Henze GP and Neumann C. Building simulation in building automation systems. *In: Building Performance Simulation for Design and Operation*. Ed. by Lamberts R and Hensen J. Routledge, 2011 :402–440

57. Xue X, Wang S, Sun Y, and Xiao F. An interactive building power demand management strategy for facilitating smart grid optimization. Applied Energy 2014; 116:297–310

58. Wang S and Xu X. Parameter estimation of internal thermal mass of building dynamic models using genetic algorithm. Energy Conversion and Management 2006; 47:1927–1941

59. Perera DW, Pfeiffer CF, and Skeie NO. Modelling the heat dynamics of a residential building unit: Application to Norwegian buildings. Modeling, Identification and Control 2014; 35:43–57

60. Bindner HW and Thavlov A. Thermal Models for Intelligent Heating of Buildings THERMAL MODELS FOR INTELLIGENT HEATING OF BUILDINGS. *Proceedings of the International Conference on Applied Energy*. 2012

61. Wolisz H, Harb H, Matthes P, Streblow R, and Müller D. Dynamic simulation of thermal capacity and charging/ discharging performance for sensible heat storage in building wall mass. *Proceedings of BS 2013: 13th Conference of the International Building Performance Simulation Association*. 2013 :2716–2723

62. Henze GP and Neumann C. Building simulation in building automation systems. *In: Building Performance Simulation for Design and Operation*. Ed. by Lamberts R and Hensen J. Figure 14.4, General structure of a model; p. 406. Routledge, 2011 :402–440

63. Foucquier A, Robert S, Suard F, Stephan L, Jay A, Foucquier A, et al. State of the art in building modelling and energy performances prediction : A review To cite this version : HAL Id : cea-01792021. Renewable and Sustainable Energy Reviews 2013; 23:272–288

64. Niu J, Tian Z, Lu Y, and Zhao H. Flexible dispatch of a building energy system using building thermal storage and battery energy storage. Applied Energy 2019; 243:274–287

65. Ferracuti F, Fonti A, Ciabattoni L, Pizzuti S, Arteconi A, Helsen L, et al. Data-driven models for short-term thermal behaviour prediction in real buildings. Applied Energy 2017; 204:1375–1387

66. Yu X, Georges L, Knudsen MD, Sartori I, and Imsland L. Investigation of the Model Structure for Low-Order Grey-Box Modelling of Residential Buildings. 2019 :5076–5083

67. Kramer R, Schijndel J van, and Schellen H. Simplified thermal and hygric building models: A literature review. Frontiers of Architectural Research 2012; 1:318–325

68. Derakhtenjani AS, Candanedo JA, Chen Y, Dehkordi VR, and Athienitis AK. Modeling approaches for the characterization of building thermal dynamics and model-based control: A case study. Science and Technology for the Built Environment 2015; 21:824–836

69. Georges L. Personal communication. Associate Professor at the Department of Energy and Process Engineering, Faculty of Engineering. Supervisor for this thesis

70. Andersen KK, Madsen H, and Hansen LH. Modelling the heat dynamics of a building using stochastic differential equations. Energy and Buildings 2000; 31:13–24

71. Lamberts R and Hensen J. Building Performance Simulation for Design and Operation. Routledge, 2011 :3–14

72. Augenbroe G. The role of simulation in performance based building. *In: Building Performance Simulation for Design and Operation*. Ed. by Lamberts R and Hensen J. Routledge, 2011 :15–36

73. Augenbroe G. The role of simulation in performance based building. *In: Building Performance Simulation for Design and Operation*. Ed. by Lamberts R and Hensen J. Figure 2.1, Performance testing requires a (virtual) experiment; p. 17. Routledge, 2011 :15–36

74. EQUA-Simulation-AB. IDA Indoor Climate and Energy. 2019. Available from: https://www.equa.se/en/ida-ice. (Accessed on 27/11/2019)

75. EQUA-Simulation-AB. User Manual IDA Indoor Climate and Energy - Version 4.5. 2013. Available from: http://www.equaonline.com/iceuser/pdf/ICE45eng.pdf. (Accessed on 27/11/2019)

76. Research-Centre-on-zero-emission-neighbourhoods-in-smart-cities. Sustainable neighbourhoods with zero greenhouse gas emissions. 2019. Available from: https://fmezen.no/. (Accessed on 27/11/2019)

77. Rønneseth Ø and Sartori I. MEHOD FOR MODELLING NORWEGIAN SINGLE-FAMILY HOUSES IN IDA ICE. Tech. rep. 10. SINTEF Building and Infrastructure, NTNU, 2018

78. Brattebø H, O'Born R, Sartori I, Klinski M, and Nørstebø B. Typologier for norske boligbygg - Eksempler på tiltak for energieffektivisering. 2014. Available from: https://www.ntnu.no/documents/1201072460/1201115133/Typologier_for_norske_boligbygg. (Accessed on 22/06/2020)

79. EnergyPlus. Weather Data. 2020. Available from: https://energyplus.net/weather. (Accessed on 15/05/2020)

80. Hole I. Generelt om passivhus. Valg og konsekvenser. Tech. rep. 473.010. SINTEF Byggforsk, 2013

81. Arnesen H, Holme J, Risholt B, Uvsløkk S, Grynning S, Jelle BP, et al. Moderne trevinduer – funksjonalitet, levetid og design. Tech. rep. 46. SINTEF Byggforsk, 2009

82. Kirkhus A. Baderom, toalettrom og vaskerom i boliger. Tech. rep. 361.216. SINTEF Byggforsk, 2017

83. MathWorks. nlinfit - Nonlinear regression. 2020. Available from: https://www.mathworks.com/help/stats/nlinfit.html. (Accessed on 31/05/2020)

84. MathWorks. What Are State-Space Models? 2020. Available from: https://www.mathworks.com/help/ident/ug/what-are-state-space-models.html. (Accessed on 15/06/2020)

Appendix A

Building envelope description

TEK87 model

The information regarding the TEK87 model is retrieved from the ZEN memo 10 [77], and is equivalent to the SH-05 model (variation 1). Table A.1 specify the building envelope characteristics, and table A.2 specify the building envelope materials for the TEK87 model defined in IDA ICE.

Table A.1: Building envelope characteristics - TEK87 model.

Characteristic	Unit	Value
U-value, external wall	W/m^2K	0.28
U-value, roof	W/m^2K	0.18
U-value, floor	W/m^2K	0.25
U-value, windows	W/m^2K	2.40
Thermal bridge value	W/m^2K	0.06
Infiltration rate	h^{-1}	4
Area ratio, windows/BRA	%	20*

*Calculated according to TEK17 [32].

Table A.2: Building envelope materials - TEK87 model.

Component	Materials/insulation	d [mm]
External Wall	Studs, mineral wool	150
Internal Wall	Gypsum boards, insulation	124
Roof	Beams, mineral wool	250
External floor	Reinforced concrete, insulation boards, sole foundation, Leca	300
Internal floor (floor divider)	Wallboard, parquet, insulated framework, gypsum	320
Windows	Double-glazed window, regular glass, air filled	-

TEK10 model

The information regarding the TEK10 model is retrieved from the ZEN memo 10 [77], and is equivalent to the SH-07 model (variation 1). Table A.3 specify the building envelope characteristics, and table A.4 specify the building envelope materials for the TEK10 model defined in IDA ICE.

Table A.3: Building envelope characteristics - TEK10 model.

Characteristic	Unit	Value
U-value of the external wall	W/m^2K	0.17
U-value of the roof	W/m^2K	0.12
U-value of the floor	W/m^2K	0.15
U-value of the windows	W/m^2K	1.20
Thermal bridge value	W/m^2K	0.05
Infiltration rate	h^{-1}	1.50
Area ratio, windows/BRA	%	20*

*Calculated value according to TEK17 [32].

Table A.4: Building envelope materials - TEK10 model.

Component	Materials/insulation	d [mm]
External Wall	Studs, mineral wool	250
Internal Wall	Gypsum boards, insulation	124
Roof	Beams, mineral wool	350
External floor	Reinforced concrete, insulation boards, sole foundation, Leca	300
Internal floor (floor divider)	Wallboard, parquet, insulated framework, gypsum	320
Windows	Double-glazed window, regular glass, air filled	-

TEK17 model

The information specified for the TEK17 model in IDA ICE is retrieved partly from the ZEN memo 10 [77], and partly from the regulations stated in TEK17. In table A.5, U-values for the external wall and roof are equivalent to the SH-07 model (variation 1) in the ZEN memo. The infiltration rate, thermal bridge value and U-values for the windows and floors are defined according to the requirements in TEK17. The material information given in table A.6 is equivalent to the SH-07 model (variation 1) in the ZEN memo.

Table A.5: Building envelope characteristics - TEK17 model.

Characteristics	**Value**	**Unit**
U-value of the external wall	W/m^2K	0.17
U-value of the roof	W/m^2K	0.12
U-value of the floor	W/m^2K	0.10
U-value of the windows	W/m^2K	0.80
Thermal bridge value	W/m^2K	0.05
Infiltration rate	h^{-1}	0.60
Area ratio, windows/BRA	%	20*

*Calculated value according to TEK17 [32].

Table A.6: Building envelope materials - TEK17 model.

Component	**Materials/insulation**	**d [mm]**
External Wall	Studs, mineral wool	250
Internal Wall	Gypsum boards, insulation	124
Roof	I-beams, mineral wool	350
External floor	Reinforced concrete, insulation boards	350
Internal floor (floor divider)	Wallboard, parquet, insulated framework, gypsum	320
Windows	3 pane glazing, clear	-

Passive house model

The information regarding the passive house model is retrieved from the ZEN memo 10 [77], and is equivalent to the SH-07 model (variation 2). Table A.1 specify the building envelope characteristics, and table A.2 specify the building envelope materials for the passive house model defined in IDA ICE.

Table A.7: Building envelope characteristics - passive house model.

Characteristics	**Value**	**Unit**
U-value of the external wall	W/m^2K	0.10
U-value of the roof	W/m^2K	0.08
U-value of the floor	W/m^2K	0.15
U-value of the windows	W/m^2K	0.8
Thermal bridge value	W/m^2K	0.03
Infiltration rate	h^{-1}	0.60
Area ratio, windows/BRA	%	20*

*Calculated value according to TEK17 [32].

Table A.8: Building envelope materials - passive house model.

Component	**Materials/insulation**	**d [mm]**
External Wall	Studs, mineral wool	340
Internal Wall	Gypsum boards, insulation	124
Roof	I-beams, mineral wool	420
External floor	Reinforced concrete, insulation boards	350
Internal floor (floor divider)	Wallboard, parquet, insulated framework, gypsum	320
Windows	3 pane glazing, clear	-

Appendix B

MATLAB script - Modify power

```
%#########################################################
%                        CHANGING POWER LOADS
%#########################################################

%Month of simulation: January
%Model: TEK17
Nominal power, living room: 1903 W

%=========================================================
% Color scheme for graphs
%=========================================================

%Pref: magenta, 'm'
%Pref+dP: yellow, 'ye'
%Tref: green, 'gr'
%Tref+dT: blue, 'blu'
%1st order model: green 'gr'
%2nd order model: black 'k'

ye = [1.0000, 0.7529, 0];
blu = [0.3010, 0.7450, 0.9330];
gr = [0.6588, 0.9294, 0.3882];

%=========================================================
% Import heat load profile from IDA ICE
%=========================================================

function modifyPower_TEK17_january

dirname = 'C:\Users\elinsto\Desktop\January\TEK17\';

startstep = 432.0;
```

```
33 dirnameC = [dirname 'closedLoop_TEK17_jan\day room, 1st
       floor\'];
34 dirnameO = [dirname 'openLoop_TEK17_jan\day room, 1st floor\
       '];
35
36 Livingroom = importdata([dirnameC 'Ideal heater.rm_heat_ctrl
       .Output_PIcontrol.prn'],' ');
37 Livingroom = Livingroom.data;
38 time_ref = Livingroom(:,1);
39 order_ref = Livingroom(:,2);
40 Psh_r = Livingroom(:,3);
41
42 %=============================================================
43 % Change power signals to real values in Watt
44 %=============================================================
45 countPr = size(Psh_r,1);
46 Psh_ref = zeros;
47
48 for i = 1:countPr
49       Psh_ref(i) = Psh_r(i) * 1903.0;
50 end
51
52 %=============================================================
53 %Graph showing the reference heat load profile
54 %=============================================================
55 figure(1)
56 plot(time_ref,Psh_ref, 'm');
57 ylabel('P [W]');
58 xlabel('Time [h]');
59 title('Reference heat load profile, January (TEK17)');
60 grid on;
61
62 %=============================================================
63 % Introducing step
64 %=============================================================
65 %Psh = Psh_ref + deltaP
66 %add a value dP to each element of Pref
67 %In the case of charge, 125 is chosen
68 %In the case of discharge, -125 is chosen
69
70 Psh = zeros;
71
72 skipstartindexC = find(time_ref > startstep,1,'first');
73 for i = 1:countPr
74       if i >= skipstartindexC
75           deltaP = 125.0;
```

```
76          else
77              deltaP = 0.0;
78          end
79          Psh(i) = Psh_ref(i) + deltaP;
80      end
81
82      deltaP = Psh - Psh_ref;
83
84      %============================================================
85      %Graph showing the reference heat load profile with charge\
            discharge
86      %============================================================
87      figure(2)
88      hold off;
89      plot(time_ref,Psh 'Color', ye, 'LineWidth', 0.5);
90      hold on;
91      plot(time_ref,Psh_ref 'm');
92      ylabel('P [W]');
93      xlabel('Time [h]');
94      legend('Pref+dP','Pref');
95      title('Charge/discharge of reference load, January (TEK17)')
            ;
96      grid on;
97
98      %============================================================
99      % Preparing power profile to go back into IDA ICE
100     %============================================================
101     % Changing Psh back to heat signals between 0 and 1
102
103     fid = fopen('newLivingroom.prn', 'W');
104     fprintf(fid,'#      time          order         picontrols\r\n
            ');
105
106     countPsh = size(Psh,2);
107     for i = 1 : countPsh
108         fprintf(fid,'%f\t%f\t%f\r\n',time_ref(i),order_ref(i),
                Psh(i)/1903.0);
109     end
110
111     fclose(fid);
112
113     %============================================================
114     % Delta T
115     %============================================================
116     %Reference temperatures obtained from closed loop
```

```
117 OpTempClosed = importdata([dirnameC 'TEMPERATURES.prn'],' ')
    ;
118 OpTempClosed = OpTempClosed.data;
119 Tsh_ref = OpTempClosed(skipstartindexC:end,3);
120 TimeC   = OpTempClosed(skipstartindexC:end,1);
121 size(Tsh_ref);
122
123 %Temperatures after change in P, obtained from open loop
124 OpTempOpen = importdata([dirnameO 'TEMPERATURES.prn'],' ');
125 OpTempOpen = OpTempOpen.data;
126 skipstartindexO = find(OpTempOpen(:,1) > startstep,1,'first'
    );
127 Tsh    = OpTempOpen(skipstartindexO:end,3);
128 TimeO = OpTempOpen(skipstartindexO:end,1);
129
130 %=============================================================
131 % Remove duplicates
132 %=============================================================
133 TimeC_unique = zeros;
134 TshC_unique = zeros;
135
136 Nc = size(Tsh_ref,1);
137 index = 1;
138 TimeC_unique(1) = TimeC(1);
139 TshC_unique(1)  = Tsh_ref(1);
140 for i = 1 : Nc-1
141     if (TimeC(i+1) > TimeC(i))
142         index = index + 1;
143         TimeC_unique(index) = TimeC(i+1);
144         TshC_unique(index) = Tsh_ref(i+1);
145     end
146 end
147
148 %=============================================================
149 TimeO_unique = zeros;
150 TshO_unique = zeros;
151
152 No = size(Tsh,1);
153 index = 1;
154 TimeO_unique(1) = TimeO(1);
155 TshO_unique(1)  = Tsh(1);
156 for i = 1 : No-1
157     if (TimeO(i+1) > TimeO(i))
158         index = index + 1;
159         TimeO_unique(index) = TimeO(i+1);
160         TshO_unique(index) = Tsh(i+1);
```

```
161     end
162 end
163
164 %=========================================================
165 Tsh_ref_onO = interp1(TimeC_unique,TshC_unique,TimeO_unique,
    'linear');
166 dTsh = TshO_unique-Tsh_ref_onO;
167 %=========================================================
168
169 %=========================================================
170 % First order interpolation
171 %=========================================================
172 modelfunO1 = @(b,x)((deltaPc/b(1))*(1-exp(-x/(b(2)))));
173 betaO1_start  = [10;10];
174 opts = statset('nlinfit');
175 opts.RobustWgtFun = 'bisquare';
176 betaO1 = nlinfit(TimeO_unique-startstep,dTsh,modelfunO1,
    betaO1_start,opts);
177 disp(['First order model U = ' num2str(betaO1(1)) ' time
    constant = ' num2str(betaO1(2)) ' and capacitance = '
    num2str(betaO1(1)*betaO1(2))]);
178 dTsh_fit01 = (deltaPc/betaO1(1))*(1-exp(-(TimeO_unique-
    startstep)/betaO1(2)));
179
180 %=========================================================
181 % Second order interpolation
182 %=========================================================
183 modelfunO2 = @(b,x)((deltaPc/b(1))*(1-b(2)*exp(-x/(b(3)))
    -(1-b(2))*exp(-x/b(4))));
184 betaO2_start  = [betaO1(1);0.6;60;1]; % This routine is not
    robust, the initial value should be chosen in a smart way
    to make the fitting converge
185 opts = statset('nlinfit');
186 opts.RobustWgtFun = 'bisquare';
187 betaO2 = nlinfit(TimeO_unique-startstep,dTsh,modelfunO2,
    betaO2_start,opts);
188 disp(['Second order model U = ' num2str(betaO2(1)) ' time
    constant 1 = ' num2str(betaO2(3)) ' time constant 2 = '
    num2str(betaO2(4)) ' and fraction ' num2str(betaO2(2))]);
189 dTsh_fit02 = (deltaPc/betaO2(1))*(1-betaO2(2)*exp(-(
    TimeO_unique-startstep)/betaO2(3))-(1-betaO2(2))*exp(-(
    TimeO_unique-startstep)/betaO2(4)));
190
191 %=========================================================
192
193
```

```
194
195 %============================================================
196 % Graph showing temperatures from closed loop and open loop
197 %============================================================
198 figure(3)
199 hold off
200 plot(TimeC,Tsh_ref,'Color', gr, 'LineWidth',0.5);
201 hold on;
202 grid on;
203 plot(TimeO,Tsh,'Color', blu, 'LineWidth',0.5);
204 ylabel('Air temperature [^{\circ}C]');
205 xlabel('Time [h]');
206 legend('Tref','Tref+dT');
207 title('Temperature change by charging\discharging, January (
    TEK17)');
208
209 %In case of discharge, the following command is used to
    invert the graph:
210 %set(gca, 'YDir', 'Reverse');
211
212 %============================================================
213 %Graph showing dT, including the first and second order
    model
214 %============================================================
215 figure(4)
216 hold off
217 plot(TimeO_unique,dTsh,'Color', blu, 'LineWidth',0.5);
218 hold on;
219 plot(TimeO_unique,dTsh_fit01,'Color', gr, 'LineWidth',0.5);
220 plot(TimeO_unique,dTsh_fit02,'k');
221 grid on;
222 ylabel('dT [^{\circ}C]');
223 xlabel('Time [h]');
224 legend('dT','dT (1st order)','dT (2nd order)');
225 title('Temperature change by charging, January (TEK17)');
226
227 %In case of discharge, the following command is used to
    invert the graph:
228 %set(gca, 'YDir', 'Reverse');
229
230 %============================================================
231 %Graph showing dT and dP
232 %============================================================
233 %Define interval corrsponding to startindex and end point
234 delP = deltaP(4321:11040);
235 timeP = time_ref(4322:11041);
```

```
236
237 figure(5)
238 subplot(2,1,1)
239 hold off
240 plot(TimeO_unique,dTsh,'Color', blu, 'LineWidth',0.5);
241 hold on;
242 plot(TimeO_unique,dTsh_fit01,'Color', gr, 'LineWidth',0.5);
243 plot(TimeO_unique,dTsh_fit02,'k');
244 grid on;
245 ylabel('dT [^{\circ}C]');
246 xlabel('Time [h]');
247 legend('dT','dT (1st order)','dT (2nd order)');
248 title('Analysis: charging in January (TEK17)');
249 ylim([0 3]);
250
251 subplot(2,1,2)
252 plot(timeP,delP,'Color', ye, 'LineWidth',0.6)
253 ylim([0 500]);
254 ylabel('dP [W]');
255 xlabel('Time [h]');
256 legend('Step response');
257 grid on;
258
259 %In case of discharge, the following command is used to
      invert the graph:
260 %set(gca, 'YDir', 'Reverse');
261
262 %==================================
263 end
264 %==================================
```

Appendix C

MATLAB scripts - Validation

C.1 Schedule and model definition

```
%##############################################
%              CHANGING POWER LOADS
%##############################################
%#####################################################
function modifyPower_validation_TEK17_january
%#####################################################
startstep = 528.0; % time when the step functions starts
dt = 0.1;          % in hour
Pn = 1903.0;       % nominal power
isexported = 1;    % "1" if export the results to new IDA
   ICE open loop file
%=====================================================
storageefffactor = 0.98;
%=====================================================
U = 62;            % identified U value first order
C  = 5239;         % identified C value first order
%=====================================================
Utot = 61;         % identified Uvalue second order
T1 = 102;          % identifed time constant in h
T2 = 1.1;          % identified second time constant in h
alpha = 0.86;      % weighting on T1

%=====================================================
% Colors
%=====================================================
ye = [1.0000, 0.7529, 0];
blu = [0.3010, 0.7450, 0.9330];
gr = [0.6588, 0.9294, 0.3882];

%=====================================================
```

```
30 Preffile = importdata('Closedloop_TEK17_jan\day room, 1st
     floor\Ideal heater.rm_heat_ctrl.Output_PIcontrol.prn',' ')
     ;
31 Treffile = importdata('Closedloop_TEK17_jan\day room, 1st
     floor\TEMPERATURES.prn',' ');
32
33 Prefdata = Preffile.data;
34 Trefdata = Treffile.data;
35 time_ref  = Prefdata(:,1);
36 order_ref = Prefdata(:,2);
37 Psh_ref   = Prefdata(:,3)*Pn;
38 Tsh_ref   = Trefdata(:,3);
39 sizeP     = size(Psh_ref,1);
40 sizeT     = size(Tsh_ref,1);
41
42 % counttime = size(time_ref,1);
43 % fid = fopen('Time.prn', 'W');
44 % fprintf(fid,'#      time          order         picontrols\r
     \n');
45 %
46 % for i = 1 : counttime
47 %     fprintf(fid,'%f\t%f\t%f\r\n',time_ref(i),order_ref(i),
     Psh_r(i));
48 % end
49 % fclose(fid);
50
51 %====================================
52 % Change the power
53 %====================================
54 skipstartindexC = find(time_ref > startstep,1,'first');
55 firstperiod1 = 0;
56 firstperiod2 = 0;
57 firstperiod3 = 0;
58 firstperiod4 = 0;
59 %==================
60 for i = 1:sizeP
61     localtime   = time_ref(i);
62     day_ref(i)  = floor(localtime/24)+ 1;
63     hour_ref(i) = localtime - floor(localtime/24)*24;
64 end
65 for i = 1:sizeP
66      localtime = time_ref(i);
67      daynumber = day_ref(i);
68      hourofday = hour_ref(i); % determine the hour of day
69      if i >= skipstartindexC
70          deltaPc = 0.0;
```

```
71          %=========================================
72          Tmin1 = 5.0;
73          Tmax1 = 7.0;
74          Tmin2 = Tmax1;
75          Tmax2 = 10.0;
76          if (hourofday >= Tmin1)&&(hourofday < Tmax1)
77              if (firstperiod1 == 0)
78                  firstperiod1 = 1;
79                  firstperiod2 = 1;
80                  firstperiod3 = 0;
81                  firstperiod4 = 0;
82                  Iinterval1   = find((hour_ref >= Tmin1)&(
                        hour_ref < Tmax1)&(day_ref == daynumber));
83                  Iinterval2   = find((hour_ref >= Tmin2)&(
                        hour_ref < Tmax2)&(day_ref == daynumber));
84                  Pinterval1   = Psh_ref(Iinterval1);
85                  Pinterval2   = Psh_ref(Iinterval2);
86                  Pmax1        = max(Pinterval1);
87                  dPmax1       = max((Pn-Pmax1),0);
88                  Pmin2        = min(Pinterval2);
89                  dPmin2       = max(Pmin2,0);
90                  duration1    = Tmax1-Tmin1;
91                  duration2    = Tmax2-Tmin2;
92                  dP1          = min(dPmax1,dPmin2*duration2/
                        duration1);
93                  dP2          = storageefffactor*dP1*
                        duration1/duration2;
94                  clear Iinterval1 Pinterval1 Iinterval2
                        Pinterval2;
95              end
96              deltaPc = dP1;
97          end
98          if (hourofday >= Tmin2)&&(hourofday < Tmax2)
99              deltaPc = -dP2;
100         end
101         %=========================================
102         Tmin3 = 15.0;
103         Tmax3 = 17.0;
104         Tmin4 = Tmax3;
105         Tmax4 = 20.0;
106         if (hourofday >= Tmin3)&&(hourofday < Tmax3)
107             if (firstperiod3 == 0)
108                 firstperiod1 = 0;
109                 firstperiod2 = 0;
110                 firstperiod3 = 1;
111                 firstperiod4 = 1;
```

```
112                     Iinterval3    = find((hour_ref >= Tmin3)&(
                           hour_ref < Tmax3)&(day_ref == daynumber));
113                     Iinterval4    = find((hour_ref >= Tmin4)&(
                           hour_ref < Tmax4)&(day_ref == daynumber));
114                     Pinterval3    = Psh_ref(Iinterval3);
115                     Pinterval4    = Psh_ref(Iinterval4);
116                     Pmax3         = max(Pinterval3);
117                     dPmax3        = max((Pn-Pmax3),0);
118                     Pmin4         = min(Pinterval4);
119                     dPmin4        = max(Pmin4,0);
120                     duration3     = Tmax3-Tmin3;
121                     duration4     = Tmax4-Tmin4;
122                     dP3           = min(dPmax3,dPmin4*duration4/
                           duration3);
123                     dP4           = storageefffactor*dP3*
                           duration3/duration4;
124                     clear Iinterval3 Pinterval3 Iinterval4
                           Pinterval4;
125                 end
126                 deltaPc = dP3;
127             end
128             if (hourofday >= Tmin4)&&(hourofday < Tmax4)
129                 deltaPc = -dP4;
130             end
131         else
132             deltaPc = 0.0;
133         end
134         Psh(i)    = Psh_ref(i) + deltaPc;
135         deltaP(i) = deltaPc;
136 end
137
138 disp(['Sum of change of power ' num2str(sum(deltaP*dt))]);
139
140 close all;
141
142 figure(2)
143 hold off;
144 plot(time_ref,Psh,'Color', ye, 'LineWidth',0.5);
145 hold on;
146 plot(time_ref,Psh_ref,'m');
147 plot(time_ref,ones(sizeP,1)*Pn,'k');
148 ylabel('P [W]');
149 xlabel('Time [h]');
150 legend('Pref+dP','Pref','Pn');
151 title('Modified heat load profile, January (TEK17)');
152 grid on;
```

```
153
154 figure(21)
155 hold off;
156 plot(time_ref,deltaP,'yeo-');
157 hold on;
158 ylabel('dP [W]');
159 xlabel('Time [h]');
160 title('Scheduled load, January (TEK17)');
161 grid on;
162
163 %=====================================
164 % Define first-order model
165 disp('Integrate first-order model');
166 A = -U/C;
167 B =  1/C;
168 C = 1.0;
169 D = 0.0;
170 ss1 = ss(A,B,C,D);
171 ym1 = lsim(ss1,deltaP,(time_ref-time_ref(1)),0,'zoh');
172 disp(['Sum of change of temperature ' num2str(sum(ym1*dt))])
    ;
173 Tmod1 = ym1 + Tsh_ref;
174
175 %=====================================
176 % Define second-order model
177 %=====================================
178
179 %.... This part is excluded from the script
180
181 %=====================================
182 figure(3)
183 hold off;
184 plot(time_ref,ym1,'bo-');
185 hold on;
186 plot(time_ref,ym2,'ko:');
187 grid on;
188 ylabel('dT');
189 xlabel('Time');
190
191 %=====================================
192 % Preparing power profile for IDA ICE
193 %=====================================
194 % Changing Psh back to heat signals between 0 and 1
195 if isexported
196     disp('Export file');
197     fid = fopen('newLivingroomDR.prn', 'W');
```

```
198     fprintf(fid,'#       time          order          picontrols
                Tref          dTmod1          dTmod2          Pref
               deltaP\r\n');
199     countPsh = size(Psh,2);
200     for i = 1 : countPsh
201         fprintf(fid,'%f\t%f\t%f\t%f\t%f\t%f\t%f\t%f\r\n',
              time_ref(i),order_ref(i),Psh(i)/Pn,Tsh_ref(i),ym1(
              i),ym2(i),Psh_ref(i),deltaP(i));
202     end
203     fclose(fid);
204 end
205 %=====================================
```

C.2 Plot of the temperatures

```
1  %#########################################
2  function plotresultsDR
3  %#########################################
4  modelTfile = importdata('newLivingroomDR.prn','\t');
5  modelTdata = modelTfile.data;
6  timeref  = modelTdata(:,1);
7  Tref     = modelTdata(:,4);
8  dTmod1   = modelTdata(:,5); % temperature change from 1st
       order model
9  dTmod2   = modelTdata(:,6); % temperature change from 2nd
       order model
10 Pref     = modelTdata(:,7);
11 dP       = modelTdata(:,8);
12 %=================================
13 IDATfile = importdata('OpenloopUp_TEK17_jan\day room, 1st
       floor\TEMPERATURES.prn',' ');
14 IDATdata = IDATfile.data;
15 timeIDA  = IDATdata(:,1);
16 TIDA     = IDATdata(:,3);
17 %=================================
18 blu = [0.3010, 0.7450, 0.9330];
19 gr = [0.6588, 0.9294, 0.3882];
20 %=================================
21 figure(1)
22 %=================================
23 hold off;
24 plot(timeref,Tref,'Color', gr, 'LineWidth',0.5);
25 hold on;
26 grid on;
27 plot(timeref,Tref+dTmod1,'r--');
28 plot(timeref,Tref+dTmod2,'m:');
```

```
29 plot(timeIDA,TIDA,'k--');
30 ylabel('Living Room Air Temperature [°C]');
31 xlabel('Time [h]');
32 legend('Reference','1st order','2nd order','IDA ICE');
33 title('Model variation TEK17');
34 %================================
```

Elin Storlien

NTNU
Norwegian University of
Science and Technology